

An Intuitive and Visual Approach to Vector Calculus and Electromagnetism

Shawn Eastwood

Introduction

Many discussions and introductions to vector calculus utilize examples and proofs that are exercises in symbolic computation. It is of this author's opinion that a symbolic approach to vector calculus does not convey core concepts in a sufficiently clear manner. Abstract proofs, abstract formulas, and examples for which the emphasis is on the algebra and symbolic computation do not convey the core essence of vector calculus.

The primary purpose of this document is to provide an introduction to vector calculus and electromagnetism **without using the language of Calculus**. The material presented below will use easy to visualize concepts and keep equations and numbers to a minimum. Any equation given will be accompanied by a high level description that will make such equations intuitive.

The primary application that will be presented will be electromagnetism and Maxwell's equations. Most approaches to electromagnetism are piece-wise. For example, basic circuit analysis is primarily concerned with voltages, currents, and resistances. Eventually inductance and mutual inductance is introduced. What is rarely mentioned in these discussions is that the electric field is not conservative, and therefore the notion of voltage itself is poorly defined. While the magnetic vector potential can be used to "complete" the electric field and create a field that is conservative, the vector potential itself is not uniquely defined and is subject to multiple "gauges". Within inductors in particular, the voltage difference across the inductor is in direct opposition to the electric field that actually exists. The voltage difference is instead the electric field that must exist to "push back" the electric field generated by the inductor itself.

The aim is to enable a visualization of electromagnetic phenomena that takes full account of Maxwell's equations. To this end, conventional depictions of vector fields as a forest of arrows will be replaced in favor of depictions that use bundles of oriented paths and layers of oriented surfaces. Using terminology from fluid mechanics, the description will be **Lagrangian** in nature as opposed to more conventional **Eulerian** descriptions. With Eulerian descriptions, the fields are tracked at **fixed points**. With the Lagrangian description, the field lines will be tracked as they sweep through space.

What will be assumed

This document will assume that the reader is familiar with basic algebra.

While a basic knowledge of Calculus is useful, an in-depth knowledge of Calculus is not required.

Since the conventional depiction of vectors as arrows is being replaced, vector algebra is also not required as a prerequisite topic. When vectors are introduced, they will be introduced as lists of numbers.

Chapter structure

Chapter 1 introduces the fundamental structures of points, paths, surfaces, and volumes. Chapters 2 to 4 introduce the basic functions involving points, paths, surfaces, and volumes. Chapters 5 and 6 establish algebraic properties involving the introduced structures and operations.

Chapter 7 introduces the system by which points, paths, surfaces, and volumes can be quantified directly with numbers and functions. It is in this chapter that a prior knowledge of differential calculus is useful.

Chapter 8 describes how the dimensionality of structures can be “inverted”, with points becoming volumes and vice versa, and with paths becoming surfaces and vice versa. It is at this point that electromagnetism is introduced assuming no changes with respect to time (i.e. statics). Many important details related to electrostatics and magnetostatics will be proven.

Chapter 9 finally introduces time. Additional functions are introduced. The computations from chapter 7 and the concept of duality from chapter 8 are extended to incorporate time.

Chapter 10 finally fully introduces electromagnetism with the incorporation of time.

Chapter 11 connects electromagnetism with force, momentum, and energy.

Contents

| | |
|---|------------|
| Introduction | iii |
| 1 Multi-structures | 1 |
| 1.1 Introduction | 1 |
| 1.2 Multi-points | 1 |
| 1.3 Multi-paths | 2 |
| 1.4 Multi-surfaces | 4 |
| 1.5 Multi-volumes | 6 |
| 1.6 Summary | 7 |
| 2 Unions | 9 |
| 2.1 Introduction | 9 |
| 2.2 point-point unions | 9 |
| 2.3 path-path unions | 10 |
| 2.4 surface-surface unions | 11 |
| 2.5 volume-volume unions | 11 |
| 2.6 Summary | 12 |
| 3 Intersections | 13 |
| 3.1 Introduction | 13 |
| 3.2 Point-volume intersections | 14 |
| 3.3 Path-surface intersections | 16 |
| 3.4 Path-volume intersections | 18 |
| 3.5 Surface-surface intersections | 20 |
| 3.6 Surface-volume intersections | 25 |
| 3.7 Volume-volume intersections | 27 |
| 3.8 Intersections that are not being considered | 28 |
| 3.8.1 Point-path intersections | 29 |
| 3.8.2 Point-surface intersections | 29 |
| 3.8.3 Path-path intersections | 30 |
| 3.9 Summary | 30 |
| 4 Boundaries | 33 |
| 4.1 Point totals | 33 |
| 4.1.1 Scanning for equivalence | 33 |
| 4.2 Path endpoints | 37 |
| 4.3 Surface boundaries | 38 |
| 4.4 Volume surfaces | 39 |
| 4.5 Summary | 40 |

| | | |
|----------|--|-----------|
| 5 | Closed loops and surfaces | 41 |
| 5.1 | Balanced multi-points | 41 |
| 5.2 | Closed loops | 42 |
| 5.3 | Closed surfaces | 43 |
| 6 | Boundaries and intersections | 45 |
| 6.1 | Introduction | 45 |
| 6.2 | The endpoints of path-volume intersections | 45 |
| 6.3 | The endpoints of surface-surface intersections | 47 |
| 6.4 | The boundaries of surface-volume intersections | 49 |
| 6.5 | The surfaces of volume-volume intersections | 50 |
| 6.6 | Summary | 50 |
| 7 | Quantifying multi-structures | 53 |
| 7.1 | Introduction | 53 |
| 7.2 | The smoothness condition | 53 |
| 7.3 | Unions revisited | 54 |
| 7.4 | Coordinate systems | 56 |
| 7.5 | Using numbers to describe multi-structures | 59 |
| 7.5.1 | Quantifying multi-points | 59 |
| 7.5.2 | Quantifying multi-paths | 59 |
| 7.5.3 | Quantifying multi-surfaces | 60 |
| 7.5.4 | Quantifying multi-volumes | 61 |
| 7.6 | Computing unions | 61 |
| 7.7 | Computing intersections | 62 |
| 7.7.1 | Computing intersections involving a multi-volume | 62 |
| 7.7.2 | Computing path-surface intersections | 62 |
| 7.7.3 | Computing surface-surface intersections | 63 |
| 7.8 | Computing boundaries | 65 |
| 7.8.1 | Computing path endpoints | 65 |
| 7.8.2 | Computing surface boundaries | 67 |
| 7.8.3 | Computing volume surfaces | 68 |
| 7.9 | Select Coordinate systems | 69 |
| 7.9.1 | Cartesian coordinates | 71 |
| 7.9.2 | Cylindrical coordinates | 73 |
| 7.9.3 | Spherical coordinates | 74 |
| 7.10 | Summary | 75 |
| 8 | Duality | 79 |
| 8.1 | Point-volume duality | 79 |
| 8.2 | Path-surface duality | 80 |
| 8.3 | Duality and intersections | 81 |
| 8.4 | Simplifying notation | 84 |
| 8.5 | Quantifying duality | 85 |
| 8.6 | Energy | 86 |
| 8.6.1 | Path energy | 86 |
| 8.6.2 | Surface energy | 86 |
| 8.6.3 | Loop-bubble duality | 86 |
| 8.6.4 | Low energy multi-path | 87 |
| 8.6.5 | Low energy multi-surface | 90 |
| 8.6.6 | The Helmholtz decomposition theorem | 92 |
| 8.7 | Inductance | 92 |

| | | |
|-----------|--|------------|
| 8.7.1 | Balanced multi-point inductance | 92 |
| 8.7.2 | Multi-loop inductance | 94 |
| 8.8 | Scalar ϵ | 96 |
| 8.9 | Electrostatics and magnetostatics | 98 |
| 8.9.1 | Special scenarios | 99 |
| 8.9.2 | Nonuniform permittivity and permeability | 99 |
| 8.9.3 | Anisotropic mediums | 99 |
| 9 | Finite element modeling | 101 |
| 10 | Introducing time | 103 |
| 10.1 | A new multi-structure | 103 |
| 10.2 | How multi-structures change with time | 103 |
| 10.2.1 | Moving points | 104 |
| 10.3 | New intersections | 105 |

Chapter 1

Multi-structures

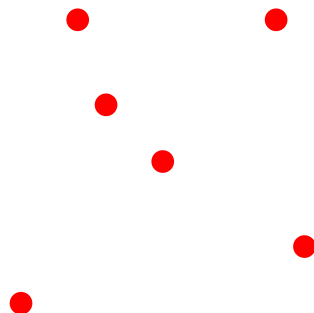
1.1 Introduction

This chapter will introduce the structures that will serve as the basis for all of the concepts that will be discussed by this book.

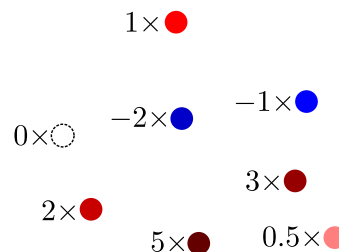
A **multi-structure** is a collection of points (a multi-point), a collection of paths (a multi-path), a collection of surfaces (a multi-surface), or a collection of volumes (a multi-volume). The “type” of a multi-structure is the status of being a multi-point, a multi-path, a multi-surface, or a multi-volume. All of these structures will be assumed to exist in **3D space**.

1.2 Multi-points

A **multi-point** is a superposition of points. One such superposition is depicted on the right.



When two points have the same position, the result is a point with a weight of 2. When three points have the same position, the result is a point with a weight of 3. Every point in a multi-point has associated with it a “weight” which is the number of how many points have been stacked into the same position. The weight can be a fraction, so there can be fractional copies of a point. The weight can also be negative, so there can be “anti-points”. If the weight is 0, then the point is simply not included. On the right is a multi-point, where the points have different weights.



A multi-point ρ is effectively a set of point (P) / weight (w) pairs. An arbitrary multi-point will be

denoted via the notation

$$\rho = w_1 P_1 + w_2 P_2 + \dots + w_N P_N$$

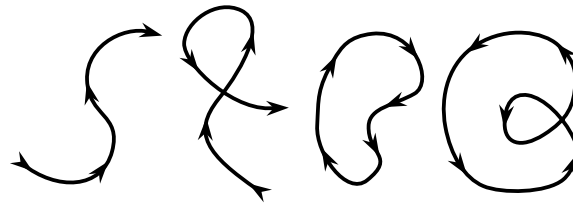
where w_i is the weight that is assigned to point P_i . This notation effectively denotes that a multi-point is a collection/sum of points.

Each weight w_i will be assumed to be nonzero, as a point with a weight of 0 is not included as part of the multi-point. Moreover, the points will be assumed to all be unique. If a point appears multiple times, then these appearances can be condensed into a single appearance whose weight is the sum of all weights from the multiple appearances.

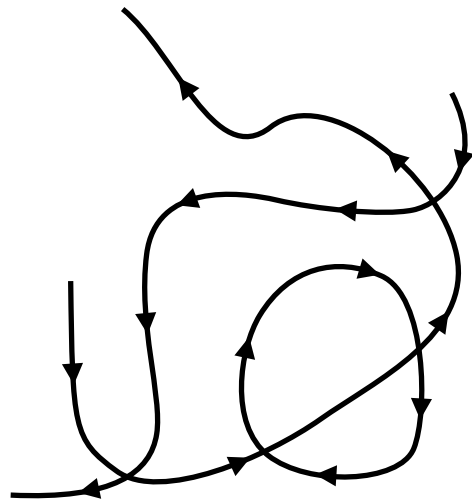
Two multi-points are equivalent if and only if the collections of constituent points are equivalent with identical weights.

1.3 Multi-paths

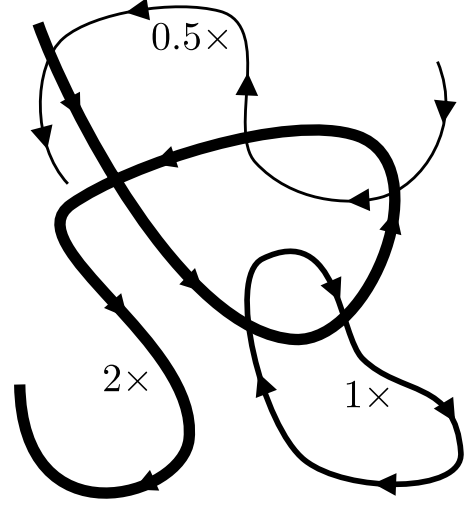
A path is 1D trail. An oriented path is a path that has a preferred direction as is depicted in the four examples below:



A **multi-path** is a superposition of oriented paths. One such superposition is depicted on the right.



When two oriented paths in the same multi-path are equivalent, the result is the common oriented path with a weight of 2. When three oriented paths in the same multi-path are the equivalent, the result is the common oriented path with a weight of 3. Every oriented path in a multi-path has associated with it a “weight” which is the number of “stacked” oriented paths. The weight can be a fraction, so there can be fractional copies of a path. **If the weight is negative, then the orientation of the path is reversed and the sign is flipped to positive.** On the right is a multi-path where the paths have different weights. Note how there are no negative weights, as a negative weight merely flips the orientation of the path.



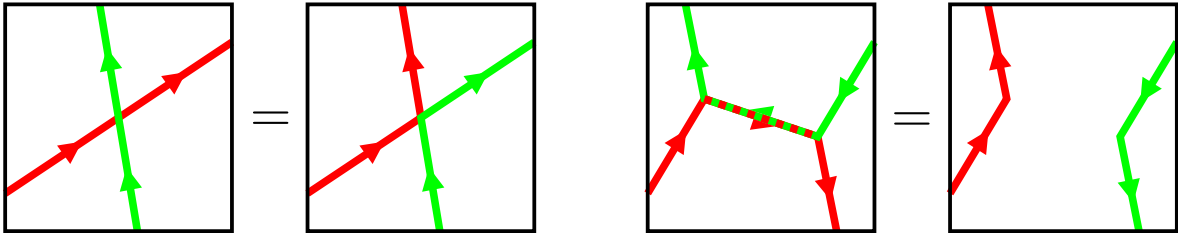
A multi-path \mathbf{J} is effectively a set of oriented path (C) / weight (w) pairs:

$$\mathbf{J} = w_1 C_1 + w_2 C_2 + \dots + w_N C_N$$

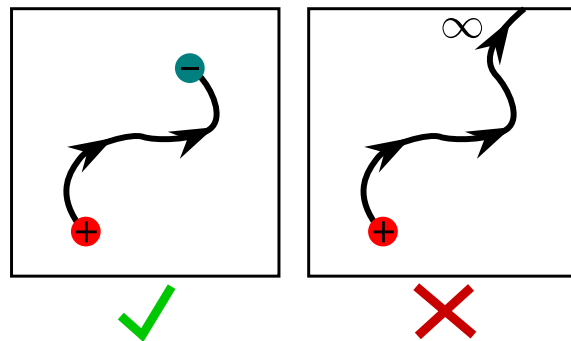
where w_i is the weight that is assigned to path C_i . This notation effectively denotes that a multi-path is a collection/sum of oriented paths.

Each weight w_i will be assumed to be strictly positive, as an oriented path with a weight of 0 is not included as part of the multi-path, and a negative weight can be made positive while reversing the path’s orientation. Moreover, the oriented paths will be assumed to all be unique. If a path appears multiple times, then these appearances can be condensed into a single appearance whose weight is the sum of all weights from the multiple appearances. If an oriented path and its reversed orientation appears, then these instances cancel out. The orientation with the smaller weight is eliminated, while the orientation with the larger weight has its weight reduced by the smaller weight. If the weights of both orientations are equal, then the orientations completely cancel each other out. It should also be noted that curves can partially cancel each other out (as illustrated below on the right).

Two multi-paths are equivalent if and only if the networks of oriented paths are equivalent, regardless of how the network is broken up into individual oriented paths, as illustrated below. In the example on the right, the segments that are on top of each other and have opposite orientations have canceled each other out.

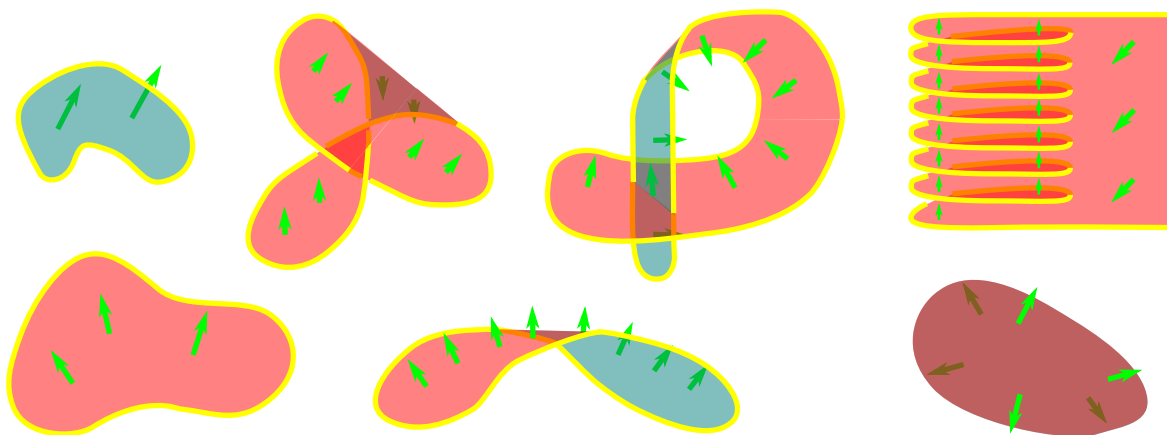


Unless otherwise specified, no path will be allowed to diverge to points that are infinitely distant.

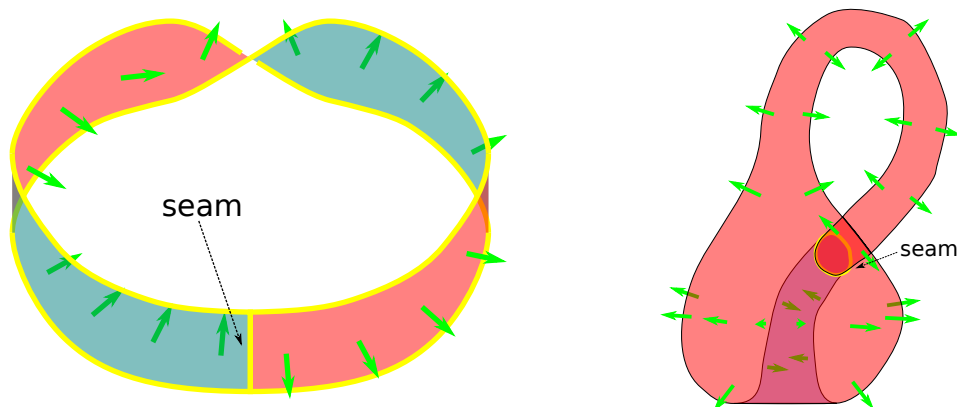


1.4 Multi-surfaces

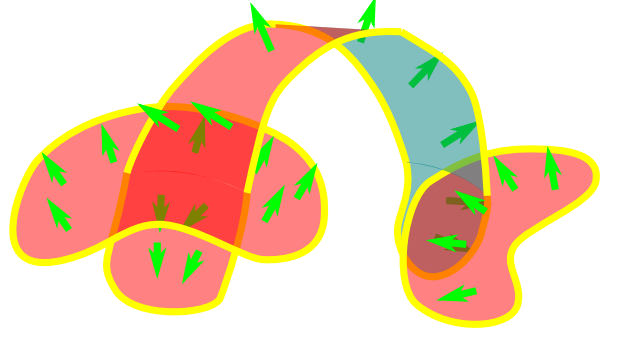
An oriented surface is a surface that has a “front” side and a “back” side. The orientation is depicted as arrows that point outwards from the front side, as depicted in the examples below.



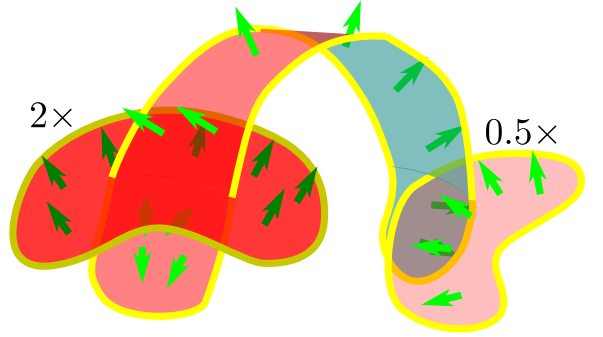
A “Mobius strip” (left) or a “Klein bottle” (right) are examples of surfaces that have only one side, and therefore cannot be oriented without the introduction of a seam.



A **multi-surface** is a superposition of oriented surfaces. One such superposition is depicted on the right.



When two oriented surfaces in the same multi-surface are equivalent, the result is the common oriented surface with a weight of 2. When three oriented surfaces in the same multi-surface are the equivalent, the result is the common oriented surface with a weight of 3. Every oriented surface in a multi-surface has associated with it a “weight” which is the number of “stacked” oriented surfaces. The weight can be a fraction, so there can be fractional copies of a surface. **If the weight is negative, then the orientation of the surface is reversed and the sign is flipped to positive.** On the right is a multi-surface where the surfaces have different weights. Note how there are no negative weights, as a negative weight merely flips the orientation of the surface.



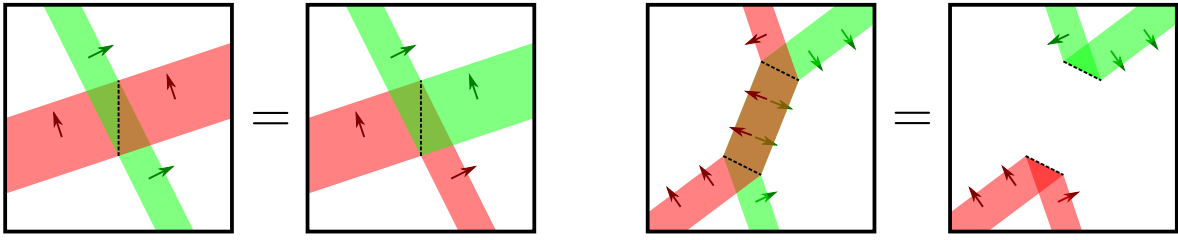
A multi-surface \mathbf{F} is effectively a set of oriented surface (σ) / weight (w) pairs:

$$\mathbf{F} = w_1\sigma_1 + w_2\sigma_2 + \dots + w_N\sigma_N$$

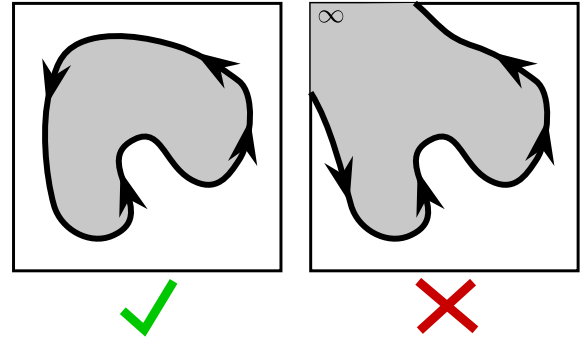
where w_i is the weight that is assigned to surface σ_i . This notation effectively denotes that a multi-surface is a collection/sum of oriented surfaces.

As with multi-paths, each weight w_i will be assumed to be strictly positive, as an oriented surface with a weight of 0 is not included as part of the multi-surface, and a negative weight can be made positive while reversing the surface’s orientation. Moreover, the oriented surfaces will be assumed to all be unique. If a surface appears multiple times, then these appearances can be condensed into a single appearance whose weight is the sum of all weights from the multiple appearances. If an oriented surface and its reversed orientation appears, then these instances cancel out. The orientation with the smaller weight is eliminated, while the orientation with the larger weight has its weight reduced by the smaller weight. If the weights of both orientations are equal, then the orientations completely cancel each other out. It should also be noted that surfaces can partially cancel each other out (as illustrated below on the right).

Two multi-surfaces are equivalent if and only if the networks of oriented surfaces are equivalent, regardless of how the network is broken up into individual oriented surfaces, as illustrated below. In the example on the right, the segments that are on top of each other and have opposite orientations have canceled each other out.



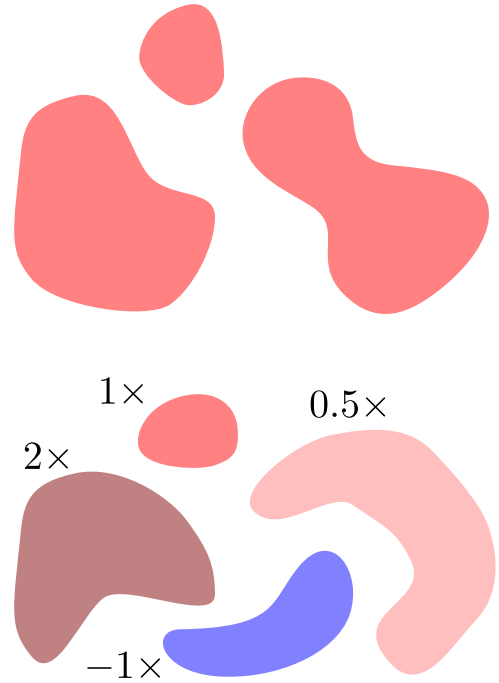
Unless otherwise specified, no surface will be allowed to diverge to points that are infinitely distant.



1.5 Multi-volumes

A **multi-volume** is a superposition of volumes. One such superposition is depicted on the right.

When two volumes in the same multi-volume are equivalent, the result is the common volume with a weight of 2. When three volumes in the same multi-volume are equivalent, the result is the common volume with a weight of 3. Every volume in a multi-volume has associated with it a “weight” which is the number of “stacked” volumes. The weight can be a fraction, so there can be fractional copies of a volume. The weight can also be negative, so there can be “anti-volume”. If the weight is 0, then the volume is simply not included. On the right is a multi-volume, where the volumes have different weights.



A multi-volume U is effectively a set of volume (Ω) /weight (w) pairs:

$$U = w_1\Omega_1 + w_2\Omega_2 + \dots + w_N\Omega_N$$

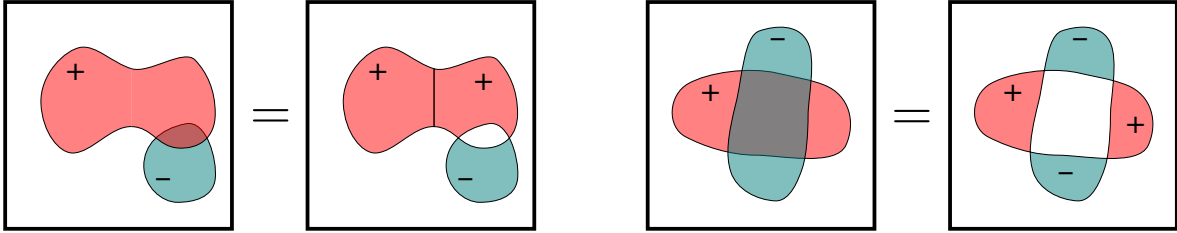
where w_i is the weight that is assigned to volume Ω_i . This notation effectively denotes that a multi-volume is a collection/sum of volumes.

Each weight w_i will be assumed to be nonzero, as a volume with a weight of 0 is not included as part of the multi-volume. Moreover, the volumes will be assumed to all be unique. If a volume appears multiple times, then these appearances can be condensed into a single appearance whose weight is the sum of all weights from the multiple appearances. It should also be noted that volumes can partially cancel each other out.

Two multi-volumes U_1 and U_2 are equivalent if and only if at every position \mathbf{q} , the net number of volumes from U_1 that contain \mathbf{q} is equal to the net number of volumes from U_2 that contain \mathbf{q} . Negative volumes subtract from the number of volumes that contain \mathbf{q} . This is illustrated below.

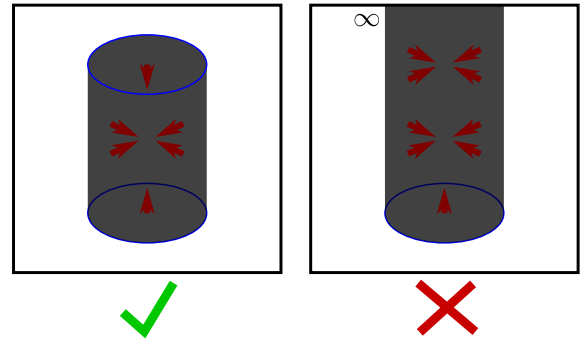
Consider the first example on the left. Left of the $=$ sign, there is a volume with a weight of $+1$, and a volume with a weight of -1 that overlap. Right of the $=$ sign, the volume with a weight of $+1$ has been broken into two separate volumes, and the overlap has been canceled out. **These two multi-volumes are equivalent.**

Consider the second example on the right. Left of the $=$ sign, there is a volume with a weight of $+1$, and a volume with a weight of -1 that overlap each other. Right of the $=$ sign, the intersection has been canceled out, breaking each of the volumes into 2 separate pieces. **These two multi-volumes are equivalent.**



In general, given an arbitrary position \mathbf{q} , and a multi-volume U , the notation $U(\mathbf{q})$ will denote the net number of volumes that contain \mathbf{q} . Multi-volumes U_1 and U_2 are equivalent if and only if $U_1(\mathbf{q}) = U_2(\mathbf{q})$ at all positions \mathbf{q} .

Unless otherwise specified, no volume will be allowed to diverge to points that are infinitely distant.



1.6 Summary

This chapter gave an introduction to the 4 types of multi-structures that will be used in the beginning chapters of this book: multi-points; multi-paths; multi-surfaces; and multi-volumes. In the later chapters

when time is introduced as a factor, an additional multi-structure called “multi-events” will be introduced.

Chapter 2

Unions

2.1 Introduction

This chapter will consist of a brief discussion of how multi-structures are “summed”. The sum is similar to computing the union of sets (more specifically multi-sets), but with major differences as will soon become apparent.

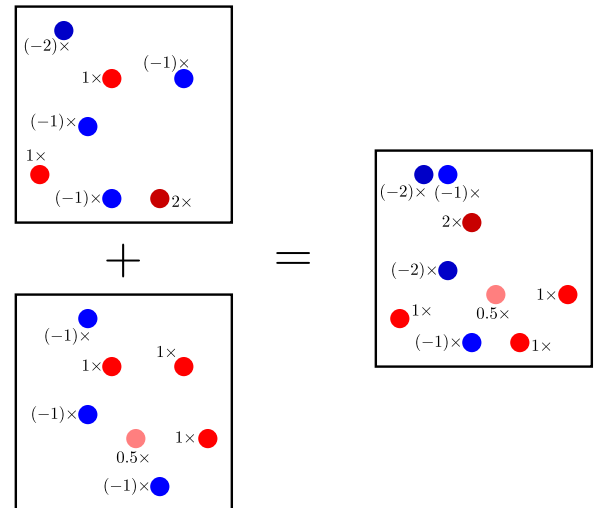
A “union” between two multi-structures of the same “type” is the result of simply “combining” the multi-structures in a straightforward manner. The addition symbol “+” denotes the union. The union of two sets typically counts the elements that are common to both sets only once, but here **the weights of structures that are common to both multi-structures are added together**.

Only multi-structures with the same type can be summed. The sum/union of multi-structures of different types will not be considered.

2.2 point-point unions

The union of multi-points ρ_1 and ρ_2 is the set of all weighted points from both multi-points. If the same points appear then their weights are added. If any resultant weight is 0, then the corresponding point disappears.

An example of such a multi-point union is depicted on the right. Illustrated are examples of points stacking up to form points of greater weight, and points canceling out, partially as well as completely.



Lastly, given a multi-point ρ and a positive integer n , then

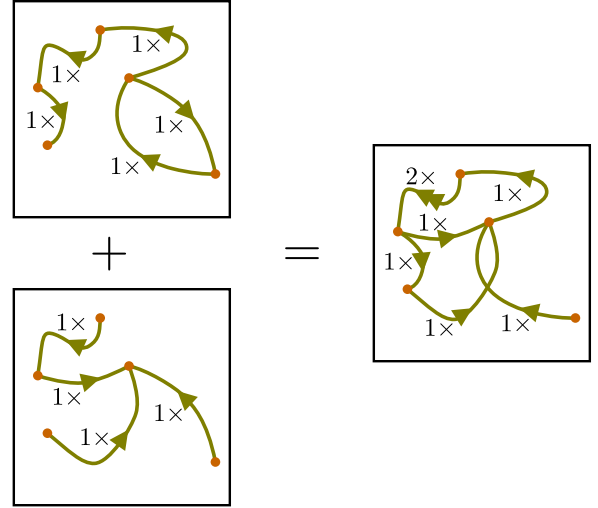
$$n \cdot \rho = \underbrace{\rho + \rho + \dots + \rho}_n$$

so “multiplying” a multi-point by n is to multiply the weight of each point by n . More generally, to multiply a multi-point by any real number k is to multiply the weight of each point by k . “Multiplication” by k is denoted by:

$$k \cdot \rho \quad \text{or} \quad k\rho \quad \text{or} \quad \rho \cdot k \quad \text{or} \quad \rho k$$

2.3 path-path unions

The union of multi-paths \mathbf{J}_1 and \mathbf{J}_2 is the set of all weighted oriented paths from both multi-paths. An example of such a union is depicted on the right. Illustrated are examples of paths with identical orientation stacking to form paths with a greater weight, and paths with opposite orientation canceling out.



Lastly, given a multi-path \mathbf{J} and a positive integer n , then

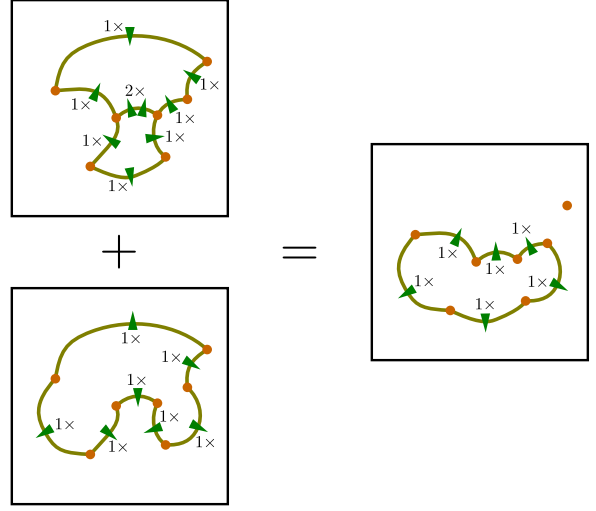
$$n \cdot \mathbf{J} = \underbrace{\mathbf{J} + \mathbf{J} + \dots + \mathbf{J}}_n$$

so “multiplying” a multi-path by n is to multiply the weight of each path by n . More generally, to multiply a multi-path by any real number k is to multiply the weight of each path by k , reversing the orientation of paths with negative weight. “Multiplication” by k is denoted by:

$$k \cdot \mathbf{J} \quad \text{or} \quad k\mathbf{J} \quad \text{or} \quad \mathbf{J} \cdot k \quad \text{or} \quad \mathbf{J}k$$

2.4 surface-surface unions

The union of multi-surfaces \mathbf{F}_1 and \mathbf{F}_2 is the set of all weighted oriented surfaces from both multi-surfaces. An example of such a union is depicted on the right (using 2D cross-sections). Illustrated are examples of surfaces with identical orientation stacking to form surfaces with a greater weight, and surfaces with opposite orientation canceling out, partially as well as completely.



Lastly, given a multi-surface \mathbf{F} and a positive integer n , then

$$n \cdot \mathbf{F} = \underbrace{\mathbf{F} + \mathbf{F} + \dots + \mathbf{F}}_n$$

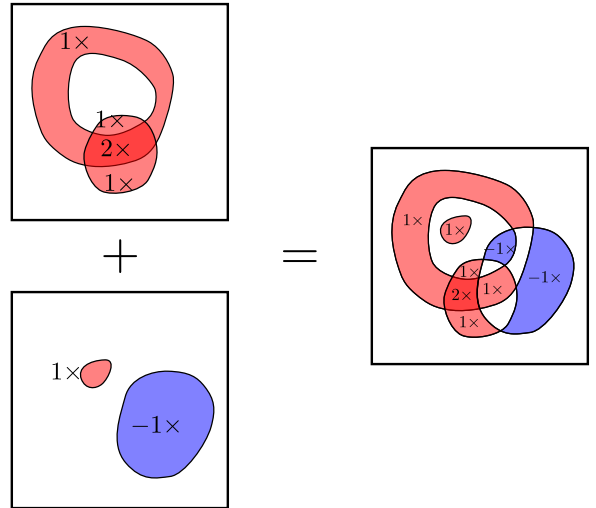
so “multiplying” a multi-surface by n is to multiply the weight of each surface by n . More generally, to multiply a multi-surface by any real number k is to multiply the weight of each surface by k , reversing the orientation of surfaces with negative weight. “Multiplication” by k is denoted by:

$$k \cdot \mathbf{F} \quad \text{or} \quad k\mathbf{F} \quad \text{or} \quad \mathbf{F} \cdot k \quad \text{or} \quad \mathbf{F}k$$

2.5 volume-volume unions

The union of multi-volumes U_1 and U_2 is the set of all weighted volumes from both multi-volumes. An example of such a union is depicted on the right (using 2D cross-sections). Illustrated are examples of volumes partially canceling each other out. Note that for a specific point \mathbf{q} , that the net number of volumes that contain \mathbf{q} in the union $U_1 + U_2$ will always be the sum of the net number of volumes that contain \mathbf{q} in each of U_1 and U_2 :

$$(U_1 + U_2)(\mathbf{q}) = U_1(\mathbf{q}) + U_2(\mathbf{q})$$



Lastly, given a multi-volume U and a positive integer n , then

$$n \cdot U = \underbrace{U + U + \dots + U}_n$$

so “multiplying” a multi-volume by n is to multiply the weight of each volume by n . More generally, to multiply a multi-volume by any real number k is to multiply the weight of each volume by k . “Multiplication” by k is denoted by:

$$k \cdot U \quad \text{or} \quad kU \quad \text{or} \quad U \cdot k \quad \text{or} \quad Uk$$

2.6 Summary

This chapter was a brief formalization of the union of two multi-structures with the same type. The union of multi-structures with different types is not allowed.

Chapter 3

Intersections

3.1 Introduction

The previous chapter discussed the union between two multi-structures, this chapter will discuss the intersection between two multi-structures. The important difference is that while the union required that both multi-structures have the same type, intersections can occur between structures with different types. In fact for some of the low dimensionality multi-structures such as points and paths, the intersection of two of these structure will not even be considered.

As is expected, the intersection of two structures is often the set of positions that are common to both structures, but this will not always be the case. 6 types of intersections will be considered:

- point-volume intersections
- path-surface intersections
- path-volume intersections
- surface-surface intersections
- surface-volume intersections
- volume-volume intersections

Other intersections will not be considered, for reasons primarily related to the fact that such intersections cannot be oriented, as will be discussed later. Intersections are generally denoted with the symbol \cap , but more specialized symbols will be introduced for each of the specific 6 types of intersections that are begin considered.

One property of intersections that will be used heavily is **linearity**. Given a set A and two sets B and C , the intersection of A with the union $B + C$ is the sum of the intersection of A with B separately and the intersection with A with C separately. This property is referred to as “linearity”, and is also frequently referred to as the “distributive law”:

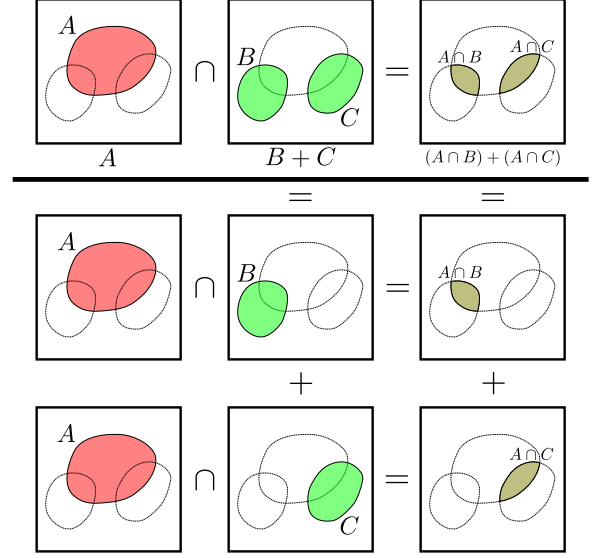
$$A \cap (B + C) = (A \cap B) + (A \cap C)$$

$$(B + C) \cap A = (B \cap A) + (C \cap A)$$

More generally if k is a real number, then the intersection of A with k copies of B is k copies of the intersection of A with B :

$$A \cap (k \cdot B) = k(A \cap B)$$

$$(k \cdot A) \cap B = k(A \cap B)$$



3.2 Point-volume intersections

Given a multi-point ρ and a multi-volume U , then the intersection between ρ and U is a multi-point and is denoted by:

$$\rho \cdot U \quad \text{or} \quad \rho U \quad \text{or} \quad U \cdot \rho \quad \text{or} \quad U \rho$$

Given a single point P , and a single volume Ω , the intersection is P if P is contained by Ω , and is nothing if P is not contained by Ω .

If a point P with a weight of w_1 is contained in a volume Ω with a weight of w_2 , then for each of the w_2 copies of Ω , w_1 copies of P are intersecting that copy. The total intersection is $w_1 \cdot w_2$ copies of P :

$$(w_1 P) \cdot (w_2 \Omega) = w_1 w_2 P$$

If a point P with a weight of w_1 is **not** contained in a volume Ω with a weight of w_2 , then for each of the w_2 copies of Ω , w_1 copies of P are not intersecting that copy. The total intersection is nothing:

$$(w_1 P) \cdot (w_2 \Omega) = 0$$

Given a multi-point $\rho = w_1 P_1 + w_2 P_2 + \dots + w_N P_N$ and a multi-volume $U = v_1 \Omega_1 + v_2 \Omega_2 + v_M \Omega_M$, then the intersection $\rho \cdot U$ is the set of all pairwise intersections of the points and volumes:

$$\rho \cdot U = \begin{cases} w_1 v_1 (P_1 \cdot \Omega_1) + w_1 v_2 (P_1 \cdot \Omega_2) + \dots + w_1 v_M (P_1 \cdot \Omega_M) \\ + w_2 v_1 (P_2 \cdot \Omega_1) + w_2 v_2 (P_2 \cdot \Omega_2) + \dots + w_2 v_M (P_2 \cdot \Omega_M) \\ \vdots \\ + w_N v_1 (P_N \cdot \Omega_1) + w_N v_2 (P_N \cdot \Omega_2) + \dots + w_N v_M (P_N \cdot \Omega_M) \end{cases}$$

In general,

- Given multi-points ρ_1 and ρ_2 , and multi-volume U , then:

$$(\rho_1 + \rho_2) \cdot U = \rho_1 \cdot U + \rho_2 \cdot U$$

- Given multi-point ρ , multi-volume U , and some real number c , then:

$$(c\rho) \cdot U = c(\rho \cdot U)$$

- Given multi-point ρ , and multi-volumes U_1 and U_2 , then:

$$\rho \cdot (U_1 + U_2) = \rho \cdot U_1 + \rho \cdot U_2$$

- Given multi-point ρ , multi-volume U , and some real number c , then:

$$\rho \cdot (cU) = c(\rho \cdot U)$$

An example of how the intersection of a multi-point and a multi-volume is the set of all pairwise intersections between the points and volumes will be given. On the right, the fact that the intersection consists of all pairs of intersections between points and volumes is illustrated with a simple example. There are two points P_1 and P_2 , and two volumes Ω_1 and Ω_2 . Points P_1 and P_2 are both contained in Ω_1 and Ω_2 . Consider the multi-point $\rho = P_1 + P_2$, and the multi-volume $U = \Omega_1 + \Omega_2$.

P_1 is contained in Ω_1 so $P_1 \cdot \Omega_1 = P_1$.

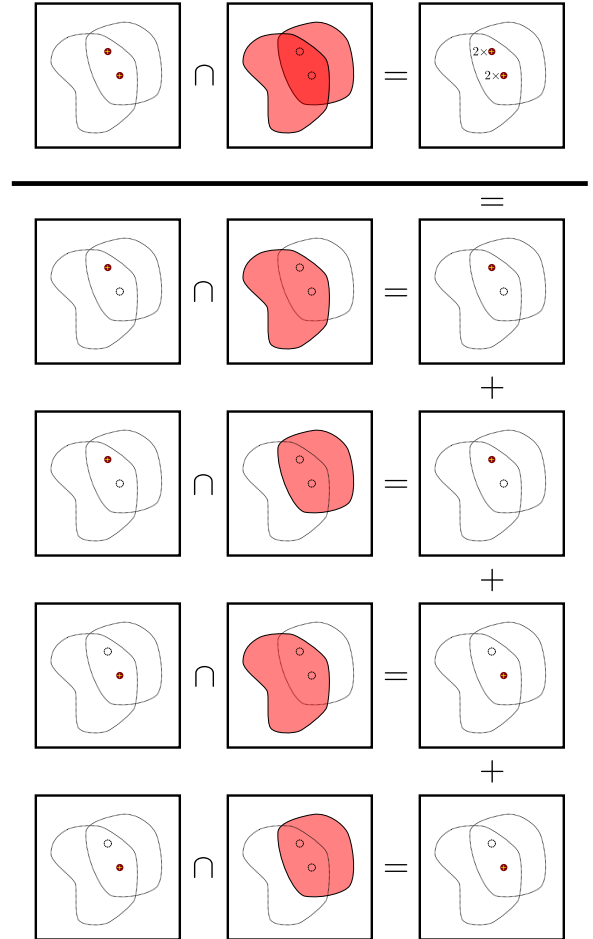
P_1 is contained in Ω_2 so $P_1 \cdot \Omega_2 = P_1$.

P_2 is contained in Ω_1 so $P_2 \cdot \Omega_1 = P_2$.

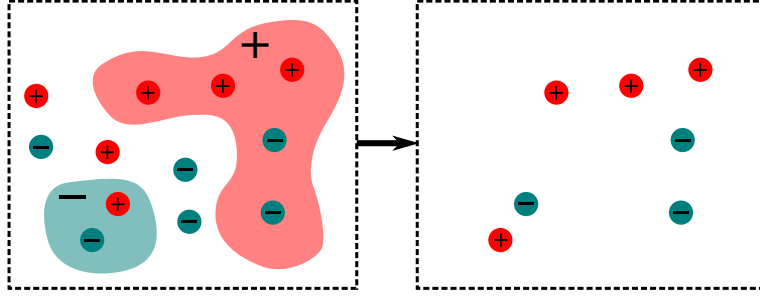
P_2 is contained in Ω_2 so $P_2 \cdot \Omega_2 = P_2$.

The total intersection of ρ with U consists of all of the pairwise intersections:

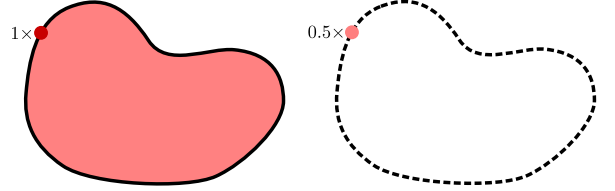
$$\rho \cdot U = P_1 + P_1 + P_2 + P_2 = 2P_1 + 2P_2$$



In the example below, the intersection between a multi-point and a multi-volume is illustrated. Note how the points that fall inside the negative volume have their polarities reversed.



If a point P with a weight of 1 lies on the edge of a volume with a weight of 1, then the intersection point P has a weight of 0.5.



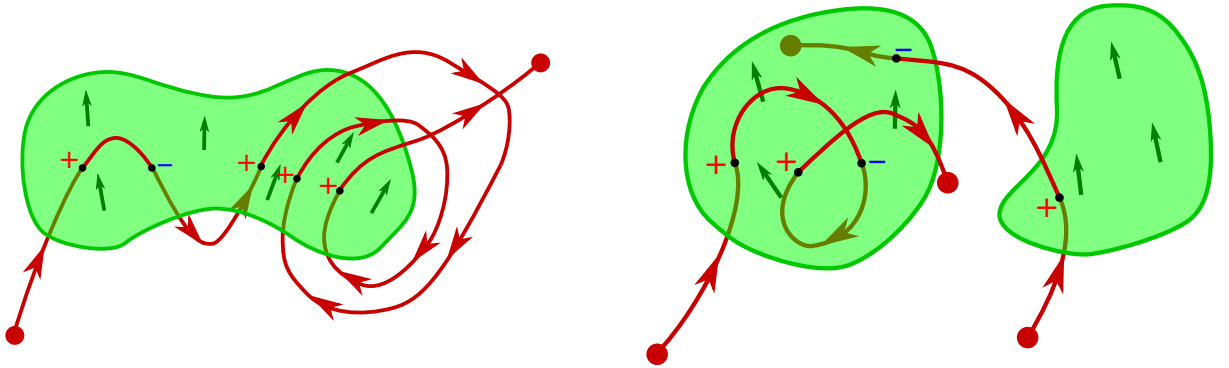
3.3 Path-surface intersections

Given a multi-path \mathbf{J} and a multi-surface \mathbf{F} , then the intersection between \mathbf{J} and \mathbf{F} is a multi-point and is denoted by:

$$\mathbf{J} \bullet \mathbf{F} \quad \text{or} \quad \mathbf{F} \bullet \mathbf{J}$$

An intersection occurs when a path pierces a surface. If a path with a weight of 1 pierces a surface with a weight of 1 in the preferred direction, then the intersection point has a weight of +1. If a path with a weight of 1 pierces a surface with a weight of 1 in the opposite direction, then the intersection point has a weight of -1. The “preferred direction” is when the path enters the surface from the back and emerges from the front. The opposite direction is when the path enters the surface from the front and emerges from the back.

In the examples below, the intersection points have a positive weight when the path intersects the surface in the preferred direction, and the intersection points have a negative weight when the path intersects the surface in the reverse direction.



If a path C with a nonnegative weight of w_1 intersects a surface σ with a nonnegative weight of w_2 in the **preferred direction** at point P , then for each of the w_2 copies of σ , w_1 copies of C are intersecting that copy. The total intersection is $w_1 \cdot w_2$ copies of P :

$$(w_1 C) \bullet (w_2 \sigma) = w_1 w_2 P$$

Contrariwise, if a path C with a weight of w_1 intersects a surface σ with a weight of w_2 in the **opposite direction** at point P , then for each of the w_2 copies of σ , w_1 copies of C are intersecting that copy in the opposite direction. The total intersection is $w_1 \cdot w_2$ copies of the anti-point $-P$:

$$(w_1 C) \bullet (w_2 \sigma) = -w_1 w_2 P$$

Given a multi-path $\mathbf{J} = w_1 C_1 + w_2 C_2 + \dots + w_N C_N$ and a multi-surface $\mathbf{F} = v_1 \sigma_1 + v_2 \sigma_2 + \dots + v_M \sigma_M$, then the intersection $\mathbf{J} \bullet \mathbf{F}$ is the set of all pairwise intersections of the paths and surfaces:

$$\mathbf{J} \bullet \mathbf{F} = \begin{cases} w_1 v_1 (C_1 \bullet \sigma_1) + w_1 v_2 (C_1 \bullet \sigma_2) + \dots + w_1 v_M (C_1 \bullet \sigma_M) \\ + w_2 v_1 (C_2 \bullet \sigma_1) + w_2 v_2 (C_2 \bullet \sigma_2) + \dots + w_2 v_M (C_2 \bullet \sigma_M) \\ \vdots \\ + w_N v_1 (C_N \bullet \sigma_1) + w_N v_2 (C_N \bullet \sigma_2) + \dots + w_N v_M (C_N \bullet \sigma_M) \end{cases}$$

In general,

- Given multi-paths \mathbf{J}_1 and \mathbf{J}_2 , and multi-surface \mathbf{F} , then:

$$(\mathbf{J}_1 + \mathbf{J}_2) \bullet \mathbf{F} = \mathbf{J}_1 \bullet \mathbf{F} + \mathbf{J}_2 \bullet \mathbf{F}$$

- Given multi-path \mathbf{J} , multi-surface \mathbf{F} , and some real number c , then:

$$(c\mathbf{J}) \bullet \mathbf{F} = c(\mathbf{J} \bullet \mathbf{F})$$

- Given multi-path \mathbf{J} , and multi-surfaces \mathbf{F}_1 and \mathbf{F}_2 , then:

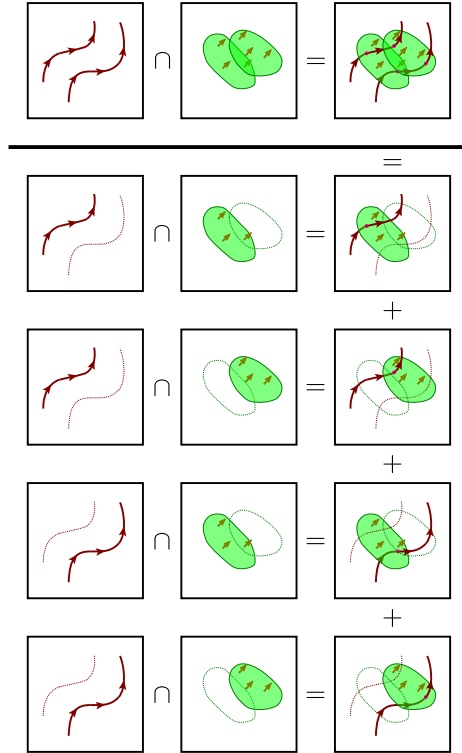
$$\mathbf{J} \bullet (\mathbf{F}_1 + \mathbf{F}_2) = \mathbf{J} \bullet \mathbf{F}_1 + \mathbf{J} \bullet \mathbf{F}_2$$

- Given multi-path \mathbf{J} , multi-surface \mathbf{F} , and some real number c , then:

$$\mathbf{J} \bullet (c\mathbf{F}) = c(\mathbf{J} \bullet \mathbf{F})$$

An example of how the intersection of a multi-path and a multi-surface is the set of all pairwise intersections between the paths and surfaces will be given. On the right, the fact that the intersection consists of all pairs of intersections between paths and surfaces is illustrated with a simple example. There are two oriented paths C_1 and C_2 , and two oriented surfaces σ_1 and σ_2 . Paths C_1 and C_2 both pass through σ_1 and σ_2 in the preferred direction. Consider the multi-path $\mathbf{J} = C_1 + C_2$, and the multi-surface $\mathbf{F} = \sigma_1 + \sigma_2$. The intersection of C_1 with σ_1 is a point $P_{1,1}$ so $C_1 \bullet \sigma_1 = P_{1,1}$. The intersection of C_1 with σ_2 is a point $P_{1,2}$ so $C_1 \bullet \sigma_2 = P_{1,2}$. The intersection of C_2 with σ_1 is a point $P_{2,1}$ so $C_2 \bullet \sigma_1 = P_{2,1}$. The intersection of C_2 with σ_2 is a point $P_{2,2}$ so $C_2 \bullet \sigma_2 = P_{2,2}$. The total intersection of \mathbf{J} with \mathbf{F} consists of all of the pairwise intersections:

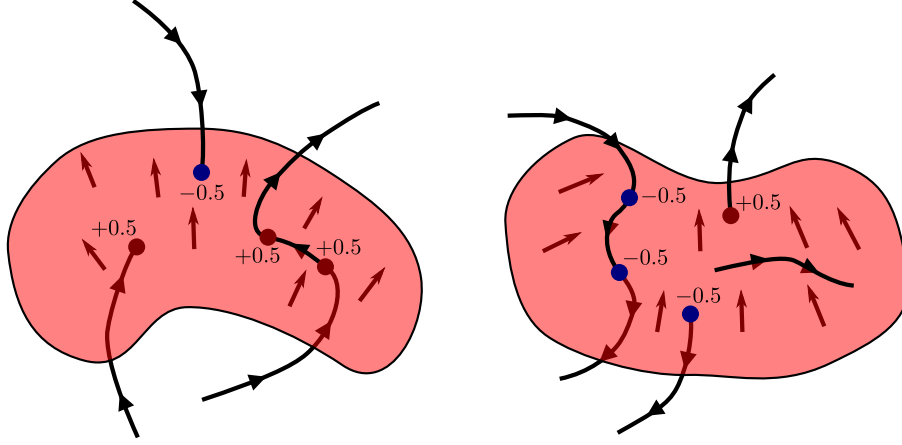
$$\mathbf{J} \bullet \mathbf{F} = P_{1,1} + P_{1,2} + P_{2,1} + P_{2,2}$$



If a path C fails to fully pass through a surface σ , then the weight of the intersection point is halved. **Paths that are embedded inside of surfaces do contribute any intersection points unless they enter or leave the surface.** It may be argued that all points along an embedded path should be counted as intersection points, but the counter argument is to ask what polarity these points should have.

If path C enters the back of σ and then continues inside of σ , then the point where C first touches σ has a weight of $+0.5$. If path C enters the front of σ and then continues inside of σ , then the point where C first touches σ has a weight of -0.5 .

If C is inside of σ and then exits the front of σ , then the exit point has a weight of $+0.5$. If C is inside of σ and then exits the back of σ , then the exit point has a weight of -0.5 .



Moreover, if the path C clips the boundary of σ , then the weight of the intersection point is also halved.

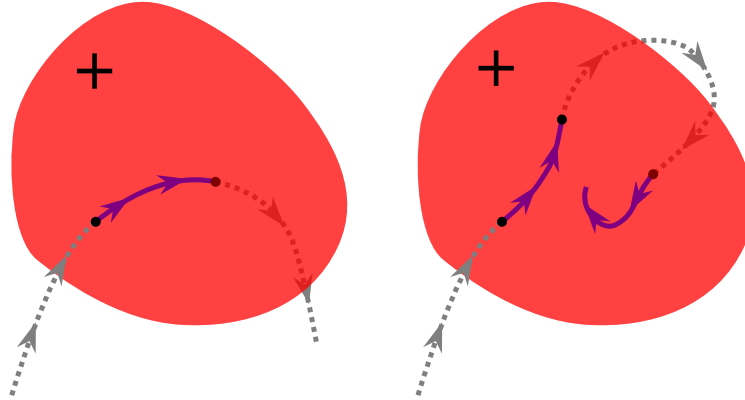
3.4 Path-volume intersections

Given a multi-path \mathbf{J} and a multi-volume U , then the intersection between \mathbf{J} and U is a multi-path and is denoted by:

$$\mathbf{J} \cdot U \quad \text{or} \quad \mathbf{J}U \quad \text{or} \quad U \cdot \mathbf{J} \quad \text{or} \quad U\mathbf{J}$$

Given an oriented path C , and a volume Ω , then the intersection is the sections of C that are contained in Ω . If the weight of Ω is negative, then the orientation of the intersection is reversed.

In the examples below, only sections of the path that are contained inside a volume are part of the intersection.



If a path C with a nonnegative weight of w_1 intersects a volume Ω with a weight of w_2 , and C' is the sections of C that are contained in Ω , then for each of the w_2 copies of Ω , w_1 copies of C are intersecting that copy. The total intersection is $w_1 \cdot w_2$ copies of C' :

$$(w_1 C) \cdot (w_2 \Omega) = w_1 w_2 C'$$

If the volume weight w_2 is negative, then both the orientation of C' and the sign of the weight $w_1 w_2$ is flipped.

Given a multi-path $\mathbf{J} = w_1 C_1 + w_2 C_2 + \dots + w_N C_N$ and a multi-volume $U = v_1 \Omega_1 + v_2 \Omega_2 + \dots + v_M \Omega_M$, then the intersection $\mathbf{J} \cdot U$ is the set of all pairwise intersections of the paths and volumes:

$$\mathbf{J} \cdot U = \begin{cases} w_1 v_1 (C_1 \cdot \Omega_1) + w_1 v_2 (C_1 \cdot \Omega_2) + \dots + w_1 v_M (C_1 \cdot \Omega_M) \\ + w_2 v_1 (C_2 \cdot \Omega_1) + w_2 v_2 (C_2 \cdot \Omega_2) + \dots + w_2 v_M (C_2 \cdot \Omega_M) \\ \vdots \\ + w_N v_1 (C_N \cdot \Omega_1) + w_N v_2 (C_N \cdot \Omega_2) + \dots + w_N v_M (C_N \cdot \Omega_M) \end{cases}$$

In general,

- Given multi-paths \mathbf{J}_1 and \mathbf{J}_2 , and multi-volume U , then:

$$(\mathbf{J}_1 + \mathbf{J}_2) \cdot U = \mathbf{J}_1 \cdot U + \mathbf{J}_2 \cdot U$$

- Given multi-path \mathbf{J} , multi-volume U , and some real number c , then:

$$(c\mathbf{J}) \cdot U = c(\mathbf{J} \cdot U)$$

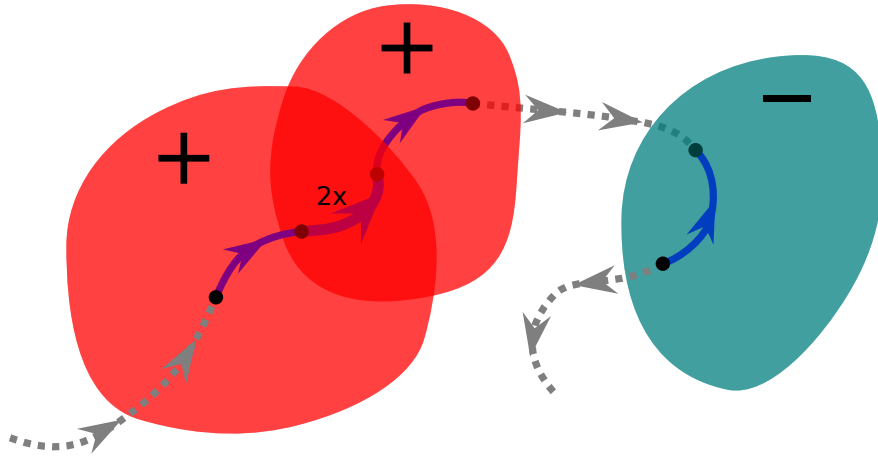
- Given multi-path \mathbf{J} , and multi-volumes U_1 and U_2 , then:

$$\mathbf{J} \cdot (U_1 + U_2) = \mathbf{J} \cdot U_1 + \mathbf{J} \cdot U_2$$

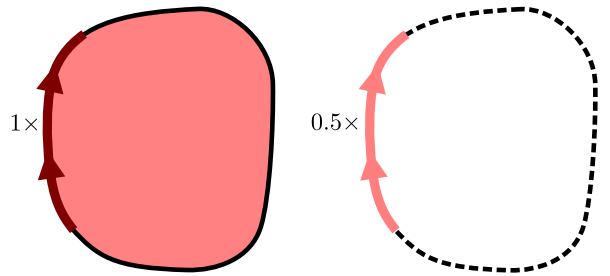
- Given multi-path \mathbf{J} , multi-volume U , and some real number c , then:

$$\mathbf{J} \cdot (cU) = c(\mathbf{J} \cdot U)$$

In the example below, the multi-volume U consists of three volumes. Two of the volumes have a weight of $+1$ and are overlapping, and the remaining separate volume has a weight of -1 . The multi-path \mathbf{J} consists of a single path that winds through each of the volumes. Outside of all of the volumes, the path is not part of the intersection. Where the path is passing through a single volume with a weight of $+1$, the intersection path from $\mathbf{J} \cdot U$ has a weight of $+1$. Where the path is passing through the overlap between the volumes with a weight of $+1$, then each volume contributes a copy of the intersection to $\mathbf{J} \cdot U$ so the weight of the path in $\mathbf{J} \cdot U$ is $+2$. Where the path is passing through the volume with a weight of -1 , the orientation of the intersection is reversed.



If a path C is on the surface of volume Ω , then the intersection is C with a weight of $+0.5$ as depicted on the right.



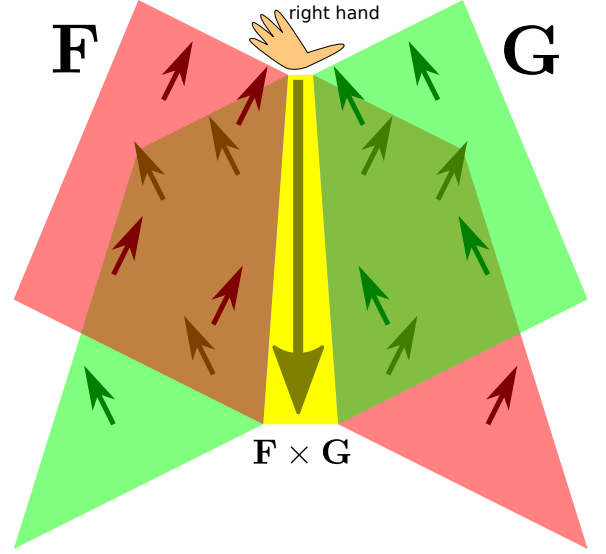
3.5 Surface-surface intersections

Given two multi-surfaces \mathbf{F}_1 and \mathbf{F}_2 , then the intersection between \mathbf{F}_1 and \mathbf{F}_2 is a multi-path and is denoted by:

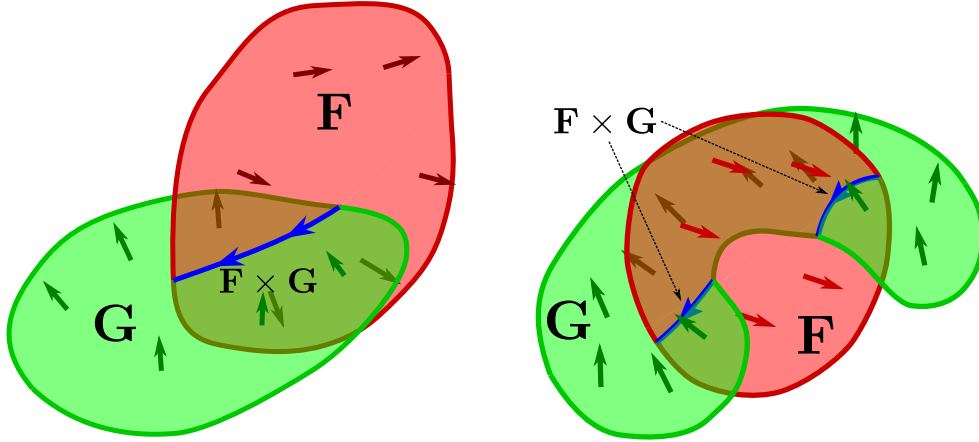
$$\mathbf{F}_1 \times \mathbf{F}_2$$

An intersection occurs when a surface slices into another surface along a curve. The orientation of the intersection curve is now to be determined.

Given two oriented surfaces σ_1 and σ_2 , the orientation of the intersection C can be determined as follows. Position your view point in the space that contains the front of σ_1 and σ_2 . When the σ_1 is on your left, and σ_2 is on your right, then the intersection is oriented towards you as depicted on the right. This is commonly referred to as the “righthand rule”.



Some examples are shown below:



Unlike other intersections, the “order” of the two surfaces impacts the orientation of the intersection path. If the order of the surfaces is reversed, then the orientation of the intersection path is also reversed:

$$\sigma_2 \cap \sigma_1 = -(\sigma_1 \cap \sigma_2)$$

so:

Theorem 1. *Given any multi-surfaces \mathbf{F}_1 and \mathbf{F}_2 , then:*

$$\mathbf{F}_2 \times \mathbf{F}_1 = -(\mathbf{F}_1 \times \mathbf{F}_2)$$

If a surface σ_1 with a nonnegative weight of w_1 intersects a surface σ_2 with a nonnegative weight of w_2 along the path C according to the righthand rule, then for each of the w_2 copies of σ_2 , w_1 copies of σ_1 are intersecting that copy. The total intersection is $w_1 \cdot w_2$ copies of C :

$$(w_1 \sigma_1) \times (w_2 \sigma_2) = w_1 w_2 C$$

Given multi-surfaces $\mathbf{F}_1 = w_1\sigma_1 + w_2\sigma_2 + \dots + w_N\sigma_N$ and $\mathbf{F}_2 = v_1\tau_1 + v_2\tau_2 + \dots + v_M\tau_M$, then the intersection $\mathbf{F}_1 \times \mathbf{F}_2$ is the set of all pairwise intersections of the surfaces:

$$\mathbf{F}_1 \times \mathbf{F}_2 = \begin{cases} w_1v_1(\sigma_1 \times \tau_1) + w_1v_2(\sigma_1 \times \tau_2) + \dots + w_1v_M(\sigma_1 \times \tau_M) \\ + w_2v_1(\sigma_2 \times \tau_1) + w_2v_2(\sigma_2 \times \tau_2) + \dots + w_2v_M(\sigma_2 \times \tau_M) \\ \vdots \\ + w_Nv_1(\sigma_N \times \tau_1) + w_Nv_2(\sigma_N \times \tau_2) + \dots + w_Nv_M(\sigma_N \times \tau_M) \end{cases}$$

In general,

- Given multi-surfaces \mathbf{F}_1 , \mathbf{F}_2 , and \mathbf{G} , then:

$$(\mathbf{F}_1 + \mathbf{F}_2) \times \mathbf{G} = \mathbf{F}_1 \times \mathbf{G} + \mathbf{F}_2 \times \mathbf{G}$$

- Given multi-surfaces \mathbf{F} and \mathbf{G} , and some real number c , then:

$$(c\mathbf{F}) \times \mathbf{G} = c(\mathbf{F} \times \mathbf{G})$$

- Given multi-surfaces \mathbf{F} , \mathbf{G}_1 , and \mathbf{G}_2 , then:

$$\mathbf{F} \times (\mathbf{G}_1 + \mathbf{G}_2) = \mathbf{F} \times \mathbf{G}_1 + \mathbf{F} \times \mathbf{G}_2$$

- Given multi-surfaces \mathbf{F} and \mathbf{G} , and some real number c , then:

$$\mathbf{F} \times (c\mathbf{G}) = c(\mathbf{F} \times \mathbf{G})$$

An example of how the intersection of two multi-surfaces is the set of all pairwise intersections between the surfaces will be given. On the right, the fact that the intersection consists of all pairs of intersections between surfaces from the two multi-surfaces is illustrated with a simple example. There are four oriented surfaces σ_1 , σ_2 (in the 1st column, and τ_1 , τ_2 (in the 2nd column). Surfaces σ_1 and σ_2 both slice into τ_1 and τ_2 . Consider the multi-surface $\mathbf{F}_1 = \sigma_1 + \sigma_2$, and the multi-surface $\mathbf{F}_2 = \tau_1 + \tau_2$.

The intersection of σ_1 with τ_1 is an oriented curve $C_{1,1}$ so $\sigma_1 \times \tau_1 = C_{1,1}$.

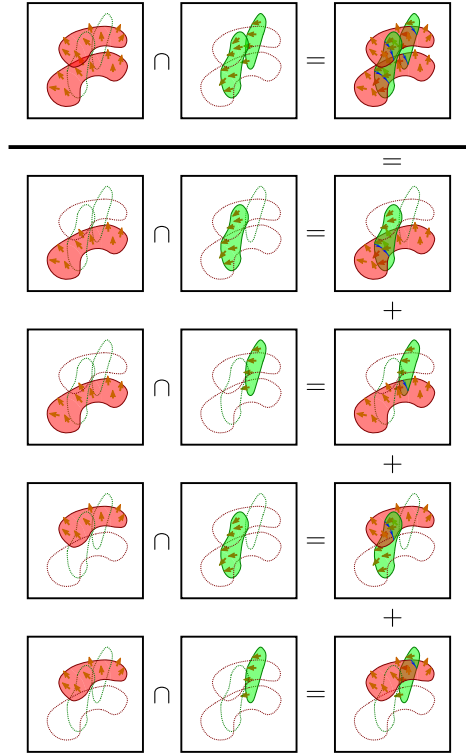
The intersection of σ_1 with τ_2 is an oriented curve $C_{1,2}$ so $\sigma_1 \times \tau_2 = C_{1,2}$.

The intersection of σ_2 with τ_1 is an oriented curve $C_{2,1}$ so $\sigma_2 \times \tau_1 = C_{2,1}$.

The intersection of σ_2 with τ_2 is an oriented curve $C_{2,2}$ so $\sigma_2 \times \tau_2 = C_{2,2}$.

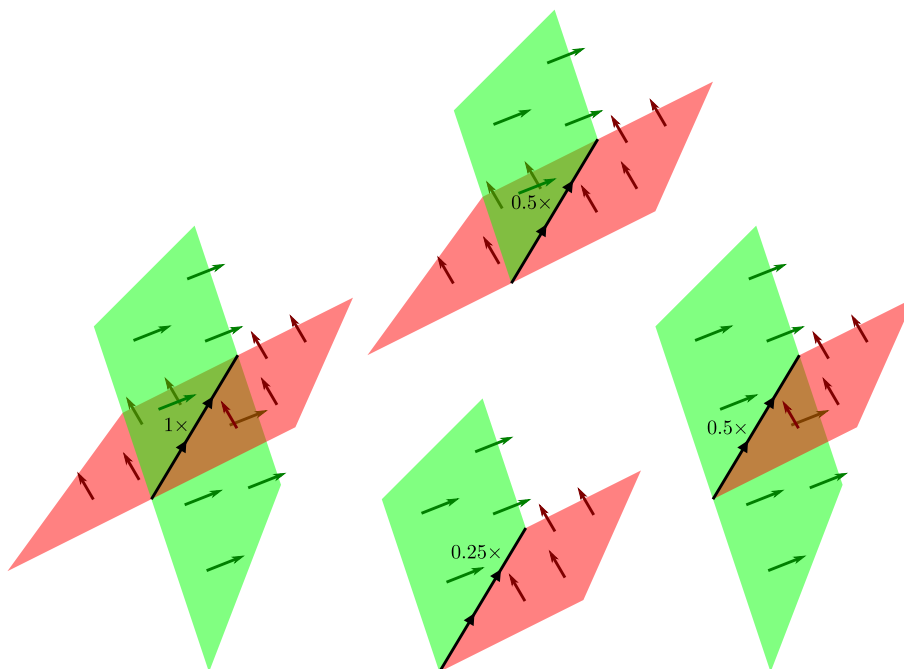
The total intersection of \mathbf{F}_1 with \mathbf{F}_2 consists of all of the pairwise intersections:

$$\mathbf{F}_1 \times \mathbf{F}_2 = C_{1,1} + C_{1,2} + C_{2,1} + C_{2,2}$$

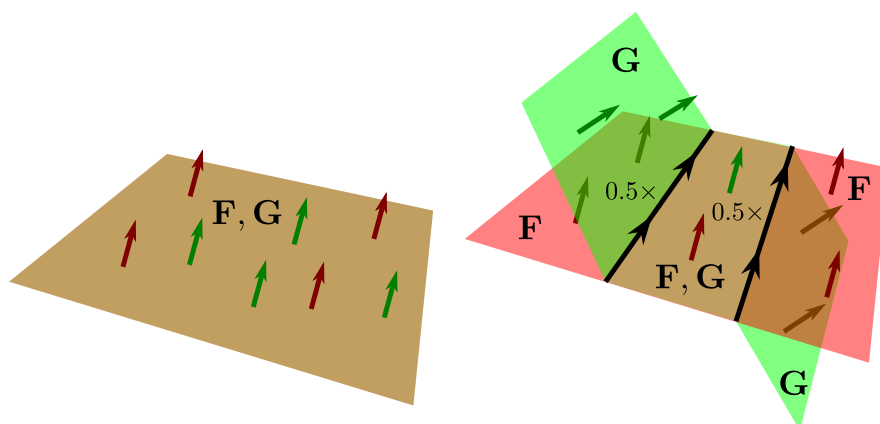


If one surface fails to fully pass through the other surface, then the weight of the intersection path is halved. Surfaces that are embedded inside of other surfaces do contribute any intersection paths unless they enter or leave the other surface.

Below are examples of surfaces intersecting each other but not fully passing through. Note the bottom example where both surfaces are truncated, so the intersection weight is further halved to 0.25.

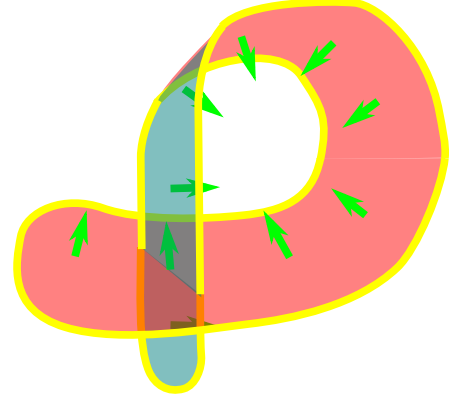


Two surfaces that are coincident do not slice through each other and therefore do not intersect. If \mathbf{F}_1 and \mathbf{F}_2 are the same flat surface as depicted below on the left, then these surfaces **do not intersect**: $\mathbf{F}_1 \times \mathbf{F}_2 = 0$. On the right, the curves where surface \mathbf{F}_2 peels away from \mathbf{F}_1 are intersection curves with weights of 0.5.



While a surface cannot intersect itself directly as explained above, a surface can still be folded over to explicitly slice through itself as depicted on the right. However, we will soon see that this type of intersection actually does not count, primarily since the intersection cannot be oriented in an objective manner. From a more mathematical perspective, consider the following: Let σ_1 and σ_2 be two flat surfaces that intersect each other, but with no self intersections that result from folding over. Let multi-surface \mathbf{G} be comprised of σ_1 and σ_2 :

$$\mathbf{G} = \sigma_1 + \sigma_2$$



The intersection of \mathbf{G} with itself is:

$$\mathbf{G} \times \mathbf{G} = (\sigma_1 + \sigma_2) \times (\sigma_1 + \sigma_2) = (\sigma_1 \times \sigma_1) + (\sigma_1 \times \sigma_2) + (\sigma_2 \times \sigma_1) + (\sigma_2 \times \sigma_2)$$

We've already established that for surfaces that do not have any self intersections from folding, do not intersect themselves in any other manner, so $\sigma_1 \times \sigma_1 = 0$ and $\sigma_2 \times \sigma_2 = 0$. It is also the case that reversing the order of σ_1 and σ_2 flips the orientation so $\sigma_2 \times \sigma_1 = -(\sigma_1 \times \sigma_2)$. Therefore:

$$\mathbf{G} \times \mathbf{G} = 0 + (\sigma_1 \times \sigma_2) + (\sigma_2 \times \sigma_1) + 0 = (\sigma_1 \times \sigma_2) - (\sigma_1 \times \sigma_2) = 0$$

In general, the intersection of a multi-surface with itself is always 0:

Theorem 2.

$$\mathbf{F} \times \mathbf{F} = 0$$

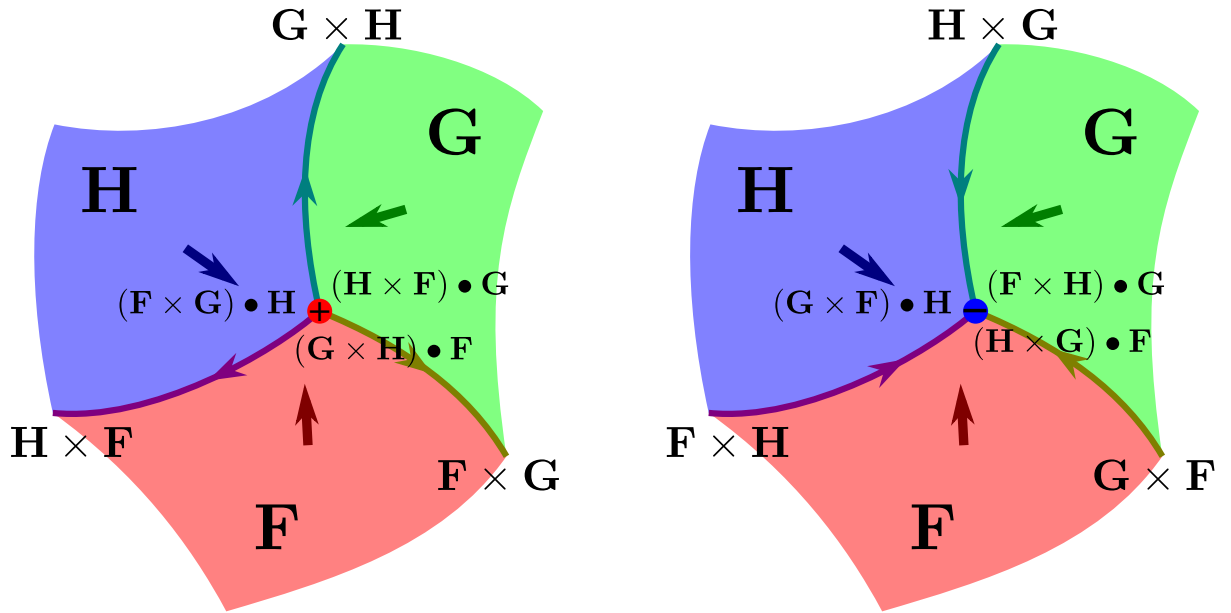
Lastly, 3 multi-surface surfaces intersect at a multi-point. Consider 3 multi-surfaces \mathbf{F} , \mathbf{G} , and \mathbf{H} . The intersection between \mathbf{F} and \mathbf{G} is the multi-path $\mathbf{F} \times \mathbf{G}$. The intersection between the multi-path $\mathbf{F} \times \mathbf{G}$ and multi-surface \mathbf{H} is the multi-point $(\mathbf{F} \times \mathbf{G}) \bullet \mathbf{H}$. This intersection can also be generated by computing the intersection of \mathbf{G} and \mathbf{H} first, or the intersection of \mathbf{H} and \mathbf{F} first:

$$(\mathbf{F} \times \mathbf{G}) \bullet \mathbf{H} = (\mathbf{G} \times \mathbf{H}) \bullet \mathbf{F} = (\mathbf{H} \times \mathbf{F}) \bullet \mathbf{G}$$

Note that swapping any two surfaces in the above intersections flips the polarity of the intersection point:

Theorem 3.

$$\begin{aligned} (\mathbf{F} \times \mathbf{G}) \bullet \mathbf{H} &= (\mathbf{G} \times \mathbf{H}) \bullet \mathbf{F} = (\mathbf{H} \times \mathbf{F}) \bullet \mathbf{G} \\ &= -(\mathbf{G} \times \mathbf{F}) \bullet \mathbf{H} = -(\mathbf{H} \times \mathbf{G}) \bullet \mathbf{F} = -(\mathbf{F} \times \mathbf{H}) \bullet \mathbf{G} \end{aligned}$$



It was previously noted that a path only “intersects” a surface when it decisively passes through the surface, and that paths that are embedded within surfaces do not contribute any intersection points. Since the intersection path $\mathbf{F} \times \mathbf{G}$ is embedded in surfaces \mathbf{F} and \mathbf{G} , then contrary to intuition, there is no intersection of $\mathbf{F} \times \mathbf{G}$ with either \mathbf{F} or \mathbf{G} :

Theorem 4.

$$\mathbf{F} \bullet (\mathbf{F} \times \mathbf{G}) = 0 \quad \text{and} \quad \mathbf{G} \bullet (\mathbf{F} \times \mathbf{G}) = 0$$

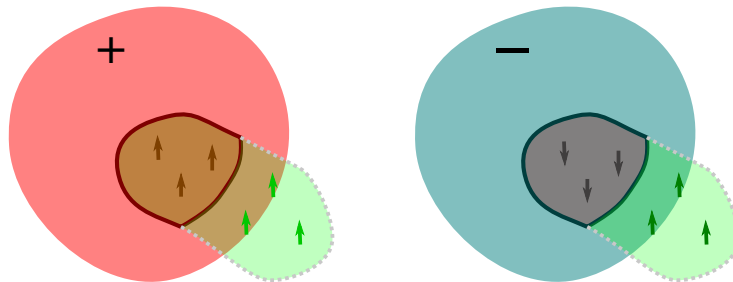
3.6 Surface-volume intersections

Given a multi-surface \mathbf{F} and a multi-volume U , then the intersection between \mathbf{F} and U is a multi-surface and is denoted by:

$$\mathbf{F} \cdot U \quad \text{or} \quad \mathbf{F}U \quad \text{or} \quad U \cdot \mathbf{F} \quad \text{or} \quad U\mathbf{F}$$

Given an oriented surface σ , and a volume Ω , then the intersection is the sections of σ that are contained in Ω . If the weight of Ω is negative, then the orientation of the intersection is reversed.

In the examples below, only sections of the surface that are contained inside a volume are part of the intersection. In the example on the right, because the volume of weight is negative, the orientation is reversed



If a surface σ with a nonnegative weight of w_1 intersects a volume Ω with a weight of w_2 and σ' is the sections of σ that are contained in Ω , then for each of the w_2 copies of Ω , w_1 copies of σ are intersecting that copy. The total intersection is $w_1 \cdot w_2$ copies of σ' :

$$(w_1\sigma) \cdot (w_2\Omega) = w_1w_2\sigma'$$

If the volume weight w_2 is negative, then both the orientation of σ' and the sign of the weight w_1w_2 is flipped.

Given a multi-surface $\mathbf{F} = w_1\sigma_1 + w_2\sigma_2 + \dots + w_N\sigma_N$ and a multi-volume $U = v_1\Omega_1 + v_2\Omega_2 + \dots + v_M\Omega_M$, then the intersection $\mathbf{F} \cdot U$ is the set of all pairwise intersections of the surfaces and volumes:

$$\mathbf{F} \cdot U = \begin{cases} w_1v_1(\sigma_1 \cdot \Omega_1) + w_1v_2(\sigma_1 \cdot \Omega_2) + \dots + w_1v_M(\sigma_1 \cdot \Omega_M) \\ + w_2v_1(\sigma_2 \cdot \Omega_1) + w_2v_2(\sigma_2 \cdot \Omega_2) + \dots + w_2v_M(\sigma_2 \cdot \Omega_M) \\ \vdots \\ + w_Nv_1(\sigma_N \cdot \Omega_1) + w_Nv_2(\sigma_N \cdot \Omega_2) + \dots + w_Nv_M(\sigma_N \cdot \Omega_M) \end{cases}$$

In general,

- Given multi-surfaces \mathbf{F}_1 and \mathbf{F}_2 , and multi-volume U , then:

$$(\mathbf{F}_1 + \mathbf{F}_2) \cdot U = \mathbf{F}_1 \cdot U + \mathbf{F}_2 \cdot U$$

- Given multi-surface \mathbf{F} , multi-volume U , and some real number c , then:

$$(c\mathbf{F}) \cdot U = c(\mathbf{F} \cdot U)$$

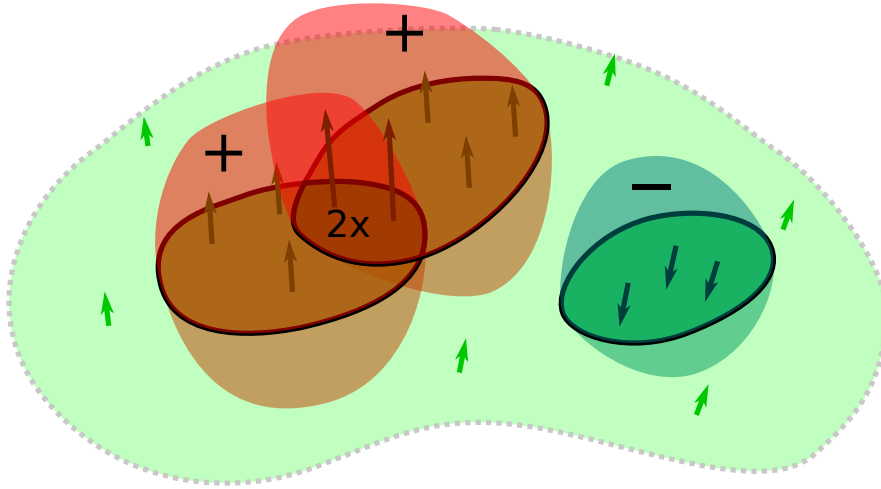
- Given multi-surface \mathbf{F} , and multi-volumes U_1 and U_2 , then:

$$\mathbf{F} \cdot (U_1 + U_2) = \mathbf{F} \cdot U_1 + \mathbf{F} \cdot U_2$$

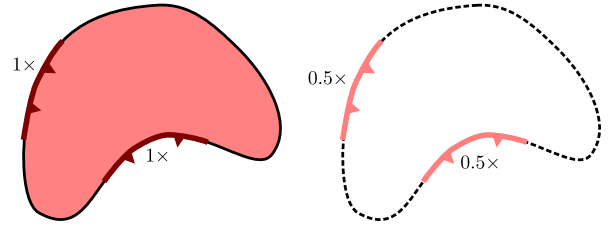
- Given multi-surface \mathbf{F} , multi-volume U , and some real number c , then:

$$\mathbf{F} \cdot (cU) = c(\mathbf{F} \cdot U)$$

In the example below, the multi-volume U consists of three volumes. Two of the volumes have a weight of +1 and are overlapping, and the remaining separate volume has a weight of -1 . The multi-path \mathbf{F} consists of a single surface that slices through all of the volumes. Outside of all of the volumes, the surface is not part of the intersection. Where the surface is inside a single volume with a weight of +1, the intersection surface from $\mathbf{F} \cdot U$ has a weight of +1. Where the surface is inside the overlap between the volumes with a weight of +1, then each volume contributes a copy of the intersection to $\mathbf{F} \cdot U$ so the weight of the surface in $\mathbf{F} \cdot U$ is +2. Where the surface is inside the volume with a weight of -1 , the orientation of the intersection is reversed.



If a surface σ is on the surface of volume Ω , then the intersection is σ with a weight of $+0.5$ as depicted on the right.



3.7 Volume-volume intersections

Given two multi-volumes U_1 and U_2 , then the intersection between U_1 and U_2 is a multi-volume and is denoted by:

$$U_1 \cdot U_2 \quad \text{or} \quad U_1 U_2$$

Given volumes Ω_1 and Ω_2 , then the intersection is the sections of Ω_1 and Ω_2 that overlap.

If a volume Ω_1 with a weight of w_1 intersects a volume Ω_2 with a weight of w_2 and Ω' is the sections of Ω_1 and Ω_2 that overlap, then for each of the w_2 copies of Ω_2 , w_1 copies of Ω_1 are intersecting that copy. The total intersection is $w_1 \cdot w_2$ copies of Ω' :

$$(w_1 \Omega_1) \cdot (w_2 \Omega_2) = w_1 w_2 \Omega'$$

Given multi-volumes $U_1 = w_1 \Omega_1 + w_2 \Omega_2 + \dots + w_N \Omega_N$ and $U_2 = v_1 \Phi_1 + v_2 \Phi_2 + \dots + v_M \Phi_M$, then the intersection $U_1 \cdot U_2$ is the set of all pairwise intersections of the volumes:

$$U_1 \cdot U_2 = \begin{cases} w_1 v_1 (\Omega_1 \cdot \Phi_1) + w_1 v_2 (\Omega_1 \cdot \Phi_2) + \dots + w_1 v_M (\Omega_1 \cdot \Phi_M) \\ + w_2 v_1 (\Omega_2 \cdot \Phi_1) + w_2 v_2 (\Omega_2 \cdot \Phi_2) + \dots + w_2 v_M (\Omega_2 \cdot \Phi_M) \\ \vdots \\ + w_N v_1 (\Omega_N \cdot \Phi_1) + w_N v_2 (\Omega_N \cdot \Phi_2) + \dots + w_N v_M (\Omega_N \cdot \Phi_M) \end{cases}$$

In general,

- Given multi-volumes U_1 , U_2 , and V , then:

$$(U_1 + U_2) \cdot V = U_1 \cdot V + U_2 \cdot V$$

- Given multi-volumes U and V , and some real number c , then:

$$(cU) \cdot V = c(U \cdot V)$$

- Given multi-volumes U , V_1 , and V_2 , then:

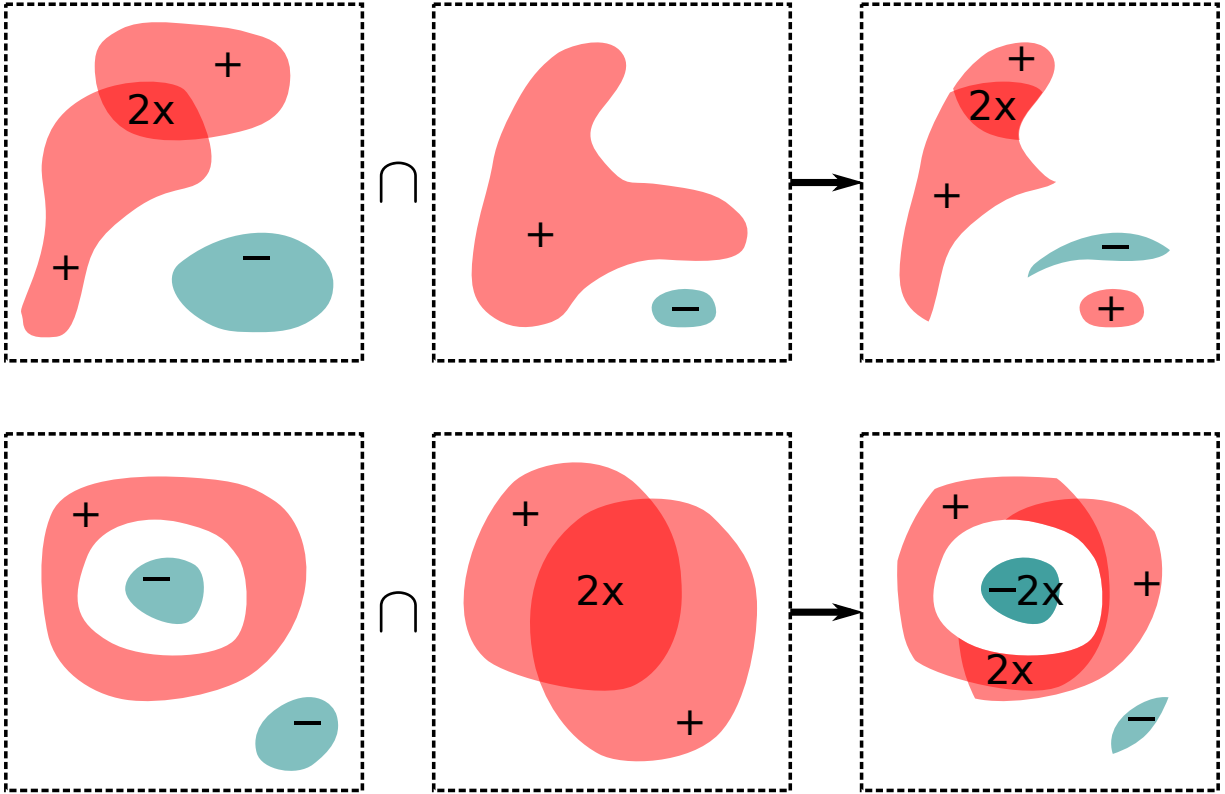
$$U \cdot (V_1 + V_2) = U \cdot V_1 + U \cdot V_2$$

- Given multi-volumes U and V , and some real number c , then:

$$U \cdot (cV) = c(U \cdot V)$$

Some examples of intersecting multi-volumes are shown below. Note that for a specific point \mathbf{q} , that the net number of volumes that contain \mathbf{q} in the intersection $U_1 \cdot U_2$ will always be the product of the net number of volumes that contain \mathbf{q} in each of U_1 and U_2 :

$$(U_1 \cdot U_2)(\mathbf{q}) = U_1(\mathbf{q}) \cdot U_2(\mathbf{q})$$

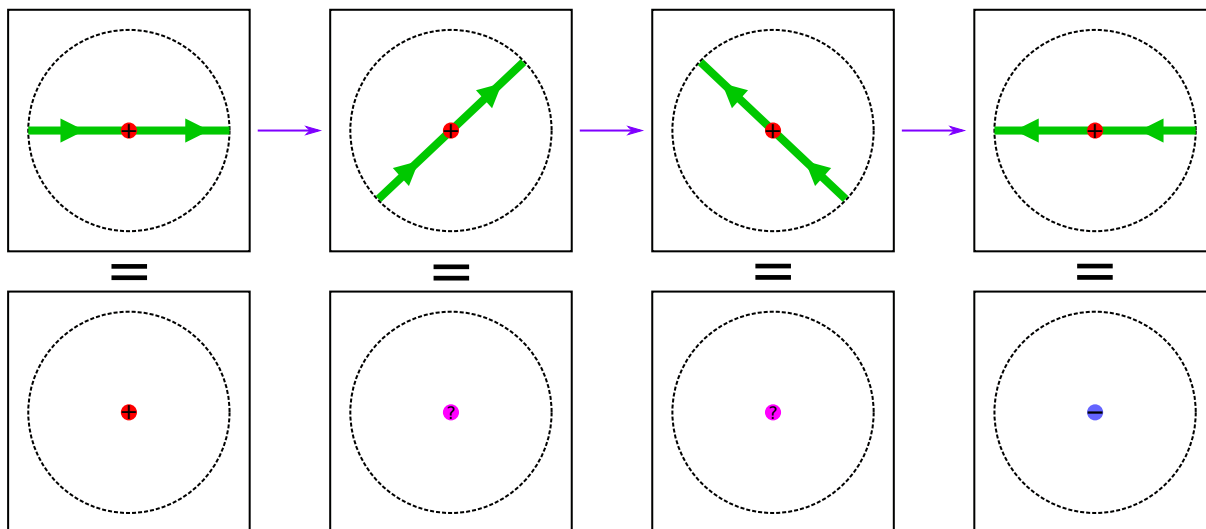


3.8 Intersections that are not being considered

What about the following other types of intersections? Namely point-point intersections, point-path intersections, point-surface intersections, and path-path intersections? With the exception of point-point intersections, these intersections cannot be oriented as will be discussed:

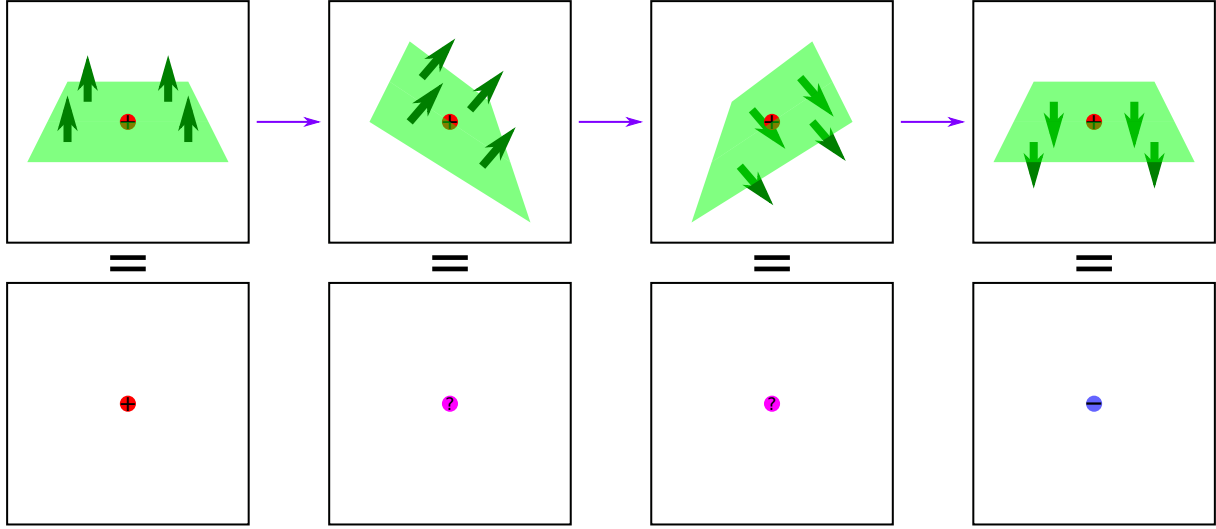
3.8.1 Point-path intersections

Why can't point-path intersections be oriented? Let P be a point and let C be an oriented path, where point P lies on C . Let the weights of P and C both be 1. What weight should point P have in the intersection? Should the orientation of C be reversed, the sign of the weight should also be flipped. Now slowly rotate C around while maintaining the intersection as depicted below. No matter the direction in which C passes through P the weight should ideally remain constant as all directions are equal. The question is at what point during the rotation does the sign of the weight flip? The answer is that the weight should always be 0, and the intersection does not exist.



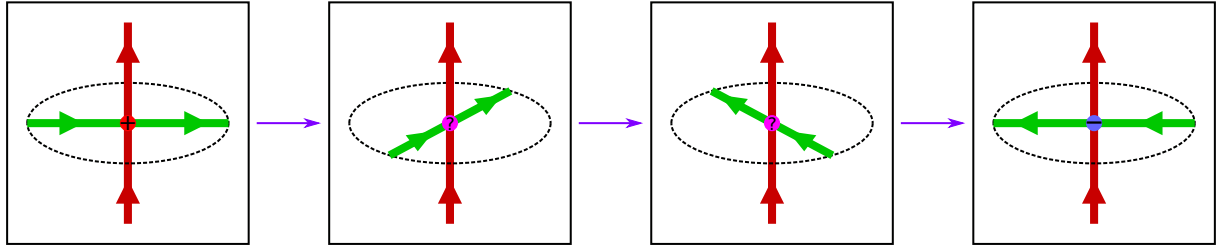
3.8.2 Point-surface intersections

Why can't point-surface intersections be oriented? Let P be a point and let σ be an oriented surface, where point P lies on σ . Let the weights of P and σ both be 1. What weight should point P have in the intersection? Should the orientation of σ be reversed, the sign of the weight should also be flipped. Now slowly rotate σ around while maintaining the intersection as depicted below. No matter the direction in which σ faces as it passes through P the weight should ideally remain constant as all directions are equal. The question is at what point during the rotation does the sign of the weight flip? The answer is that the weight should always be 0, and the intersection does not exist.



3.8.3 Path-path intersections

Why can't path-path intersections be oriented? Let C_1 and C_2 be oriented paths that intersect at point P . Let the weights of C_1 and C_2 both be 1. What weight should point P have in the intersection? Should the orientation of C_1 xor C_2 be reversed, the sign of the weight should also be flipped. Now slowly rotate C_2 around while maintaining the intersection as depicted below. Also, at no point during the rotation C_2 will have the same direction of C_1 . No matter the direction in which C_2 intersects C_1 the weight should ideally remain constant as all directions are equal (except if C_1 and C_2 share the same direction). The question is at what point during the rotation does the sign of the weight flip? The answer is that the weight should always be 0, and the intersection does not exist.



3.9 Summary

A summary of the notations used for various intersections is given below:

| Intersections | point ρ_2 {0} | path \mathbf{J}_2 {1} | surface \mathbf{F}_2 {2} | volume U_2 {3} |
|----------------------------|------------------------------|---|---|--------------------------------------|
| point ρ_1 {0} | N/A | N/A | N/A | point $\rho_1 \cdot U_2$ {0} |
| path \mathbf{J}_1 {1} | N/A | N/A | point $\mathbf{J}_1 \bullet \mathbf{F}_2$ {0} | path $\mathbf{J}_1 \cdot U_2$ {1} |
| surface \mathbf{F}_1 {2} | N/A | point $\mathbf{F}_1 \bullet \mathbf{J}_2$ {0} | path $\mathbf{F}_1 \times \mathbf{F}_2$ {1} | surface $\mathbf{F}_1 \cdot U_2$ {2} |
| volume U_1 {3} | point $U_1 \cdot \rho_2$ {0} | path $U_1 \cdot \mathbf{J}_2$ {1} | surface $U_1 \cdot \mathbf{F}_2$ {2} | volume $U_1 \cdot U_2$ {3} |

In red is indicated the “dimensionality” of the multi-structure. Points have 0 dimensions; paths have 1

dimension; surfaces have 2 dimensions; and volumes have 3 dimensions. The number of dimensions of the intersection is the sum of the dimensions minus 3. When the resultant number of dimensions is less than 0, the intersection does not exist.

Chapter 4

Boundaries

Now will be discussed are the multi-structures that constitute the boundaries of other multi-structures. There will be the endpoints of multi-paths, the boundaries of multi-surfaces, and the surfaces of multi-volumes. Throughout the discussion the symbol “ ∇ ”, referred to as a “nabla”, will see frequent use. One possible interpretation of ∇ is:

$$\nabla = \text{“the inwards oriented surface of reality”}$$

By “inwards oriented surface of reality”, reality is in “front” of ∇ , and “un-reality” is behind ∇ . ∇ is **not an actual 2D surface**, but this interpretation is useful regardless.

4.1 Point totals

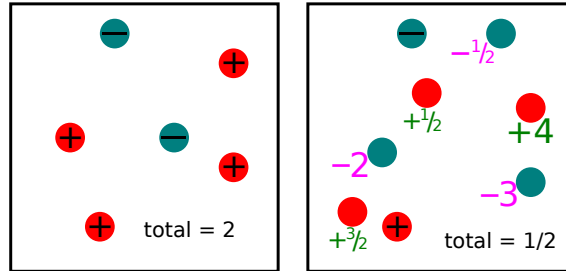
Given a multi-point ρ , the total sum of the weights of all of the points that comprise ρ is denoted by:

$$\int \rho$$

The elongated S , \int , literally stands for sum.

If $\rho = w_1 P_1 + w_2 P_2 + \dots + w_N P_N$ where P_1, P_2, \dots, P_N are single points, then

$$\int \rho = \int (w_1 P_1 + w_2 P_2 + \dots + w_N P_N) = w_1 + w_2 + \dots + w_N$$



4.1.1 Scanning for equivalence

In chapter 1, descriptions of what it means for two multi-structures to be equivalent were briefly given.

- Two multi-points ρ_1 and ρ_2 are equivalent if and only if the collections of constituent points are equivalent with identical weights.
- Two multi-paths \mathbf{J}_1 and \mathbf{J}_2 are equivalent if and only if the networks of oriented paths are equivalent, regardless of how the network is broken up into individual oriented paths. Within the same multi-path, path sections with opposite orientations cancel each other out.
- Two multi-surfaces \mathbf{F}_1 and \mathbf{F}_2 are equivalent if and only if the networks of oriented surfaces are equivalent, regardless of how the network is broken up into individual oriented surfaces. Within the same multi-surface, surface sections with opposite orientations cancel each other out.
- Two multi-volumes U_1 and U_2 are equivalent if and only if at every position \mathbf{q} , the net number of volumes from U_1 that contain \mathbf{q} is equal to the net number of volumes from U_2 that contain \mathbf{q} . Negative volumes subtract from the number of volumes that contain \mathbf{q} .

The equivalence of two multi-structures can alternately be determined by moving around a small “scanning window” and then comparing the total intersection point weights found within the scanning window. If the numbers of detected intersection points are equivalent between the two multi-structures no matter the choice of scanning window, then the two multi-structures must be equivalent. This is elaborated in more detail below

Scanning multi-points

Two multi-points can be determined to be equal by “scanning” for differences between the two multi-points using a small volume “scanning window”. Let ρ denote an arbitrary multi-point. If U is a tiny single volume, then $\int(\rho \cdot U)$ is the number of points (weighted accordingly) from ρ that are found within the tiny “scanning window” U . By moving the scanning window U around as well as adjusting the size, and then computing $\int(\rho \cdot U)$, the constituent points from ρ can effectively be “felt” for, and differences between the multi-points identified.

Theorem 5. *If ρ_1 and ρ_2 are equivalent multi-points: $\rho_1 = \rho_2$, then for any choice of multi-volume U ,*

$$\int(\rho_1 \cdot U) = \int(\rho_2 \cdot U)$$

Conversely, if ρ_1 and ρ_2 are multi-points, but it is instead known that for any choice of multi-volume U that $\int(\rho_1 \cdot U) = \int(\rho_2 \cdot U)$, then ρ_1 and ρ_2 are in fact equivalent:

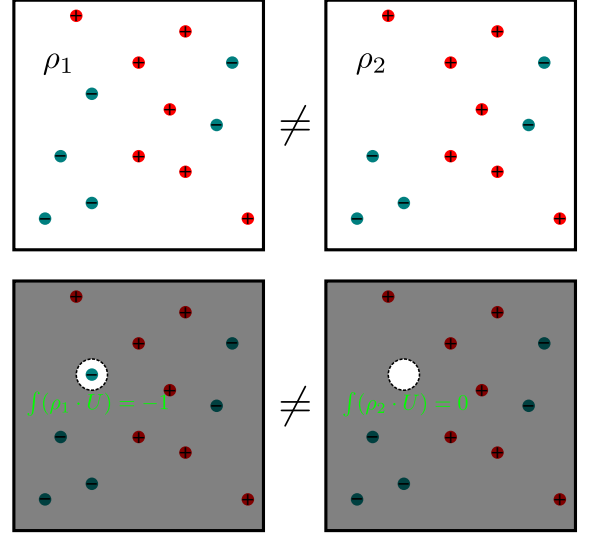
$$\rho_1 = \rho_2$$

Proof:

If $\rho_1 = \rho_2$, then it is fairly obvious from the equivalence of ρ_1 and ρ_2 that $\int(\rho_1 \cdot U) = \int(\rho_2 \cdot U)$ for all choices of multi-volume U .

With respect to the converse, assume that $\rho_1 \neq \rho_2$. Since $\rho_1 \neq \rho_2$, there must exist some point in ρ_1 that has a different weight, possibly 0, in ρ_2 . There will then exist some small scanning window U that wraps the point in question, and captures a different amount of point weight in ρ_1 than in ρ_2 .

In the image on the right, the difference between ρ_1 and ρ_2 is targeted by the scanning window U . A different amount of point weight is captured by U for ρ_1 and ρ_2 , so $\int(\rho_1 \cdot U) \neq \int(\rho_2 \cdot U)$.



□

Scanning multi-paths

Two multi-paths can be determined to be equal by “scanning” for differences between the two multi-paths using a small surface “scanning window”. Let \mathbf{J} denote an arbitrary multi-path. If \mathbf{F} is a tiny single surface, then $\int(\mathbf{J} \bullet \mathbf{F})$ is the number of intersection points (weighted accordingly) resulting from \mathbf{J} intersecting the tiny “scanning window” \mathbf{F} . By moving the scanning window \mathbf{F} around as well as adjusting the size, and then computing $\int(\mathbf{J} \bullet \mathbf{F})$, the constituent paths from \mathbf{J} can effectively be “felt” for, and differences between the multi-paths identified.

Theorem 6. *If \mathbf{J}_1 and \mathbf{J}_2 are equivalent multi-paths: $\mathbf{J}_1 = \mathbf{J}_2$, then for any choice of multi-surface \mathbf{F} ,*

$$\int(\mathbf{J}_1 \bullet \mathbf{F}) = \int(\mathbf{J}_2 \bullet \mathbf{F})$$

Conversely, if \mathbf{J}_1 and \mathbf{J}_2 are multi-paths, but it is instead known that for any choice of multi-surface \mathbf{F} that $\int(\mathbf{J}_1 \bullet \mathbf{F}) = \int(\mathbf{J}_2 \bullet \mathbf{F})$, then \mathbf{J}_1 and \mathbf{J}_2 are in fact equivalent:

$$\mathbf{J}_1 = \mathbf{J}_2$$

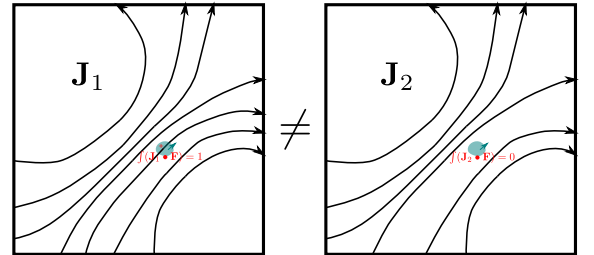
Proof:

If $\mathbf{J}_1 = \mathbf{J}_2$, then it is fairly obvious from the equivalence of \mathbf{J}_1 and \mathbf{J}_2 that $\int(\mathbf{J}_1 \bullet \mathbf{F}) = \int(\mathbf{J}_2 \bullet \mathbf{F})$ for all choices of multi-surface \mathbf{F} .

With respect to the converse, assume that $\mathbf{J}_1 \neq \mathbf{J}_2$. Since $\mathbf{J}_1 \neq \mathbf{J}_2$, there must exist some path in \mathbf{J}_1 that has a different weight, possibly 0, or a different shape in \mathbf{J}_2 . There will then exist some small scanning window \mathbf{F} that intersects the path in question, and records a different amount of intersection point weight from \mathbf{J}_1 than from \mathbf{J}_2 .

In the image on the right, the difference between \mathbf{J}_1 and \mathbf{J}_2 is targeted by the scanning window \mathbf{F} . A different amount of intersection point weight is captured by \mathbf{F} for \mathbf{J}_1 and \mathbf{J}_2 , so $\int(\mathbf{J}_1 \bullet \mathbf{F}) \neq \int(\mathbf{J}_2 \bullet \mathbf{F})$.

□



Scanning multi-surfaces

Two multi-surfaces can be determined to be equal by “scanning” for differences between the two multi-surfaces using a small path “scanning window”. Let \mathbf{F} denote an arbitrary multi-surface. If \mathbf{J} is a tiny single path, then $\int(\mathbf{F} \bullet \mathbf{J})$ is the number of intersection points (weighted accordingly) resulting from \mathbf{F} intersecting the tiny “scanning window” \mathbf{J} . By moving the scanning window \mathbf{J} around as well as adjusting the length, and then computing $\int(\mathbf{F} \bullet \mathbf{J})$, the constituent surfaces from \mathbf{F} can effectively be “felt” for, and differences between the multi-surfaces identified.

Theorem 7. *If \mathbf{F}_1 and \mathbf{F}_2 are equivalent multi-surfaces: $\mathbf{F}_1 = \mathbf{F}_2$, then for any choice of multi-path \mathbf{J} ,*

$$\int(\mathbf{F}_1 \bullet \mathbf{J}) = \int(\mathbf{F}_2 \bullet \mathbf{J})$$

Conversely, if \mathbf{F}_1 and \mathbf{F}_2 are multi-surfaces, but it is instead known that for any choice of multi-path \mathbf{J} that $\int(\mathbf{F}_1 \bullet \mathbf{J}) = \int(\mathbf{F}_2 \bullet \mathbf{J})$, then \mathbf{F}_1 and \mathbf{F}_2 are in fact equivalent:

$$\mathbf{F}_1 = \mathbf{F}_2$$

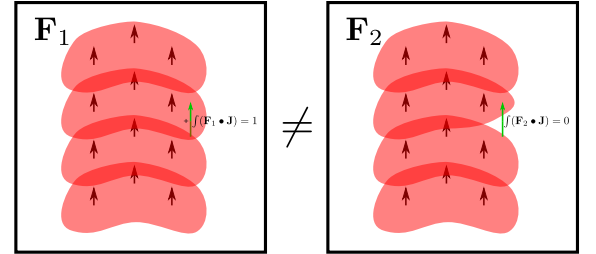
Proof:

If $\mathbf{F}_1 = \mathbf{F}_2$, then it is fairly obvious from the equivalence of \mathbf{F}_1 and \mathbf{F}_2 that $\int(\mathbf{F}_1 \bullet \mathbf{J}) = \int(\mathbf{F}_2 \bullet \mathbf{J})$ for all choices of multi-path \mathbf{J} .

With respect to the converse, assume that $\mathbf{F}_1 \neq \mathbf{F}_2$. Since $\mathbf{F}_1 \neq \mathbf{F}_2$, there must exist some surface in \mathbf{F}_1 that has a different weight, possibly 0, or a different shape in \mathbf{F}_2 . There will then exist some small scanning window \mathbf{J} that intersects the surface in question, and records a different amount of intersection point weight from \mathbf{F}_1 than from \mathbf{F}_2 .

In the image on the right, the difference between \mathbf{F}_1 and \mathbf{F}_2 is targeted by the scanning window \mathbf{J} . A different amount of intersection point weight is captured by \mathbf{J} for \mathbf{F}_1 and \mathbf{F}_2 , so $\int(\mathbf{F}_1 \bullet \mathbf{J}) \neq \int(\mathbf{F}_2 \bullet \mathbf{J})$.

□



Scanning multi-volumes

Two multi-volumes can be determined to be equal by “scanning” for differences between the two multi-volumes using “point probes”. Let U denote an arbitrary multi-volume. If ρ is a single point, then $\int(U \cdot \rho)$ is the number of volumes (weighted accordingly) from U that contain the probe ρ . By moving the probe ρ around, and then computing $\int(U \cdot \rho)$, the constituent volumes from U can effectively be “felt” for, and differences between the multi-volumes identified.

Theorem 8. *If U_1 and U_2 are equivalent multi-volumes: $U_1 = U_2$, then for any choice of multi-point ρ ,*

$$\int(U_1 \cdot \rho) = \int(U_2 \cdot \rho)$$

Conversely, if U_1 and U_2 are multi-volumes, but it is instead known that for any choice of multi-point ρ that $\int(U_1 \cdot \rho) = \int(U_2 \cdot \rho)$, then U_1 and U_2 are in fact equivalent:

$$U_1 = U_2$$

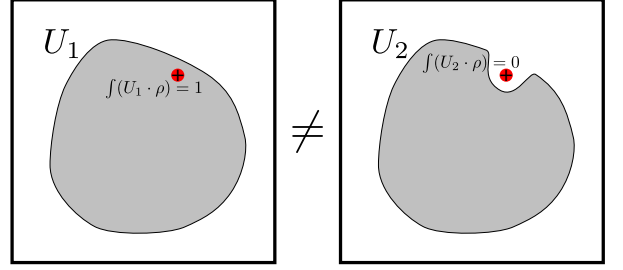
Proof:

If $U_1 = U_2$, then it is fairly obvious from the equivalence of U_1 and U_2 that $\int(U_1 \cdot \rho) = \int(U_2 \cdot \rho)$ for all choices of multi-point ρ .

With respect to the converse, assume that $U_1 \neq U_2$. Since $U_1 \neq U_2$, there must exist some volume in U_1 that has a different weight, possibly 0, or a different shape in U_2 . There will then exist some point probe ρ that targets the difference in question, and records a different amount of volumes in U_1 than in U_2 .

In the image on the right, the difference between U_1 and U_2 is targeted by the point probe ρ . A different amount of volumes is recorded by ρ for U_1 and U_2 , so $\int(U_1 \cdot \rho) \neq \int(U_2 \cdot \rho)$.

□



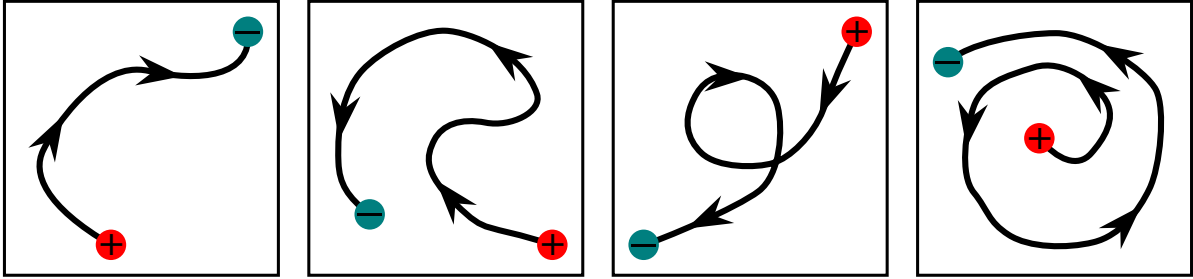
4.2 Path endpoints

Given a multi-path \mathbf{J} , the “endpoints” of \mathbf{J} is a multi-point that is denoted by:

$$\nabla \bullet \mathbf{J}$$

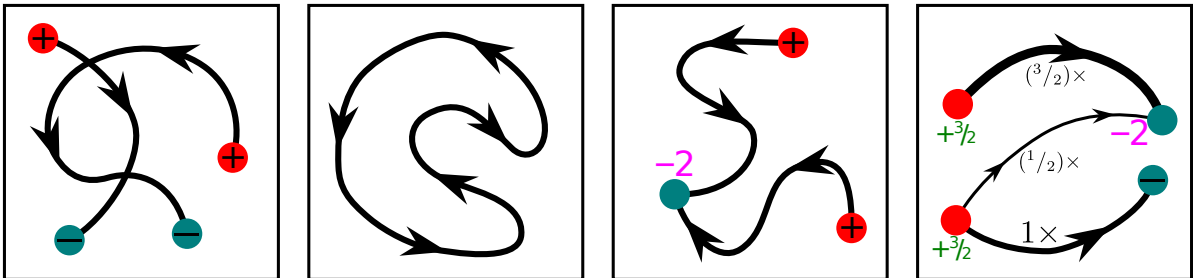
Given an oriented path C , let P_0 be the starting point of C , and let P_1 be the finishing point of C . The multi-point that is the endpoints of C consists of P_0 with a weight of +1 and P_1 with a weight of -1:

$$\nabla \bullet C = P_0 - P_1$$



The endpoints of a multi-path is the sum of the endpoints of all of the constituent paths:

$$\nabla \bullet (w_1 C_1 + w_2 C_2 + \dots + w_N C_N) = w_1 (\nabla \bullet C_1) + w_2 (\nabla \bullet C_2) + \dots + w_N (\nabla \bullet C_N)$$



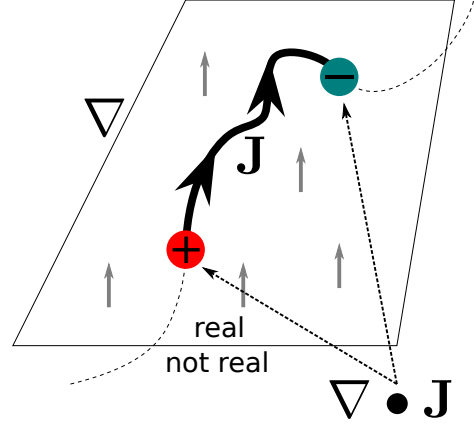
Theorem 9. *It should be noted that a closed loop has a net endpoint of 0. If multi-path \mathbf{J} consists of only closed loops, then $\nabla \bullet \mathbf{J} = 0$.*

It has already been established that paths are not allowed to extend to infinity, hence every starting point must be paired with a finishing point. Starting points have weights of +1, while finishing points have weights of -1. This means that for an arbitrary multi-path \mathbf{J} , that the sum of all of the endpoint weights is 0:

Theorem 10. *For any multi-path \mathbf{J} ,*

$$\int (\nabla \bullet \mathbf{J}) = 0$$

A logical question is why the notation $\nabla \bullet \mathbf{J}$ is used to denote the endpoints of multi-path \mathbf{J} . The notation $\mathbf{F} \bullet \mathbf{J}$ denotes the intersection of multi-path \mathbf{J} with multi-surface \mathbf{F} in the preferred direction. With ∇ denoting the inwards oriented surface of reality, $\nabla \bullet \mathbf{J}$ consists of points where \mathbf{J} enters reality with a weight of +1, and leaves reality with a weight of -1. This is illustrated on the right.



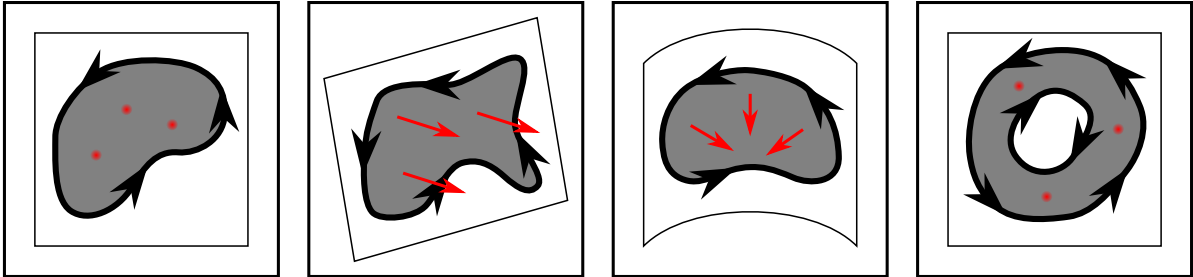
4.3 Surface boundaries

Given a multi-surface \mathbf{F} , the “boundaries” of \mathbf{F} is a multi-path that is denoted by:

$$\nabla \times \mathbf{F}$$

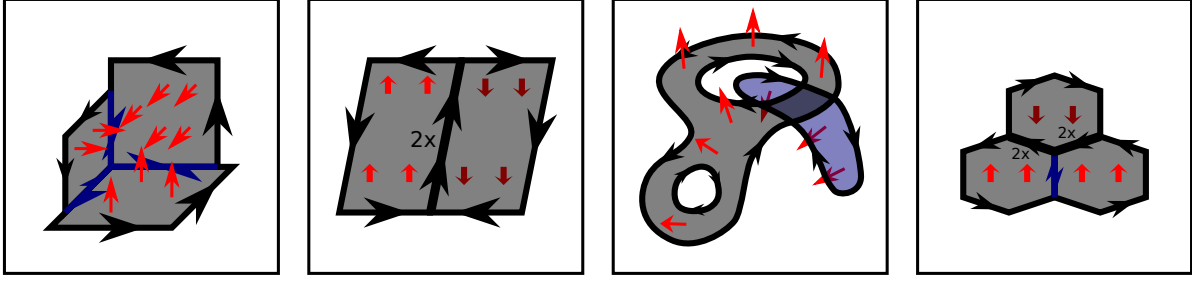
Given an oriented surface σ , the boundary of σ is its **counterclockwise** oriented boundary. The counterclockwise orientation is the orientation that traverses the boundary in a counterclockwise direction when the front of the surface is visible.

More exactly, the counterclockwise orientation is determined as follows. Position your view point so that the front of σ is visible. When σ is on your right, the boundary is oriented towards you. This is demonstrated in the rightmost example below where the boundary circles the hole in a clockwise direction.



The counterclockwise boundary of a multi-surface is the sum of the boundaries of all of the constituent surfaces:

$$\nabla \times (w_1\sigma_1 + w_2\sigma_2 + \dots + w_N\sigma_N) = w_1(\nabla \times \sigma_1) + w_2(\nabla \times \sigma_2) + \dots + w_N(\nabla \times \sigma_N)$$



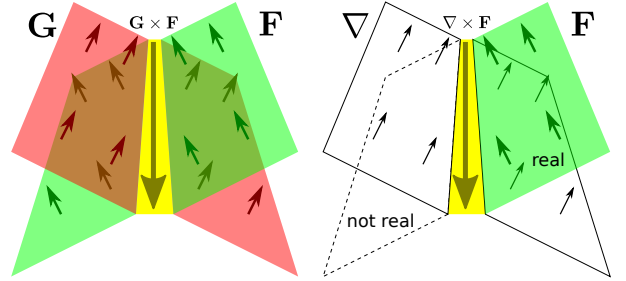
Theorem 11. *It should be noted that a closed surface (a bubble) has no boundaries. If multi-surface \mathbf{F} consists of only closed surfaces (bubbles), then $\nabla \times \mathbf{F} = 0$.*

The boundaries of surfaces do not abruptly end, and must be closed loops. The counterclockwise boundaries do not have end points.

Theorem 12. *For any multi-surface \mathbf{F} ,*

$$\nabla \bullet (\nabla \times \mathbf{F}) = 0$$

A logical question is why the notation $\nabla \times \mathbf{F}$ is used to denote the counterclockwise boundary of multi-surface \mathbf{F} . The notation $\mathbf{G} \times \mathbf{F}$ denotes the intersection of multi-surface \mathbf{G} with multi-surface \mathbf{F} , with \mathbf{F} as the 2nd surface. With ∇ denoting the inwards oriented surface of reality, $\nabla \times \mathbf{F}$ consists of the path where \mathbf{F} slices into and out of reality. This is illustrated on the right.

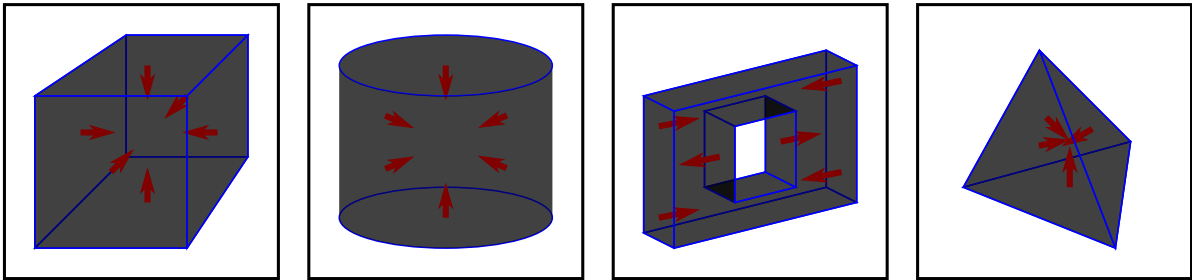


4.4 Volume surfaces

Given a multi-volume U , the “surfaces” of U is a multi-surface that is denoted by:

$$\nabla U$$

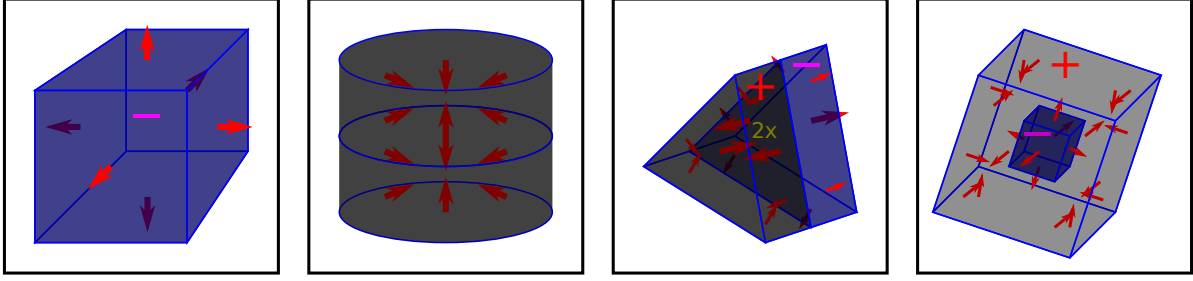
Given a volume Ω , the surface of Ω is **inwards-oriented**.



The inwards oriented surface of a multi-volume is the sum of the inwards oriented surfaces of all of the constituent volumes:

$$\nabla(w_1\Omega_1 + w_2\Omega_2 + \dots + w_N\Omega_N) = w_1(\nabla\Omega_1) + w_2(\nabla\Omega_2) + \dots + w_N(\nabla\Omega_N)$$

In the examples depicted below, the “inwards oriented surfaces” of volumes that have a negative weight are in fact oriented outwards.

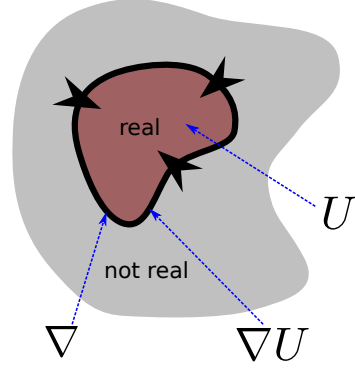


The surfaces of volumes are bubbles that have no boundaries.

Theorem 13. For any multi-volume U ,

$$\nabla \times (\nabla U) = 0$$

A logical question is why the notation ∇U is used to denote the inwards oriented surface of multi-volume U . The notation $\mathbf{F}U$ denotes the intersection of multi-volume U with multi-surface \mathbf{F} . With ∇ denoting the inwards oriented surface of reality, ∇U consists of the surface where U pushes into and out of reality. The surface is inwards oriented since ∇ is inwards oriented. This is illustrated on the right.



4.5 Summary

A summary of the notations used for the different boundaries is given below. In addition, we have observed that the boundaries have no boundaries themselves.

| multi-structure | boundary | orientation | no boundary of the boundary property |
|--------------------------|---------------------------------------|------------------------------|---|
| point ρ {0} | N/A | N/A | N/A |
| path \mathbf{J} {1} | point $\nabla \bullet \mathbf{J}$ {0} | positive start, negative end | $\int (\nabla \bullet \mathbf{J}) = 0$ |
| surface \mathbf{F} {2} | path $\nabla \times \mathbf{F}$ {1} | counterclockwise | $\nabla \bullet (\nabla \times \mathbf{F}) = 0$ |
| volume U {3} | surface ∇U {2} | inwards-oriented | $\nabla \times (\nabla U) = 0$ |

In **red** is indicated the “dimensionality” of the multi-structure. Points have 0 dimensions; paths have 1 dimension; surfaces have 2 dimensions; and volumes have 3 dimensions. The number of dimensions of the boundary is the number of dimensions minus 1. When the resultant number of dimensions is less than 0, the boundary does not exist.

Chapter 5

Closed loops and surfaces

5.1 Balanced multi-points

Consider a multi-path \mathbf{J} . Since no paths extend to infinity, every starting point, which has a weight of $+1$, is paired with a finishing point, which has a weight of -1 . The total weight of all the endpoints is 0:

$$\int (\nabla \cdot \mathbf{J}) = 0$$

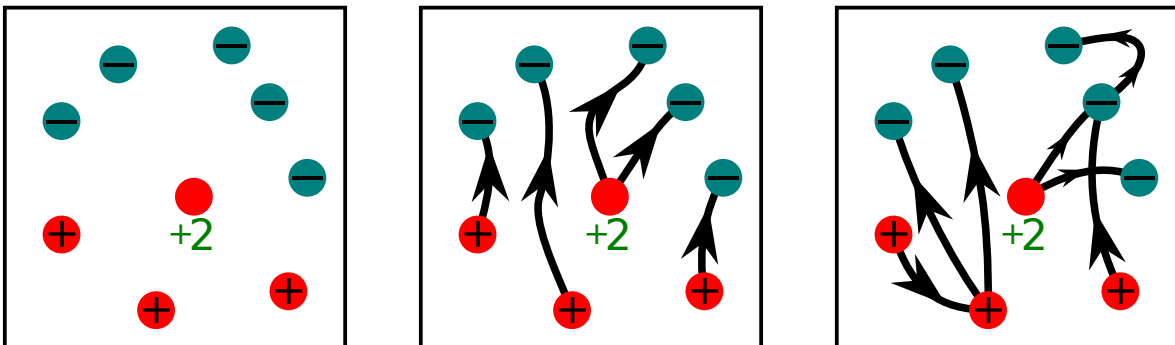
If multi-point ρ has a net total weight of 0, then ρ will be referred to as being a **balanced multi-point**.

$$\rho \text{ is balanced if and only if } \int \rho = 0$$

While the endpoints of any multi-path are balanced, it is also the case that given an arbitrary balanced multi-point ρ , that there exists some multi-path whose endpoints are ρ :

Theorem 14. *If multi-point ρ is such that $\int \rho = 0$ then there exists a multi-path \mathbf{J} such that $\nabla \cdot \mathbf{J} = \rho$*

This multi-path \mathbf{J} can be created by drawing oriented paths in a “dot-to-dot” fashion starting from points with positive weight and ending on points with negative weight. The resultant multi-path is **not unique**, as there are infinitely many ways to link the endpoints. The image below shows a balanced multi-point and two possible multi-paths whose endpoints are the given balanced multi-point.



5.2 Closed loops

Consider a multi-surface \mathbf{F} . The boundary of surfaces have no endpoints, and are “closed loops”:

$$\nabla \bullet (\nabla \times \mathbf{F}) = 0$$

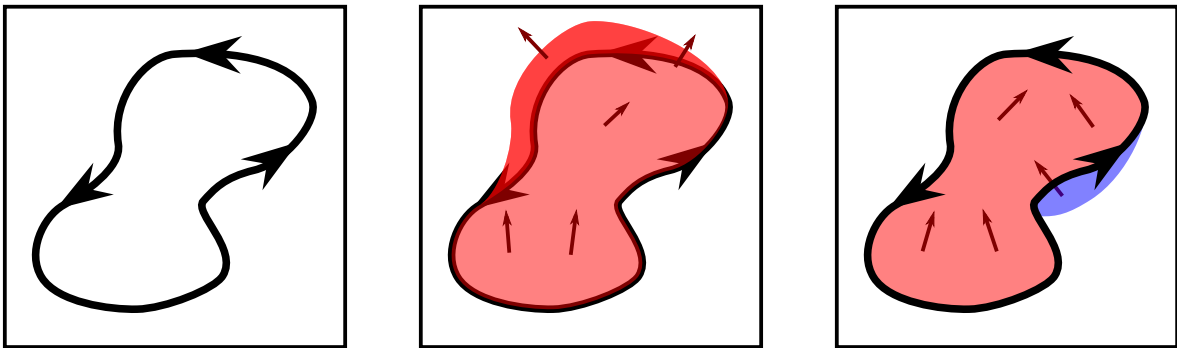
If multi-path \mathbf{J} has no endpoints, then \mathbf{J} will be referred to as being a **multi-loop**.

$$\mathbf{J} \text{ is a multi-loop (closed loop) if and only if } \nabla \bullet \mathbf{J} = 0$$

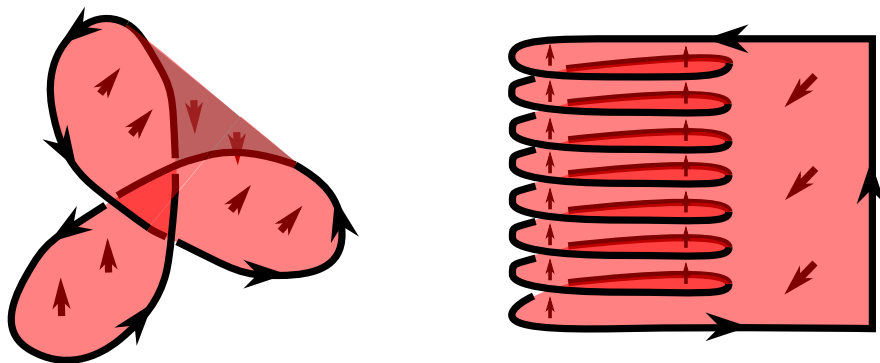
While the boundary of any multi-surface is a multi-loop, it is also the case that given an arbitrary multi-loop \mathbf{J} , that there exists some multi-surface whose boundary is \mathbf{J} :

Theorem 15. *If multi-path \mathbf{J} is such that $\nabla \bullet \mathbf{J} = 0$ then there exists a multi-surface \mathbf{F} such that $\nabla \times \mathbf{F} = \mathbf{J}$*

This multi-surface \mathbf{F} can be created by filling each loop with a surface that has the correct orientation. This filling can be done by starting at a specific point on the loop, and then “extending” a film by following the loop. The resultant multi-surface is **not unique**, as there are infinitely many ways to fill a loop. The image below shows a multi-loop and two possible multi-surfaces whose boundaries are the given multi-loop.



Below are examples of filling in more exotic loops with surfaces. On the left, there is the trefoil knot, while on the right, there is a helical coil. Helical coils have important applications in electronics and electromagnetism.



5.3 Closed surfaces

Consider a multi-volume U . The surfaces of volumes have no boundaries, and are “closed surfaces/bubbles”:

$$\nabla \times (\nabla U) = 0$$

If multi-surface \mathbf{F} has no boundary, then \mathbf{F} will be referred to as being a **multi-bubble**.

$$\mathbf{F} \text{ is a multi-bubble (closed surface) if and only if } \nabla \times \mathbf{F} = 0$$

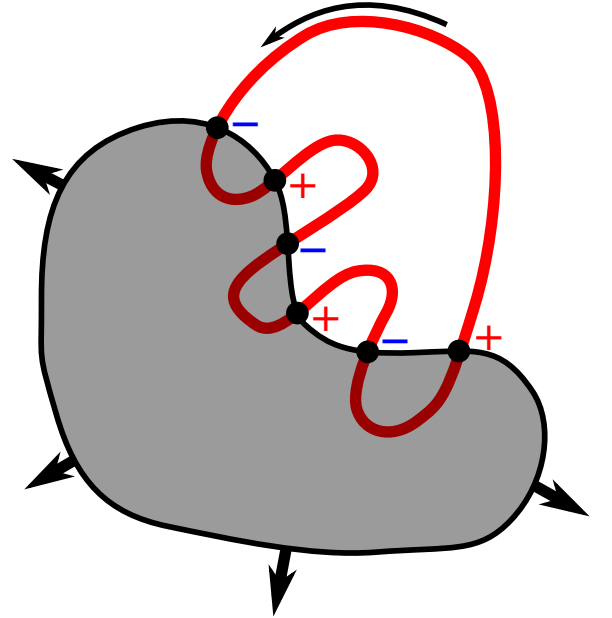
While the surface of any multi-volume is a multi-bubble, it is also the case that given an arbitrary multi-bubble \mathbf{F} , that there exists a **unique** multi-volume whose surface is \mathbf{F} :

Theorem 16. *If multi-surface \mathbf{F} is such that $\nabla \times \mathbf{F} = 0$ then there exists a **unique** multi-volume U such that $\nabla U = \mathbf{F}$*

This multi-volume U can be created by filling each of the bubbles with a volume that has the correct weight (outwards oriented bubbles are filled with negative volume). The resultant multi-volume is **unique**, as there is only one way to fill a bubble, unlike filling a boundary or connecting two points.

Given a multi-loop \mathbf{J} and a multi-bubble \mathbf{F} , the net number of times loop \mathbf{J} enters bubble \mathbf{F} is equal to the net number of times loop \mathbf{J} leaves bubble \mathbf{F} . Entrance points have an equal and opposite weight to exit points. This means that the net total of all the intersection points is 0: $\int \mathbf{J} \bullet \mathbf{F} = 0$.

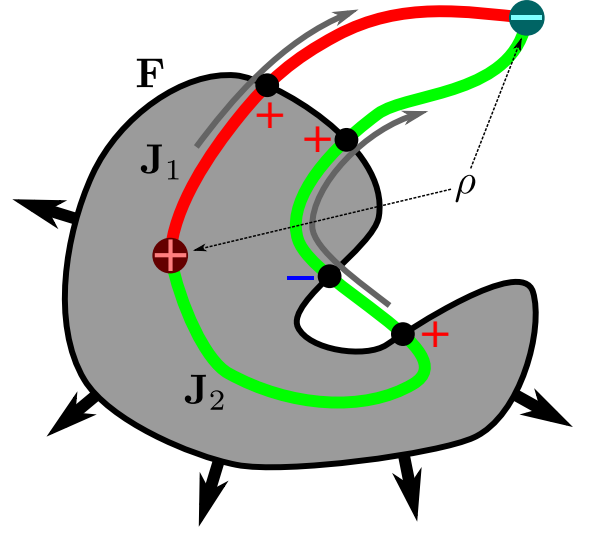
Theorem 17. *If multi-path \mathbf{J} is such that $\nabla \bullet \mathbf{J} = 0$, and multi-surface \mathbf{F} is such that $\nabla \times \mathbf{F} = 0$, then $\int (\mathbf{J} \bullet \mathbf{F}) = 0$*



Consider a balanced multi-point ρ and a multi-bubble \mathbf{F} . If \mathbf{J} is a multi-path whose endpoints are ρ , then the net number of times \mathbf{J} intersects \mathbf{F} **does not depend** on the choice of \mathbf{J} .

Theorem 18. *If multi-point ρ is such that $\int \rho = 0$, and multi-surface \mathbf{F} is such that $\nabla \times \mathbf{F} = 0$, and multi-paths \mathbf{J}_1 and \mathbf{J}_2 are two choices of multi-paths where $\nabla \bullet \mathbf{J} = \rho$, then $\int(\mathbf{J}_1 \bullet \mathbf{F}) = \int(\mathbf{J}_2 \bullet \mathbf{F})$*

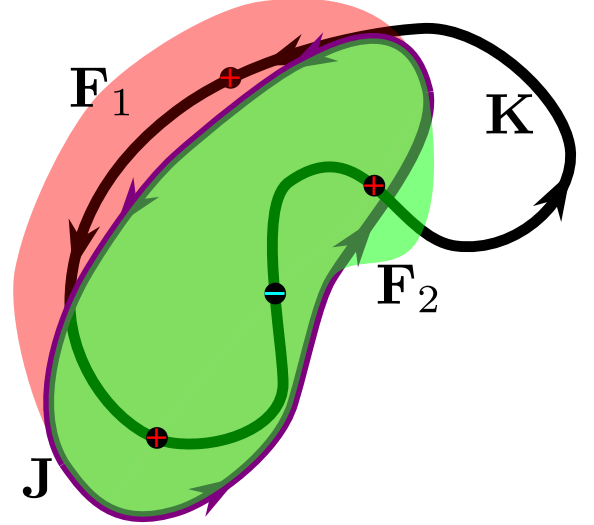
This is illustrated on the right where the two choices of paths result in the same net number of intersections with the bubble.



Consider two multi-loops \mathbf{J} and \mathbf{K} . If \mathbf{F} is a multi-surface whose counterclockwise boundary is \mathbf{J} , then the net number of times \mathbf{F} intersects \mathbf{K} **does not depend** on the choice of \mathbf{F} .

Theorem 19. *If multi-path \mathbf{J} is such that $\nabla \bullet \mathbf{J} = 0$, and multi-path \mathbf{K} is such that $\nabla \bullet \mathbf{K} = 0$, and multi-surfaces \mathbf{F}_1 and \mathbf{F}_2 are two choices of multi-surfaces where $\nabla \times \mathbf{F} = \mathbf{J}$, then $\int(\mathbf{F}_1 \bullet \mathbf{K}) = \int(\mathbf{F}_2 \bullet \mathbf{K})$*

This is illustrated on the right where the two choices of surfaces result in the same net number of intersections with the loop.



Chapter 6

Boundaries and intersections

6.1 Introduction

This chapter will derive various formulas that quantify the boundaries of the intersections. Many useful equations will be derived.

6.2 The endpoints of path-volume intersections

Consider an arbitrary multi-path \mathbf{J} and an arbitrary multi-volume U . The intersection $\mathbf{J} \cdot U$ is a multi-path, and the endpoints of this intersection are what will be sought: $\nabla \bullet (\mathbf{J} \cdot U)$

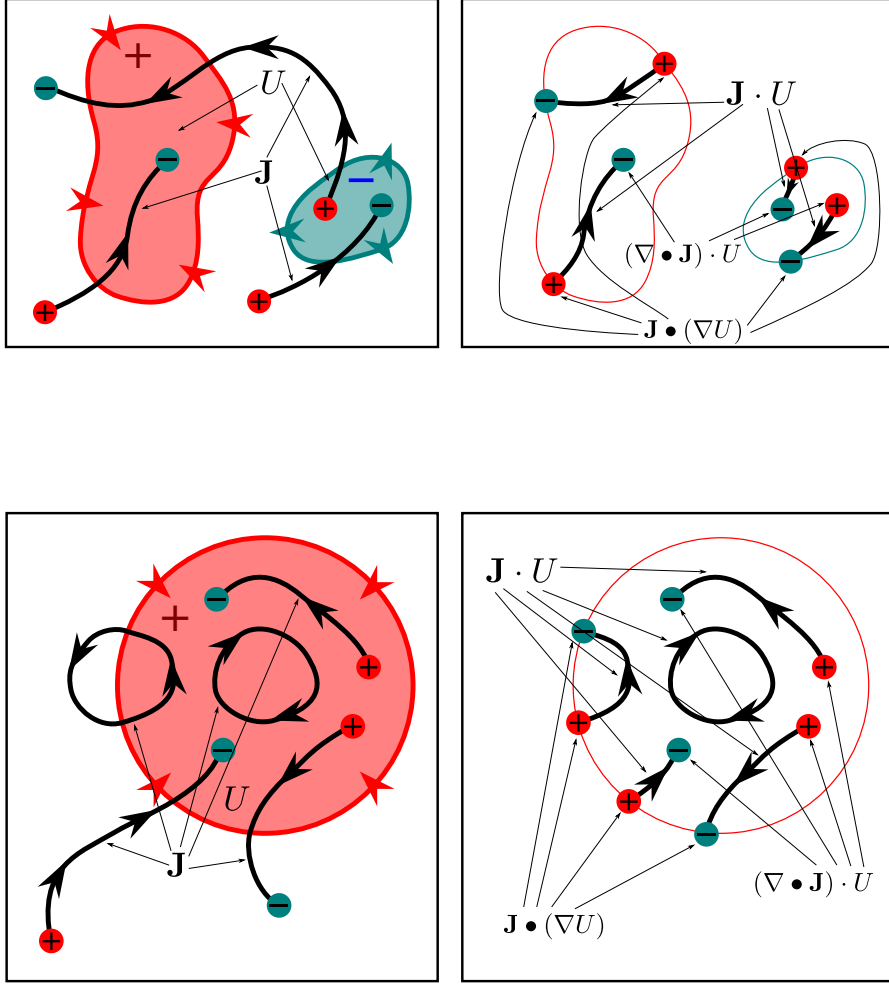
Given an oriented path C and a volume Ω , there are two sources of endpoints for $C \cdot \Omega$. The endpoints of C that happen to be inside of Ω are also endpoints of $C \cdot \Omega$. In addition, when C enters and exits Ω , this also creates endpoints for the intersection $C \cdot \Omega$. When C enters Ω , C passes through the inwards oriented surface $\nabla \Omega$ in the preferred direction. This intersection point, which has a weight of $+1$, is a starting point for the intersection $C \cdot \Omega$. When C leaves Ω , C passes through the inwards oriented surface $\nabla \Omega$ in the opposite direction. This intersection point, which has a weight of -1 , is an ending point for the intersection $C \cdot \Omega$.

Consider a multi-path \mathbf{J} and a multi-volume U . The endpoints of \mathbf{J} that are contained in U , $(\nabla \bullet \mathbf{J}) \cdot U$, are endpoints of $\mathbf{J} \cdot U$. In addition, the intersection of \mathbf{J} with the inwards oriented surface of U , $\mathbf{J} \bullet (\nabla U)$, also generates endpoints for $\mathbf{J} \cdot U$. In total,

Theorem 20.

$$\nabla \bullet (\mathbf{J} \cdot U) = (\nabla \bullet \mathbf{J}) \cdot U + \mathbf{J} \bullet (\nabla U)$$

Below are examples of the endpoints of the intersection of a multi-path and a multi-volume. On the left, the multi-path and multi-volume is shown alongside the endpoints of the multi-path and the surface of the multi-volume. On the right, the intersection of the multi-path and multi-volume is shown alongside its endpoints.



Moreover, since the total endpoint weight is always 0, $\int \nabla \bullet (\mathbf{J} \cdot U) = 0$ so $\int ((\nabla \bullet \mathbf{J}) \cdot U + \mathbf{J} \bullet (\nabla U)) = 0$ so:

Theorem 21.

$$\int \mathbf{J} \bullet (\nabla U) = \int -(\nabla \bullet \mathbf{J}) \cdot U$$

This statement reads that the net number of times path \mathbf{J} enters volume U , where exits count against entrances, is equal to the net number of finishing points left inside of U , where starting points count against finishing points. This statement is referred to as either the **gradient theorem** or the **divergence theorem**.

In the example on the right, there is a multi-path \mathbf{J} (which consists of a single path) passing through a multi-volume U . The total number of times \mathbf{J} enters U is:

$$\int \mathbf{J} \bullet (\nabla U) = +1 - 1 - 1 + 1 + 1 + 1 - 1 + 1 + 1 + 1 = 4$$

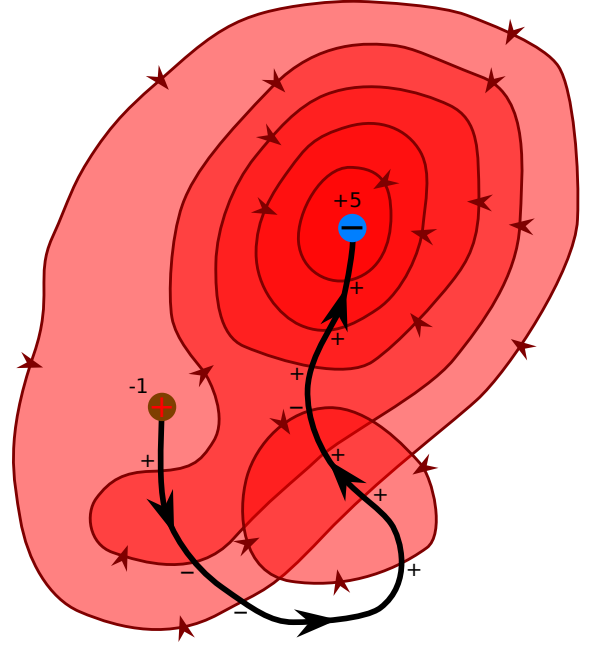
The total number of finishing points left in U is:

$$\int -(\nabla \bullet \mathbf{J}) \cdot U = +5 - 1 = 4$$

The +5 comes from the fact that the finishing point sits inside 5 volumes, while the -1 comes from the starting point sitting inside 1 volume.

It is clear that in this example:

$$\int \mathbf{J} \bullet (\nabla U) = \int -(\nabla \bullet \mathbf{J}) \cdot U$$



In the next example on the right, there is a multi-path \mathbf{J} passing through a multi-volume U (which consists of a single volume). The total number of times \mathbf{J} enters U is:

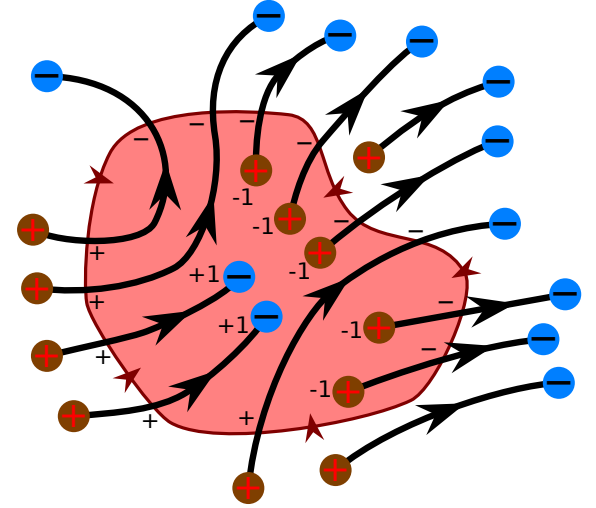
$$\int \mathbf{J} \bullet (\nabla U) = 5 \times (+1) + 8 \times (-1) = -3$$

The total number of finishing points left in U is:

$$\int -(\nabla \bullet \mathbf{J}) \cdot U = 2 \times (+1) + 5 \times (-1) = -3$$

It is clear that in this example:

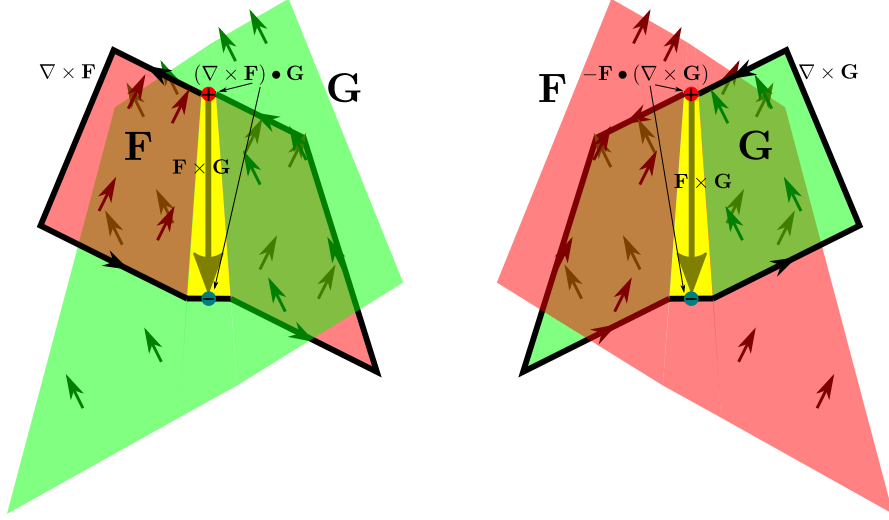
$$\int \mathbf{J} \bullet (\nabla U) = \int -(\nabla \bullet \mathbf{J}) \cdot U$$



6.3 The endpoints of surface-surface intersections

Consider arbitrary multi-surfaces \mathbf{F} and \mathbf{G} . The intersection $\mathbf{F} \times \mathbf{G}$ is a multi-path, and the endpoints of this intersection are what will be sought: $\nabla \bullet (\mathbf{F} \times \mathbf{G})$

Endpoints of $\mathbf{F} \times \mathbf{G}$ occur whenever a boundary of \mathbf{F} intersects \mathbf{G} , or vice versa as depicted below.



On the left, when the counterclockwise boundary of \mathbf{F} intersects \mathbf{G} in the preferred direction, starting points of $\mathbf{F} \times \mathbf{G}$ are created, and when the counterclockwise boundary of \mathbf{F} intersects \mathbf{G} in the opposite direction, finishing points of $\mathbf{F} \times \mathbf{G}$ are created. Therefore the intersection of the boundary of \mathbf{F} with the multi-surface \mathbf{G} contributes endpoints to $\mathbf{F} \times \mathbf{G}$. This intersection is $(\nabla \times \mathbf{F}) \bullet \mathbf{G}$

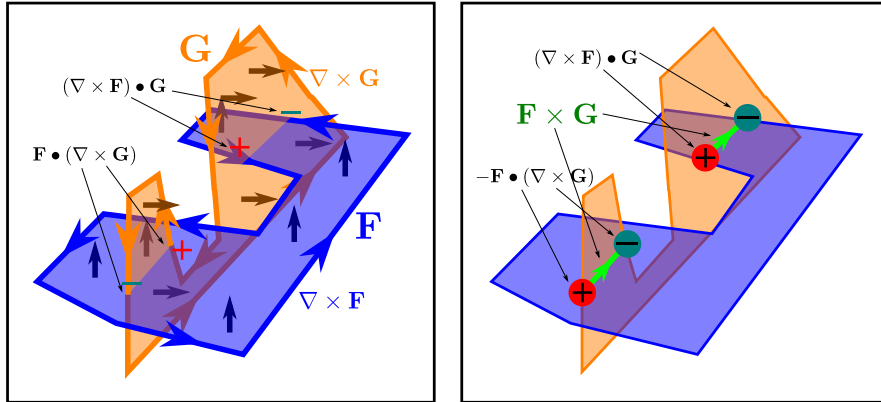
On the right, when the counterclockwise boundary of \mathbf{G} intersects \mathbf{F} in the preferred direction, finishing points of $\mathbf{F} \times \mathbf{G}$ are created, and when the counterclockwise boundary of \mathbf{G} intersects \mathbf{F} in the opposite direction, starting points of $\mathbf{F} \times \mathbf{G}$ are created. Therefore the intersection of the boundary of \mathbf{G} with the multi-surface \mathbf{F} contributes endpoints to $\mathbf{F} \times \mathbf{G}$, but the **polarity of the intersection points must be flipped to match the endpoints**. This intersection is $-\mathbf{F} \bullet (\nabla \times \mathbf{G})$

In total:

Theorem 22.

$$\nabla \bullet (\mathbf{F} \times \mathbf{G}) = (\nabla \times \mathbf{F}) \bullet \mathbf{G} - \mathbf{F} \bullet (\nabla \times \mathbf{G})$$

Another example is depicted below, where both of the intersections $(\nabla \times \mathbf{F}) \bullet \mathbf{G}$ and $\mathbf{F} \bullet (\nabla \times \mathbf{G})$ are nonzero. On the left, \mathbf{F} and \mathbf{G} are both depicted; along with their counterclockwise oriented boundaries $\nabla \times \mathbf{F}$ and $\nabla \times \mathbf{G}$; and also the intersections $(\nabla \times \mathbf{F}) \bullet \mathbf{G}$ and $\mathbf{F} \bullet (\nabla \times \mathbf{G})$. On the right, the intersection $\mathbf{F} \times \mathbf{G}$ is depicted along with the endpoints $\nabla \bullet (\mathbf{F} \times \mathbf{G})$.



Moreover, since the total endpoint weight is always 0, $\int \nabla \bullet (\mathbf{F} \times \mathbf{G}) = 0$ so $\int ((\nabla \times \mathbf{F}) \bullet \mathbf{G} - \mathbf{F} \bullet (\nabla \times \mathbf{G})) = 0$ so:

Theorem 23.

$$\int (\nabla \times \mathbf{F}) \bullet \mathbf{G} = \int \mathbf{F} \bullet (\nabla \times \mathbf{G})$$

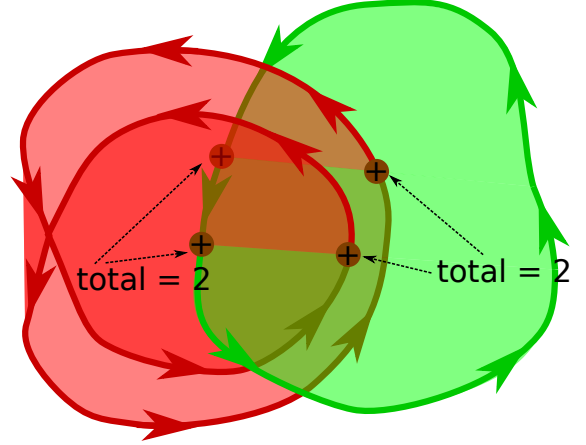
This statement reads that the net number of times the counterclockwise boundary of \mathbf{F} passes through \mathbf{G} , is equal to the net number of times that the counterclockwise boundary of \mathbf{G} passes through \mathbf{F} . This statement is generally referred to as **Stokes' Theorem**.

If \mathbf{A} and \mathbf{B} are multi-loops, and \mathbf{F} and \mathbf{G} are multi-surfaces whose counter-clockwise boundaries are respectively \mathbf{A} and \mathbf{B} , then:

$$\int \mathbf{A} \bullet \mathbf{G} = \int \mathbf{B} \bullet \mathbf{F}$$

$\int \mathbf{A} \bullet \mathbf{G}$ is the number of times multi-loop \mathbf{A} loops through multi-loop \mathbf{B} , while $\int \mathbf{B} \bullet \mathbf{F}$ is the number of times multi-loop \mathbf{B} loops through multi-loop \mathbf{A} .

In the image on the right, the two loops link through each other 2 times.



6.4 The boundaries of surface-volume intersections

Consider an arbitrary multi-surface \mathbf{F} and an arbitrary multi-volume U . The intersection $\mathbf{F} \cdot U$ is a multi-surface, and the counterclockwise boundary of this intersection is what will be sought: $\nabla \times (\mathbf{F} \cdot U)$

Given an oriented surface σ and a volume Ω , there are two sources of boundaries for $\sigma \cdot \Omega$. The sections of the boundaries of σ that happen to be inside of Ω are also sections of the boundary of $\sigma \cdot \Omega$. In addition, when σ slices into Ω , this also creates sections of the boundary for the intersection $\sigma \cdot \Omega$.

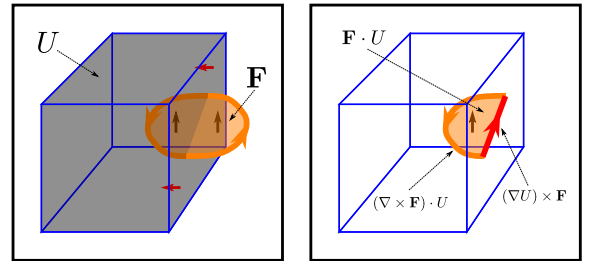
Consider a multi-surface \mathbf{F} and a multi-volume U . The sections of the counterclockwise boundary of \mathbf{F} that are contained in U , $(\nabla \times \mathbf{F}) \cdot U$, are sections of the counterclockwise boundary of $\mathbf{F} \cdot U$. In addition, the intersection of the inwards oriented surface of U with \mathbf{F} , $(\nabla U) \times \mathbf{F}$, also generates sections of the counterclockwise boundary for $\mathbf{F} \cdot U$. The intersection $(\nabla U) \times \mathbf{F}$ has the correct orientation as opposed to $\mathbf{F} \times (\nabla U)$, as illustrated below. In total,

Theorem 24.

$$\nabla \times (\mathbf{F} \cdot U) = (\nabla \times \mathbf{F}) \cdot U + (\nabla U) \times \mathbf{F}$$

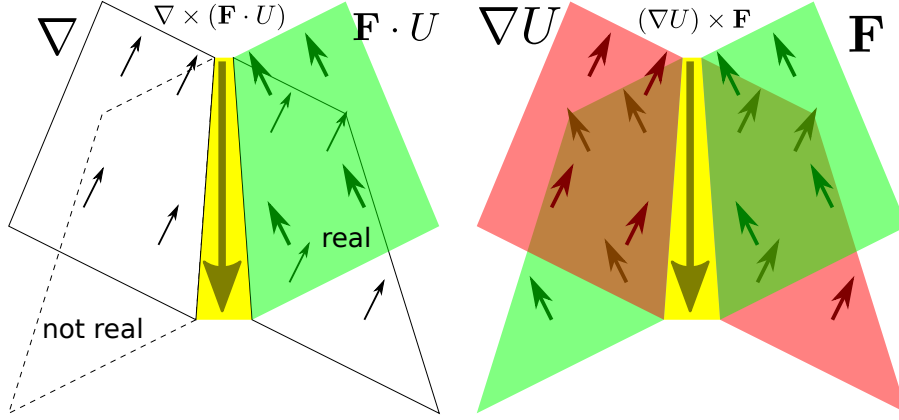
To the right, an example surface \mathbf{F} and volume U is shown, where \mathbf{F} is partially embedded in U . The boundary of intersection $\mathbf{F} \cdot U$ consists of two parts:
The first part is the section of $\nabla \times \mathbf{F}$ that is embedded in U , $(\nabla \times \mathbf{F}) \cdot U$.

The second part is the intersection of \mathbf{F} with the inwards oriented surface of U instead of with the inwards oriented surface of reality: $(\nabla U) \times \mathbf{F}$ instead of $\nabla \times \mathbf{F}$.



The ordering of the factors in the 2nd term $(\nabla U) \times \mathbf{F}$ can be easily remembered as opposed to $\mathbf{F} \times (\nabla U)$ using the following mnemonic. In the second term $(\nabla U) \times \mathbf{F}$, the inwards oriented surface of U , ∇U , replaces

the inwards oriented surface of reality, ∇ , in the expression $\nabla \times \mathbf{F}$. In the image below, on the left is the boundary $\nabla \times (\mathbf{F} \cdot U)$, and on the right is the intersection $(\nabla U) \times \mathbf{F}$.



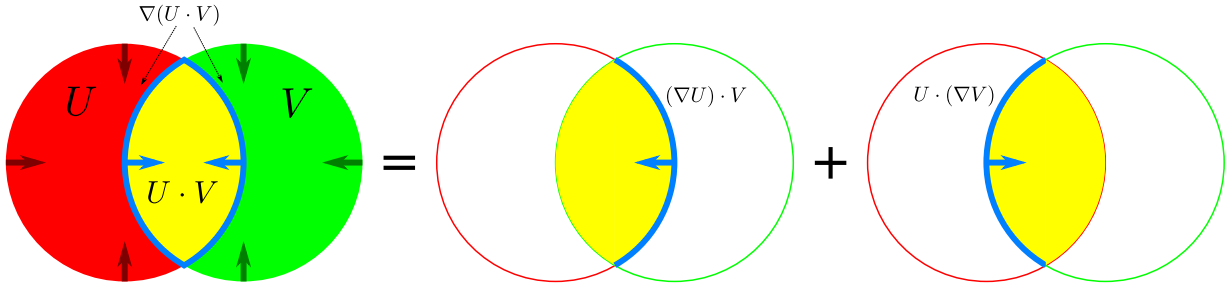
6.5 The surfaces of volume-volume intersections

Lastly, consider two multi-volumes U and V . The intersection $U \cdot V$ is a multi-volume, and the inwards-oriented surface of this intersection is what will be sought: $\nabla(U \cdot V)$

The surface of the intersection $U \cdot V$ consists of the surface of U that is embedded in V , plus the surface of V that is embedded in U , as depicted below:

Theorem 25.

$$\nabla(U \cdot V) = (\nabla U) \cdot V + U \cdot (\nabla V)$$



6.6 Summary

To summarize the boundaries of the various intersections,

| multi-structure 1 | multi-structure 2 | intersection | intersection boundary |
|----------------------|----------------------|---------------------------------------|---|
| point ρ | volume U | point $\rho \cdot U$ | N/A |
| path \mathbf{J} | surface \mathbf{F} | point $\mathbf{J} \bullet \mathbf{F}$ | N/A |
| path \mathbf{J} | volume U | path $\mathbf{J} \cdot U$ | point $\nabla \bullet (\mathbf{J} \cdot U) = (\nabla \bullet \mathbf{J}) \cdot U + \mathbf{J} \bullet (\nabla U)$ |
| surface \mathbf{F} | surface \mathbf{G} | path $\mathbf{F} \times \mathbf{G}$ | point $\nabla \bullet (\mathbf{F} \times \mathbf{G}) = (\nabla \times \mathbf{F}) \bullet \mathbf{G} - \mathbf{F} \bullet (\nabla \times \mathbf{G})$ |
| surface \mathbf{F} | volume U | surface $\mathbf{F} \cdot U$ | path $\nabla \times (\mathbf{F} \cdot U) = (\nabla \times \mathbf{F}) \cdot U + (\nabla U) \times \mathbf{F}$ |
| volume U | volume V | volume $U \cdot V$ | surface $\nabla(U \cdot V) = (\nabla U) \cdot V + U \cdot (\nabla V)$ |

In addition it was observed that:

Given an arbitrary multi-path \mathbf{J} and an arbitrary multi-volume U , then

$$\int \mathbf{J} \bullet (\nabla U) = - \int (\nabla \bullet \mathbf{J}) \cdot U$$

Given multi-surfaces \mathbf{F} and \mathbf{G} , then

$$\int (\nabla \times \mathbf{F}) \bullet \mathbf{G} = \int \mathbf{F} \bullet (\nabla \times \mathbf{G})$$

(this is **Stokes' theorem**)

Chapter 7

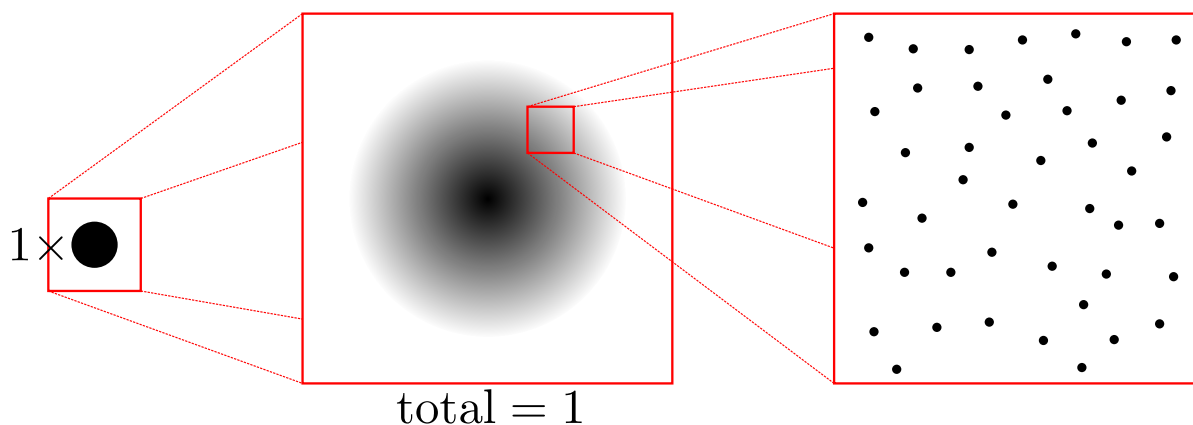
Quantifying multi-structures

7.1 Introduction

Here, the actual shape and arrangement of multi-structures will be quantified through the use of numbers, or lists of numbers. Before this can be properly done however, the multi-structures will need to be “smoothed out”, so that their “structure” at extremely small “**infinitesimal**” scales is uniform and bereft of “sharp” boundaries.

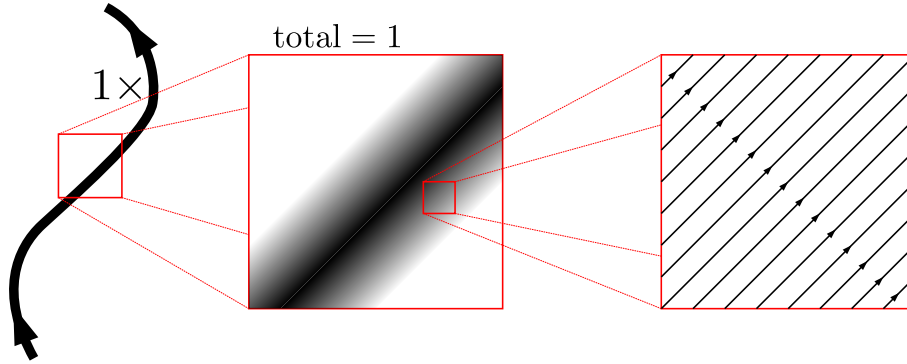
7.2 The smoothness condition

To ensure that the structure of multi-points remain uniform at infinitesimal scales, each point will be envisioned as a “cloud” of an infinite number of points, each with an infinitely small, **infinitesimal** weight. When the zoom is increased to infinite scales, the point resembles a cloud of points with the highest density at the center, rapidly dropping of to 0 further from the center. Further increases to the scale result in a uniform spread of an infinite number of points each with an infinitesimal weight. By doing this, points have a “soft/smooth” boundary. This smoothing is illustrated below:

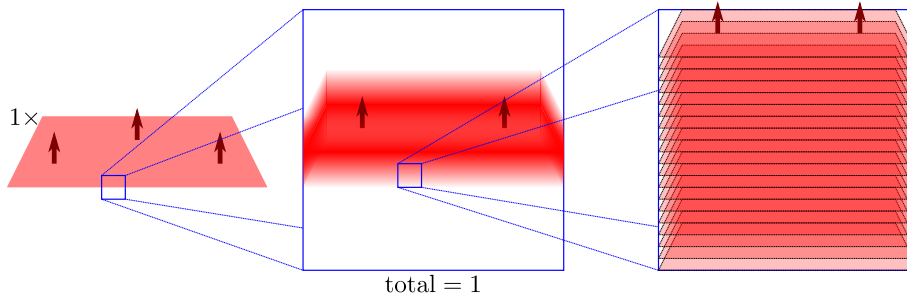


To ensure that the structure of multi-paths remain uniform at infinitesimal scales, each path will be envisioned as a “bundle” of an infinite number of paths, each with an infinitely small, infinitesimal weight. When the zoom is increased to infinite scales, the path resembles a bundle of paths with the highest density at the center, rapidly dropping of to 0 further from the center. Further increases to the scale result in a

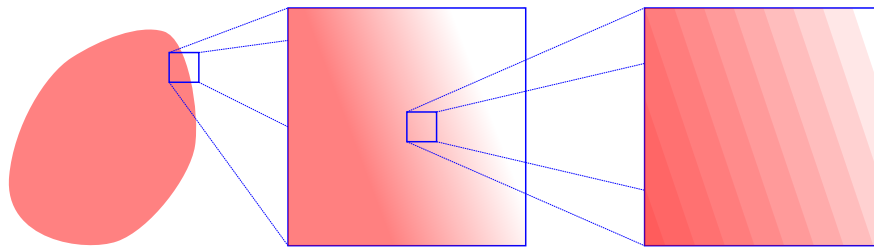
uniform spread of an infinite number of paths each with an infinitesimal weight. By doing this, paths have a “soft/smooth” boundary. This smoothing is illustrated below:



To ensure that the structure of multi-surfaces remain uniform at infinitesimal scales, each surface will be envisioned as a “stack” of an infinite number of surfaces, each with an infinitely small, infinitesimal weight. When the zoom is increased to infinite scales, the surface resembles a stack of surfaces with the highest density at the center, rapidly dropping of to 0 further from the center. Further increases to the scale result in a uniform spread of an infinite number of surfaces each with an infinitesimal weight. By doing this, surfaces have a “soft/smooth” boundary. This smoothing is illustrated below:



Lastly, volumes are “smoothed” by blurring their boundaries at an infinitesimal scale. Each volume is given an infinitely thin “crust” that consists of onion-like layers of diminishing weight closer to the outside. Essentially, the volume’s surface itself is being smoothed as discussed above. This smoothing is illustrated below:

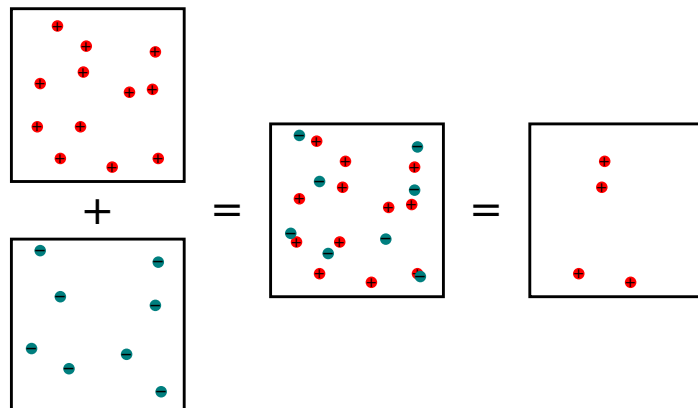


7.3 Unions revisited

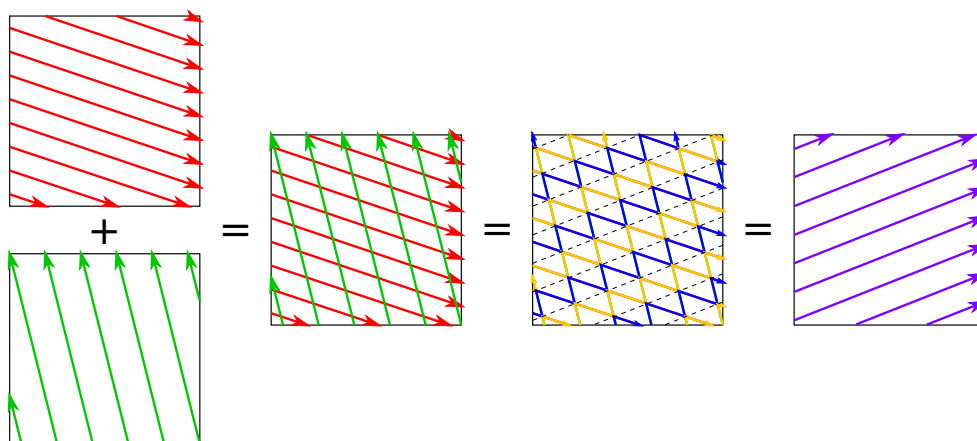
Now that the smoothness requirements on multi-points, multi-paths, multi-surfaces, and multi-volumes have been established, the addition/union of multi-structures now needs to be reconsidered in order to preserve

the smoothness requirement. Unions function almost identically to how they functioned previously, but now subtle post-union modifications are made at infinitesimal scales in order to preserve smoothness.

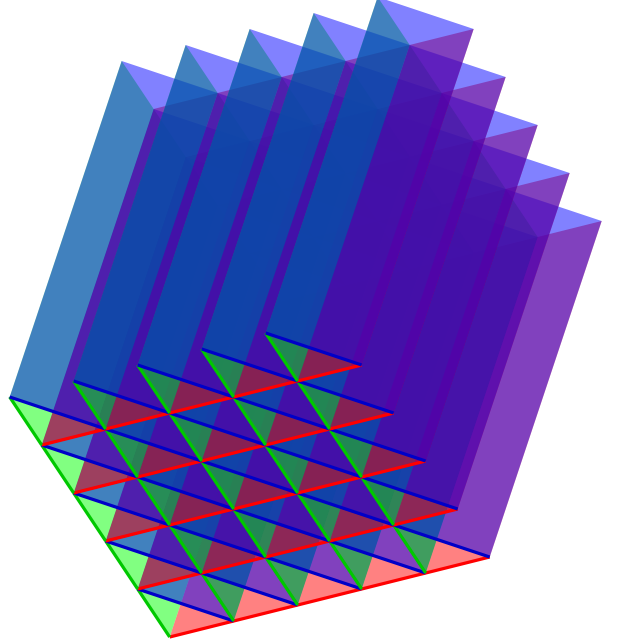
Below is depicted the union of two clouds of infinitesimally weighted points. The magnification factor is infinite, and after the union, points are moved to “annihilate” with nearby points with the opposite polarity.



Below is depicted the union of two bundles of infinitesimally weighted paths. One bundle is red in color, and the other is green in color. The magnification factor is infinite, and after the union, the paths are broken apart and restitched together into a bundle of “zigzags”, that all have roughly the same overall direction. The zigzags are then ironed out to form a bundle of parallel paths, which is the smoothed union.



To the right is depicted the union of two stacks of infinitesimally weighted surfaces, which proceeds in a virtually identical manner to the union of paths. One stack is red in color, and the other is green in color. The magnification factor is infinite, and after the union, the surfaces are broken apart and restitched together into a stack of corrugated surfaces. The corrugated surfaces are then ironed out to form the stack of blue parallel surfaces, which is the smoothed union.



Lastly, when the union of two multi-volumes occurs, the surfaces of the sum need to be smoothed out in a manner similar to what was described above.

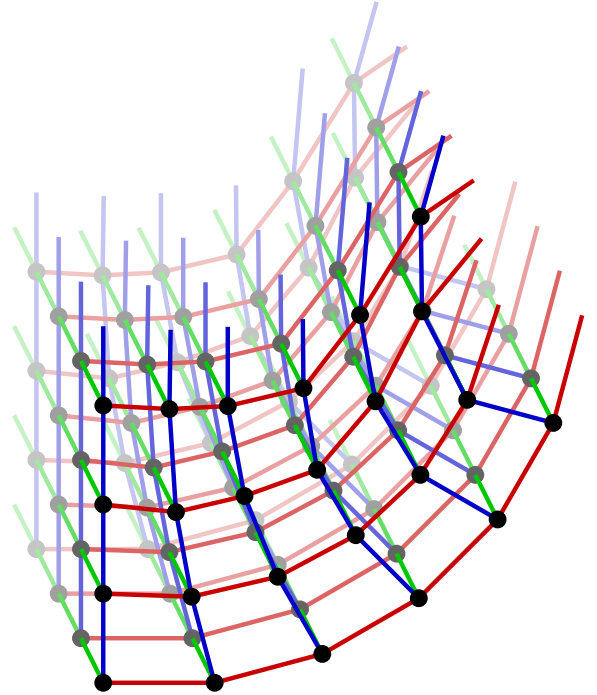
It is important to note that smoothing does not impact any of the properties regarding unions, intersections, and boundaries that were mentioned in the previous chapters.

7.4 Coordinate systems

A coordinate system labels each point with a triple of numbers (c_1, c_2, c_3) . On the right, a “coordinate lattice” is depicted where each point in the lattice is determined by a unique triple (c_1, c_2, c_3) . Changing one coordinate while holding the others constant moves the point along one of the lattice lines. Principal direction i is the direction of the line traced out by increasing c_i .

The coordinate system will be assumed to be **right handed**. With both the c_1 and c_2 directions oriented upwards, and the c_1 direction is on your left, the c_2 direction on your right, then the c_3 direction is oriented away from the viewer.

Some important notation to keep track of is as follows: The coordinates are indexed from 1 to 3. If variable i **denotes an index** with the range 1, 2, 3, then the expression $i + 1$ adds 1 to index i while **wrapping the values around** so that increasing from 3 returns to 1: $3 + 1 = 1$. The expression $i + 2$ adds 2 to index i while **wrapping the values around** so that increasing from 3 returns to 1: $2 + 2 = 1$ and $3 + 2 = 2$. Given an index i , the **other indices** are $i + 1$ and $i + 2$.



The coordinate values c_1 , c_2 , and c_3 may not be dimensionless and may instead have units of measurement. For example, with Cartesian coordinates, all coordinates are measured using units of length. The units that measure c_1 , c_2 , and c_3 will be denoted by “c_1_units”; “c_2_units”; and “c_3_units” respectively.

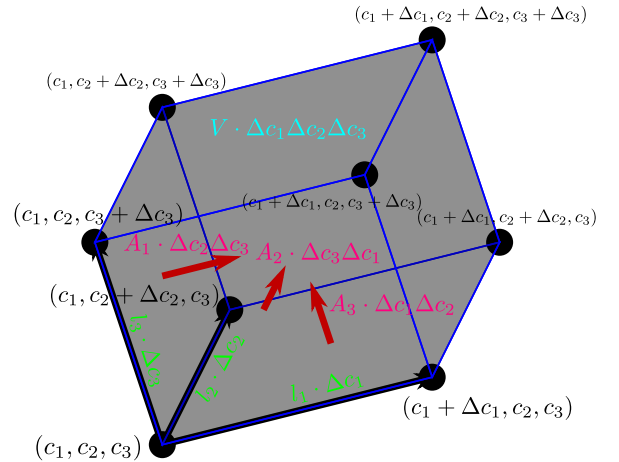
A **vector** is a **list of numbers**, while a **scalar** often refers to a single number. Vectors are often denoted by listing their numbers vertically within square braces, or horizontally within triangular braces:

$$\begin{bmatrix} F_1 \\ F_2 \\ \vdots \\ F_n \end{bmatrix} \quad \text{or} \quad \langle F_1, F_2, \dots, F_n \rangle$$

If the entries of a vector are computed via the expression $F(i)$, where i (from the range $1, 2, \dots, n$) is the index of the entry being computed, then the vector itself is denoted via the expression $[i : F(i)]$ or $\langle i : F(i) \rangle$.

Lastly, given an expression $F(i)$ where i is an index from the range $1, 2, \dots, n$, then $\sum_i F(i)$ denotes the sum $F(1) + F(2) + \dots + F(n)$.

A **parallelepiped** is the 3D analog to the parallelogram. When the coordinates c_1 , c_2 , and c_3 are changed by the respective infinitesimal (infinitely small) amounts Δc_1 , Δc_2 , and Δc_3 , the set of all points where c_1 , c_2 , and c_3 are in between their old and new values is approximately a parallelepiped, such as depicted on the right. The various dimensions of this parallelepiped are proportional to Δc_1 , Δc_2 , and Δc_3 .



For each dimension $i = 1, 2, 3$, when coordinate c_i changes by the infinitesimal amount Δc_i , the point moves a distance of $l_i \cdot \Delta c_i$. The quantity l_i is the distance traversed by the point per unit of c_i (for infinitesimal changes in c_i). **Principal direction** i is the direction of the edge traced out by increasing c_i . The values of l_1 , l_2 , and l_3 are measured using the following respective units: $\text{m}/c_1\text{-units}$, $\text{m}/c_2\text{-units}$, and $\text{m}/c_3\text{-units}$.

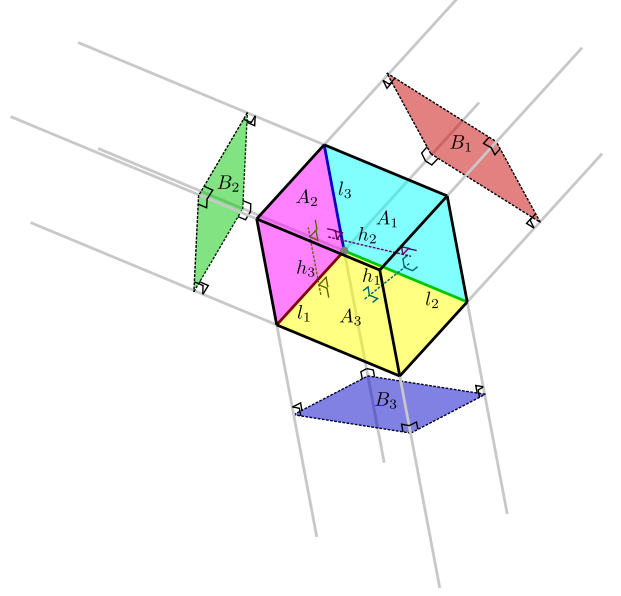
For each dimension $i = 1, 2, 3$, when the other coordinates c_{i+1} and c_{i+2} change by the respective infinitesimal amounts Δc_{i+1} and Δc_{i+2} , the area of the parallelogram formed by all points where c_{i+1} and c_{i+2} are in between their old and new values is $A_i \cdot \Delta c_{i+1} \Delta c_{i+2}$. **Co-principal direction** i is the direction perpendicular to this parallelogram (illustrated by the red arrows). The values of A_1 , A_2 , and A_3 are measured using the following respective units: $\text{m}^2/(c_2\text{-units} \cdot c_3\text{-units})$, $\text{m}^2/(c_3\text{-units} \cdot c_1\text{-units})$, and $\text{m}^2/(c_1\text{-units} \cdot c_2\text{-units})$.

Lastly when all coordinates c_1 , c_2 , and c_3 change by the respective infinitesimal amounts Δc_1 , Δc_2 , and Δc_3 , the volume of the parallelepiped (3D parallelogram) formed by all points where c_1 , c_2 , and c_3 are in between their old and new values is $V \cdot \Delta c_1 \Delta c_2 \Delta c_3$. The value of V is measured using the units: $\text{m}^3/(c_1\text{-units} \cdot c_2\text{-units} \cdot c_3\text{-units})$

In addition to the quantities $l_1, l_2, l_3, A_1, A_2, A_3$, and V , additional quantities will be introduced. For each $i = 1, 2, 3$, $B_i \cdot \Delta c_{i+1} \Delta c_{i+2}$ is the cross-sectional area when the parallelepiped is cleaved perpendicular to the c_i direction, and $h_i \cdot \Delta c_i$ is the thickness/height of the parallelepiped when placed flat along the c_{i+1} and c_{i+2} directions. All of these quantities are illustrated on the right. For simplicity, the factors $\Delta c_1, \Delta c_2$, and Δc_3 have been omitted. h_1, h_2 , and h_3 have the same units of measurement as l_1, l_2 , and l_3 respectively. B_1, B_2 , and B_3 have the same units of measurement as A_1, A_2 , and A_3 respectively.

The relationship between these quantities, derived from computing the volume in multiple different ways, are:

$$\begin{aligned} V &= l_1 B_1 = l_2 B_2 = l_3 B_3 \\ &= h_1 A_1 = h_2 A_2 = h_3 A_3 \end{aligned}$$



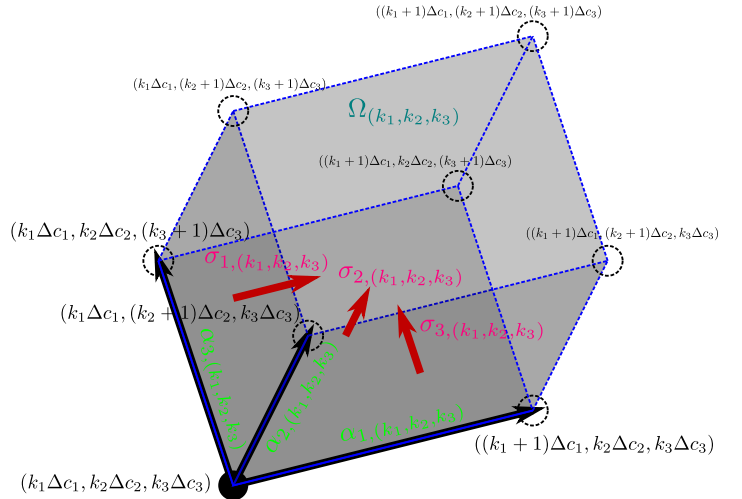
All of the quantities $l_1, l_2, l_3, A_1, A_2, A_3, V, B_1, B_2, B_3, h_1, h_2$, and h_3 **may change with respect to position**.

To assist in describing multi-structures and computing various quantities, space will be broken in a lattice of “cells”. Infinitesimal increments $\Delta c_1, \Delta c_2$, and Δc_3 will be fixed. For any choice of **integers** k_1, k_2 , and k_3 , the **cell** indexed by the triple (k_1, k_2, k_3) is the parallelepiped where for each index $i = 1, 2, 3$, that coordinate c_i is confined to the narrow interval $k_i \Delta c_i \leq c_i < (k_i + 1) \Delta c_i$. Note that the upper bound on the interval is excluded.

Point $\theta_{(k_1, k_2, k_3)}$ is a lattice note with the coordinate $(k_1 \Delta c_1, k_2 \Delta c_2, k_3 \Delta c_3)$.

For each index $i = 1, 2, 3$; $\alpha_{i, (k_1, k_2, k_3)}$ is the lattice curve/edge that consists of all points where c_i increases from $k_i \Delta c_i$ to $(k_i + 1) \Delta c_i$ and the other coordinates are held constant: $c_{i+1} = k_{i+1} \Delta c_{i+1}$ and $c_{i+2} = k_{i+2} \Delta c_{i+2}$. This curve starts at $\theta_{(k_1, k_2, k_3)}$ and does not include the end point where $c_i = (k_i + 1) \Delta c_i$.

For each index $i = 1, 2, 3$; $\sigma_{i, (k_1, k_2, k_3)}$ is the lattice surface/tile that consists of all points where $c_i = k_i \Delta c_i$ and $k_{i+1} \Delta c_{i+1} \leq c_{i+1} < (k_{i+1} + 1) \Delta c_{i+1}$ and $k_{i+2} \Delta c_{i+2} \leq c_{i+2} < (k_{i+2} + 1) \Delta c_{i+2}$. The surface faces in the direction of increasing c_i and does not include the points where $c_{i+1} = (k_{i+1} + 1) \Delta c_{i+1}$ or $c_{i+2} = (k_{i+2} + 1) \Delta c_{i+2}$.



$\Omega_{(k_1, k_2, k_3)}$ is the cell itself. Note that points where $c_1 = (k_1 + 1) \Delta c_1$ or $c_2 = (k_2 + 1) \Delta c_2$ or $c_3 = (k_3 + 1) \Delta c_3$ are not included.

Associated with each cell are the aforementioned quantities $l_1, l_2, l_3, A_1, A_2, A_3, V, B_1, B_2, B_3, h_1, h_2$, and h_3 . **These quantities may change from cell to cell.**

7.5 Using numbers to describe multi-structures

Multi-structures will be denoted by functions whose input is a point and space, and whose return values are numbers that describe the total-multi structure at that point. Given an arbitrary point (c_1, c_2, c_3) , the indices (k_1, k_2, k_3) of the cell that contains (c_1, c_2, c_3) are:

$$(k_1, k_2, k_3) = \left(\left\lfloor \frac{c_1}{\Delta c_1} \right\rfloor, \left\lfloor \frac{c_2}{\Delta c_2} \right\rfloor, \left\lfloor \frac{c_3}{\Delta c_3} \right\rfloor \right)$$

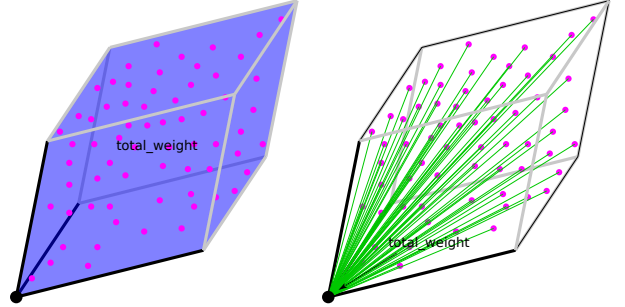
The notation $\lfloor x \rfloor$ means to round x *down* to the nearest integer provided x is not an integer. If x is already an integer $\lfloor x \rfloor = x$.

The first step in quantifying a multi-structure is to “approximate” the multi-structure using *only* the lattice nodes θ for multi-points, the lattice edges α_i for multi-paths, the lattice tiles σ_i for multi-surfaces, and the lattice cells Ω for multi-volumes.

7.5.1 Quantifying multi-points

A multi-point ρ is quantified by a function $\rho(\mathbf{q})$ whose input is a position \mathbf{q} .

Let triple (k_1, k_2, k_3) index the cell that contains \mathbf{q} . At the scales of Δc_1 , Δc_2 , and Δc_3 , the magnification results in the points resembling a uniform spread of infinitesimal points thanks to the smoothness condition, as depicted in the leftmost image on the right. The approximation takes the total point weight inside the cell and condenses it onto the lattice point $\theta_{(k_1, k_2, k_3)}$, as depicted in the rightmost image on the right. **This is the approximation that will be used for various calculations.**



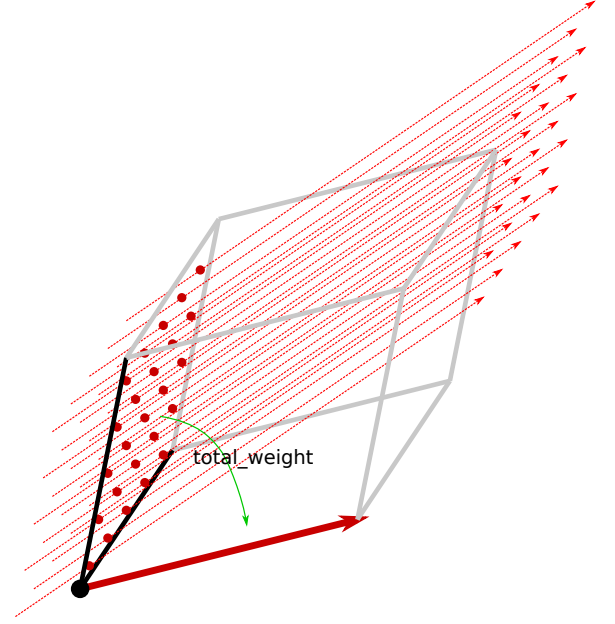
What about the value of $\rho(\mathbf{q})$ itself? The weight w_θ assigned to the lattice point $\theta_{(k_1, k_2, k_3)}$ is infinitely small, so the average density over the cell volume is used for $\rho(\mathbf{q})$ instead: $\rho(\mathbf{q}) = \frac{w_\theta}{V \cdot \Delta c_1 \Delta c_2 \Delta c_3}$. Contrariwise, if $\rho(\mathbf{q})$ is known, then the weight assigned to $\theta_{(k_1, k_2, k_3)}$ is $\rho(\mathbf{q}) \cdot V \cdot \Delta c_1 \Delta c_2 \Delta c_3$. In essence, $\rho(\mathbf{q})$ is the point weight density.

If length is being measured in meters (m), and weight is being measured using an arbitrary unit of measurement referred to as “w_units”, then the value of $\rho(\mathbf{q})$ is measured in w_units/m³ (i.e. w_units per unit volume).

7.5.2 Quantifying multi-paths

A multi-path \mathbf{J} is quantified by a vector valued function $\mathbf{J}(\mathbf{q}) = [i : J_i(\mathbf{q})] = \begin{bmatrix} J_1(\mathbf{q}) \\ J_2(\mathbf{q}) \\ J_3(\mathbf{q}) \end{bmatrix}$ whose input is a position \mathbf{q} .

Let triple (k_1, k_2, k_3) index the cell that contains \mathbf{q} . At the scales of Δc_1 , Δc_2 , and Δc_3 , the magnification results in the paths resembling a uniform bundle of infinitesimally weighted paths thanks to the smoothness condition. For each direction $i = 1, 2, 3$, the total weight of all of the intersections with the lattice tile $\sigma_{i,(k_1,k_2,k_3)}$ is the total path weight that crosses the current cell in principal direction i , and this total weight is subsequently assigned to the lattice edge $\alpha_{i,(k_1,k_2,k_3)}$ which itself crosses the current cell in principal direction i . **This is the approximation that will be used for various calculations.**



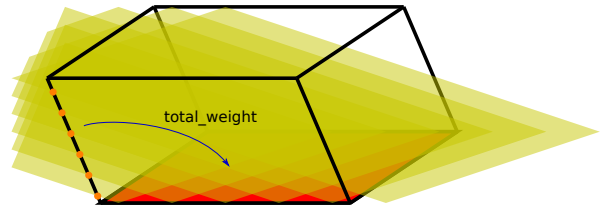
What about the value of $J_i(\mathbf{q})$ itself? The weight $w_{\alpha,i}$ assigned to the lattice edge $\alpha_{i,(k_1,k_2,k_3)}$ is infinitely small, so the average density over the cross-sectional area of the cell is used for $J_i(\mathbf{q})$ instead: $J_i(\mathbf{q}) = \frac{w_{\alpha,i}}{B_i \cdot \Delta c_{i+1} \Delta c_{i+2}}$. Contrariwise, if $J_i(\mathbf{q})$ is known, then the weight assigned to $\alpha_{i,(k_1,k_2,k_3)}$ is $J_i(\mathbf{q}) \cdot B_i \cdot \Delta c_{i+1} \Delta c_{i+2}$.

If length is being measured in meters (m), and weight is being measured using an arbitrary unit of measurement referred to as “w_units”, then the values of $\mathbf{J}(\mathbf{q})$ are measured in w_units/m² (i.e. w_units per unit cross sectional area).

7.5.3 Quantifying multi-surfaces

A multi-surface \mathbf{F} is quantified by a vector valued function $\mathbf{F}(\mathbf{q}) = [i : F_i(\mathbf{q})]$ whose input is a position \mathbf{q} .

Let triple (k_1, k_2, k_3) index the cell that contains \mathbf{q} . At the scales of Δc_1 , Δc_2 , and Δc_3 , the magnification results in the surfaces resembling a uniform stack of infinitesimally weighted surfaces thanks to the smoothness condition. For each direction $i = 1, 2, 3$, the total weight of all of the intersections with the lattice edge $\alpha_{i,(k_1,k_2,k_3)}$ is assigned to the lattice tile $\sigma_{i,(k_1,k_2,k_3)}$. **This is the approximation that will be used for various calculations.**



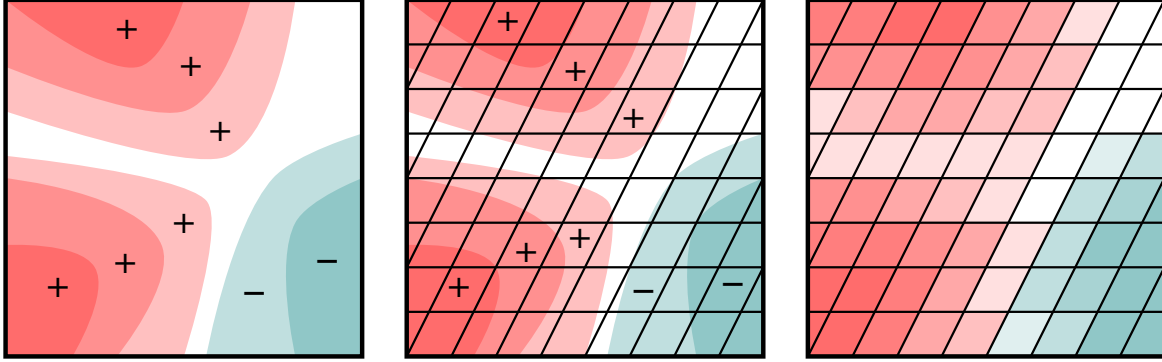
What about the value of $F_i(\mathbf{q})$ itself? The weight $w_{\sigma,i}$ assigned to the lattice tile $\sigma_{i,(k_1,k_2,k_3)}$ is infinitely small, so the average density over the thickness of the cell is used for $F_i(\mathbf{q})$ instead: $F_i(\mathbf{q}) = \frac{w_{\sigma,i}}{h_i \cdot \Delta c_i}$. Contrariwise, if $F_i(\mathbf{q})$ is known, then the weight assigned to $\sigma_{i,(k_1,k_2,k_3)}$ is $F_i(\mathbf{q}) \cdot h_i \cdot \Delta c_i$.

If length is being measured in meters (m), and weight is being measured using an arbitrary unit of measurement referred to as “w_units”, then the values of $\mathbf{F}(\mathbf{q})$ are measured in w_units/m (i.e. w_units per unit thickness).

7.5.4 Quantifying multi-volumes

A multi-volume U is quantified by a function $U(\mathbf{q})$ whose input is a position \mathbf{q} . In earlier sections, $U(\mathbf{q})$ was defined as the net number of volumes that contain position \mathbf{q} . This definition will remain, but an approximation of U using the cells $\Omega_{(k_1, k_2, k_3)}$ will be established.

For each triple (k_1, k_2, k_3) the weight assigned to cell $\Omega_{(k_1, k_2, k_3)}$ is the average value of $U(\mathbf{q})$ for all positions from said cell. This has the effect of “pixelating” U using the cells $\Omega_{(k_1, k_2, k_3)}$, as is depicted below. For all positions \mathbf{q} in cell (k_1, k_2, k_3) , the net number of volumes that contain \mathbf{q} is approximately the weight w_Ω assigned to the cell $\Omega_{(k_1, k_2, k_3)}$: $U(\mathbf{q}) \approx w_\Omega$. **This is the approximation that will be used for various calculations.**



If length is being measured in meters (m), and weight is being measured using an arbitrary unit of measurement referred to as “w_units”, then the value of $U(\mathbf{q})$ is also measured in w_units (no extra dimensions are added).

To simplify notation, unless explicitly included, the position parameter \mathbf{q} will be suppressed in the notation. Be mindful of the various quantities that do change with position.

7.6 Computing unions

Computing the unions of two multi-structures of the same type is obvious: just add the functions.

Theorem 26. *Given the two multi-points ρ and μ , the union is simply the sum of the functions:*

$$\rho + \mu = \rho(\mathbf{q}) + \mu(\mathbf{q})$$

Given the two multi-paths $\mathbf{J} = [i : J_i] = \begin{bmatrix} J_1 \\ J_2 \\ J_3 \end{bmatrix}$ and $\mathbf{K} = [i : K_i] = \begin{bmatrix} K_1 \\ K_2 \\ K_3 \end{bmatrix}$, the entries of the union is the sum of the corresponding entries from \mathbf{J} and \mathbf{K} :

$$\mathbf{J} + \mathbf{K} = \begin{bmatrix} J_1 \\ J_2 \\ J_3 \end{bmatrix} + \begin{bmatrix} K_1 \\ K_2 \\ K_3 \end{bmatrix} = \begin{bmatrix} J_1 + K_1 \\ J_2 + K_2 \\ J_3 + K_3 \end{bmatrix} = [i : J_i + K_i]$$

Given the two multi-surfaces $\mathbf{F} = [i : F_i] = \begin{bmatrix} F_1 \\ F_2 \\ F_3 \end{bmatrix}$ and $\mathbf{G} = [i : G_i] = \begin{bmatrix} G_1 \\ G_2 \\ G_3 \end{bmatrix}$, the entries of the union is the sum of the corresponding entries from \mathbf{F} and \mathbf{G} :

$$\mathbf{F} + \mathbf{G} = \begin{bmatrix} F_1 \\ F_2 \\ F_3 \end{bmatrix} + \begin{bmatrix} G_1 \\ G_2 \\ G_3 \end{bmatrix} = \begin{bmatrix} F_1 + G_1 \\ F_2 + G_2 \\ F_3 + G_3 \end{bmatrix} = [i : F_i + G_i]$$

Given the two multi-volumes U and T , the union is simply the sum of the functions:

$$U + T = U(\mathbf{q}) + T(\mathbf{q})$$

7.7 Computing intersections

7.7.1 Computing intersections involving a multi-volume

Consider a multi-volume T , and either a multi-point ρ , a multi-path $\mathbf{J} = [i : J_i(\mathbf{q})] = \begin{bmatrix} J_1(\mathbf{q}) \\ J_2(\mathbf{q}) \\ J_3(\mathbf{q}) \end{bmatrix}$, a multi-surface $\mathbf{F} = [i : F_i(\mathbf{q})] = \begin{bmatrix} F_1(\mathbf{q}) \\ F_2(\mathbf{q}) \\ F_3(\mathbf{q}) \end{bmatrix}$, or another multi-volume U . The intersection with T is easy to compute, as $T(\mathbf{q})$ is multiplier that is applied to all weights at point \mathbf{q} . The value of the function at each point is multiplied by $T(\mathbf{q})$:

Theorem 27.

$$\begin{aligned} \rho \cdot T &= \rho(\mathbf{q}) \cdot T(\mathbf{q}) & \mathbf{J} \cdot T &= [i : J_i(\mathbf{q}) \cdot T(\mathbf{q})] = \begin{bmatrix} J_1(\mathbf{q}) \cdot T(\mathbf{q}) \\ J_2(\mathbf{q}) \cdot T(\mathbf{q}) \\ J_3(\mathbf{q}) \cdot T(\mathbf{q}) \end{bmatrix} \\ \mathbf{F} \cdot T &= [i : F_i(\mathbf{q}) \cdot T(\mathbf{q})] = \begin{bmatrix} F_1(\mathbf{q}) \cdot T(\mathbf{q}) \\ F_2(\mathbf{q}) \cdot T(\mathbf{q}) \\ F_3(\mathbf{q}) \cdot T(\mathbf{q}) \end{bmatrix} & U \cdot T &= U(\mathbf{q}) \cdot T(\mathbf{q}) \end{aligned}$$

7.7.2 Computing path-surface intersections

Consider a multi-path $\mathbf{J} = [i : J_i] = \begin{bmatrix} J_1 \\ J_2 \\ J_3 \end{bmatrix}$ and a multi-surface $\mathbf{F} = [i : F_i] = \begin{bmatrix} F_1 \\ F_2 \\ F_3 \end{bmatrix}$. The multi-point intersection $\mathbf{J} \bullet \mathbf{F}$ can be computed as follows:

For simplicity, the parameter \mathbf{q} will be hidden in the notation.

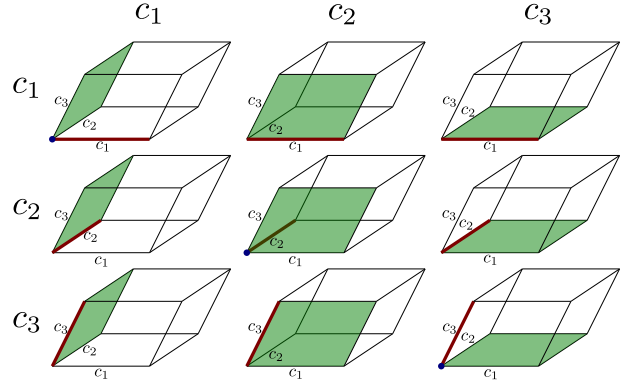
Consider an arbitrary point \mathbf{q} , and let (k_1, k_2, k_3) index the cell at \mathbf{q} .

For each $i = 1, 2, 3$, the weight assigned to the lattice edge $\alpha_{i,(k_1,k_2,k_3)}$ by \mathbf{J} is the path density J_i multiplied by the cross sectional area of the cell to get $J_i \cdot B_i \cdot \Delta c_{i+1} \Delta c_{i+2}$.

For each $j = 1, 2, 3$, the weight assigned to the lattice tile $\sigma_{j,(k_1,k_2,k_3)}$ by \mathbf{F} is the surface density F_j multiplied by the thickness of the cell to get $F_j \cdot h_j \cdot \Delta c_j$.

When $i = j$, the intersection of $\alpha_{i,(k_1,k_2,k_3)}$ with $\sigma_{j,(k_1,k_2,k_3)}$ is the lattice point $\theta_{(k_1,k_2,k_3)}$ (as depicted on the right). The total weight of this intersection is:

$$\begin{aligned} & (J_i \cdot B_i \cdot \Delta c_{i+1} \Delta c_{i+2}) \cdot (F_i \cdot h_i \cdot \Delta c_i) \\ &= J_i F_i B_i h_i \Delta c_i \Delta c_{i+1} \Delta c_{i+2} \\ &= J_i F_i B_i h_i \Delta c_1 \Delta c_2 \Delta c_3 \end{aligned}$$



intersection points.

When $i \neq j$, these paths and surfaces are parallel and no intersections take place.

In summary,

$$\alpha_{i,(k_1,k_2,k_3)} \bullet \sigma_{j,(k_1,k_2,k_3)} = \begin{cases} \theta_{(k_1,k_2,k_3)} & (i = j) \\ 0 & (i \neq j) \end{cases}$$

The total weight of point $\theta_{(k_1,k_2,k_3)}$ is:

$$J_1 F_1 B_1 h_1 \Delta c_1 \Delta c_2 \Delta c_3 + J_2 F_2 B_2 h_2 \Delta c_1 \Delta c_2 \Delta c_3 + J_3 F_3 B_3 h_3 \Delta c_1 \Delta c_2 \Delta c_3 = \left(\sum_i J_i F_i B_i h_i \right) \Delta c_1 \Delta c_2 \Delta c_3$$

The density over the current cell is the point weight divided by the volume:

$$\frac{(\sum_i J_i F_i B_i h_i) \Delta c_1 \Delta c_2 \Delta c_3}{V \Delta c_1 \Delta c_2 \Delta c_3} = \sum_i J_i F_i \frac{B_i h_i}{V}$$

The intersection is therefore:

Theorem 28.

$$\mathbf{J} \bullet \mathbf{F} = \begin{bmatrix} J_1 \\ J_2 \\ J_3 \end{bmatrix} \bullet \begin{bmatrix} F_1 \\ F_2 \\ F_3 \end{bmatrix} = \frac{B_1 h_1}{V} J_1 F_1 + \frac{B_2 h_2}{V} J_2 F_2 + \frac{B_3 h_3}{V} J_3 F_3 = \sum_i \frac{B_i h_i}{V} J_i F_i$$

7.7.3 Computing surface-surface intersections

Consider the multi-surfaces $\mathbf{F} = [i : F_i] = \begin{bmatrix} F_1 \\ F_2 \\ F_3 \end{bmatrix}$ and $\mathbf{G} = [i : G_i] = \begin{bmatrix} G_1 \\ G_2 \\ G_3 \end{bmatrix}$. The multi-path intersection

$\mathbf{F} \times \mathbf{G}$ can be computed as follows:

For simplicity, the parameter \mathbf{q} will be hidden in the notation.

Consider an arbitrary point \mathbf{q} , and let (k_1, k_2, k_3) index the cell at \mathbf{q} .

For each $i = 1, 2, 3$, the weight assigned to the lattice tile $\sigma_{i,(k_1,k_2,k_3)}$ by \mathbf{F} is the surface density F_i multiplied by the thickness of the cell to get $F_i \cdot h_i \cdot \Delta c_i$.

For each $j = 1, 2, 3$, the weight assigned to the lattice tile $\sigma_{j,(k_1,k_2,k_3)}$ by \mathbf{G} is the surface density G_j multiplied by the thickness of the cell to get $G_j \cdot h_j \cdot \Delta c_j$.

When $i = j$, the lattice tiles $\sigma_{i,(k_1,k_2,k_3)}$ and $\sigma_{j,(k_1,k_2,k_3)}$ are parallel (as depicted on the right), and there is no intersection.

When $i \neq j$, the lattice tiles $\sigma_{i,(k_1,k_2,k_3)}$ and $\sigma_{j,(k_1,k_2,k_3)}$ intersect.

When $j = i + 1$, $\sigma_{i,(k_1,k_2,k_3)} \times \sigma_{i+1,(k_1,k_2,k_3)} = \alpha_{i+2,(k_1,k_2,k_3)}$, as depicted on the right.

When $j = i + 2$, $\sigma_{i,(k_1,k_2,k_3)} \times \sigma_{i+2,(k_1,k_2,k_3)} = -\alpha_{i+1,(k_1,k_2,k_3)}$, as depicted on the right. **Note the reversed orientation.**

In summary,

$$\sigma_{i,(k_1,k_2,k_3)} \times \sigma_{j,(k_1,k_2,k_3)} = \begin{cases} 0 & (j = i) \\ \alpha_{i+2,(k_1,k_2,k_3)} & (j = i + 1) \\ -\alpha_{i+1,(k_1,k_2,k_3)} & (j = i + 2) \end{cases}$$

Now putting everything together, for each index $i = 1, 2, 3$, the path $\alpha_{i,(k_1,k_2,k_3)}$ is the intersection of $\sigma_{i+1,(k_1,k_2,k_3)}$ with $\sigma_{i+2,(k_1,k_2,k_3)}$, as well as the reverse of the intersection of $\sigma_{i+2,(k_1,k_2,k_3)}$ with $\sigma_{i+1,(k_1,k_2,k_3)}$.

Since the weight of tile $\sigma_{j,(k_1,k_2,k_3)}$ is $F_j h_j \Delta c_j$ for \mathbf{F} , and $G_j h_j \Delta c_j$ for \mathbf{G} , the total weight of path $\alpha_{i,(k_1,k_2,k_3)}$ is:

$$\begin{aligned} & (F_{i+1} h_{i+1} \Delta c_{i+1})(G_{i+2} h_{i+2} \Delta c_{i+2}) - (F_{i+2} h_{i+2} \Delta c_{i+2})(G_{i+1} h_{i+1} \Delta c_{i+1}) \\ &= F_{i+1} G_{i+2} h_{i+1} h_{i+2} \Delta c_{i+1} \Delta c_{i+2} - F_{i+2} G_{i+1} h_{i+2} h_{i+1} \Delta c_{i+2} \Delta c_{i+1} \\ &= (F_{i+1} G_{i+2} - F_{i+2} G_{i+1}) h_{i+1} h_{i+2} \Delta c_{i+1} \Delta c_{i+2} \end{aligned}$$

The path density is the path weight divided by the cross sectional area:

$$\frac{(F_{i+1} G_{i+2} - F_{i+2} G_{i+1}) h_{i+1} h_{i+2} \Delta c_{i+1} \Delta c_{i+2}}{B_i \Delta c_{i+1} \Delta c_{i+2}} = (F_{i+1} G_{i+2} - F_{i+2} G_{i+1}) \frac{h_{i+1} h_{i+2}}{B_i}$$

The intersection is therefore:

Theorem 29.

$$\mathbf{F} \times \mathbf{G} = \begin{bmatrix} F_1 \\ F_2 \\ F_3 \end{bmatrix} \times \begin{bmatrix} G_1 \\ G_2 \\ G_3 \end{bmatrix} = \begin{bmatrix} \frac{h_2 h_3}{B_1} (F_2 G_3 - F_3 G_2) \\ \frac{h_3 h_1}{B_2} (F_3 G_1 - F_1 G_3) \\ \frac{h_1 h_2}{B_3} (F_1 G_2 - F_2 G_1) \end{bmatrix} = \left[i : \frac{h_{i+1} h_{i+2}}{B_i} (F_{i+1} G_{i+2} - F_{i+2} G_{i+1}) \right]$$

Summary

- Given a multi-path $\mathbf{J} = [i : J_i] = \begin{bmatrix} J_1 \\ J_2 \\ J_3 \end{bmatrix}$ and a multi-surface $\mathbf{F} = [i : F_i] = \begin{bmatrix} F_1 \\ F_2 \\ F_3 \end{bmatrix}$, then the intersection is the multi-point:

$$\mathbf{J} \bullet \mathbf{F} = \begin{bmatrix} J_1 \\ J_2 \\ J_3 \end{bmatrix} \bullet \begin{bmatrix} F_1 \\ F_2 \\ F_3 \end{bmatrix} = \frac{B_1 h_1}{V} J_1 F_1 + \frac{B_2 h_2}{V} J_2 F_2 + \frac{B_3 h_3}{V} J_3 F_3 = \sum_i \frac{B_i h_i}{V} J_i F_i$$

- Given multi-surfaces $\mathbf{F} = [i : F_i] = \begin{bmatrix} F_1 \\ F_2 \\ F_3 \end{bmatrix}$ and $\mathbf{G} = [i : G_i] = \begin{bmatrix} G_1 \\ G_2 \\ G_3 \end{bmatrix}$, then the intersection is the multi-path:

$$\mathbf{F} \times \mathbf{G} = \begin{bmatrix} F_1 \\ F_2 \\ F_3 \end{bmatrix} \times \begin{bmatrix} G_1 \\ G_2 \\ G_3 \end{bmatrix} = \begin{bmatrix} \frac{h_2 h_3}{B_1} (F_2 G_3 - F_3 G_2) \\ \frac{h_3 h_1}{B_2} (F_3 G_1 - F_1 G_3) \\ \frac{h_1 h_2}{B_3} (F_1 G_2 - F_2 G_1) \end{bmatrix} = \left[i : \frac{h_{i+1} h_{i+2}}{B_i} (F_{i+1} G_{i+2} - F_{i+2} G_{i+1}) \right]$$

7.8 Computing boundaries

Given a function $f(c_1, c_2, c_3)$, the notation $\frac{\partial}{\partial c_1}(f(c_1, c_2, c_3))$ will denote the rate of change of the quantity $f(c_1, c_2, c_3)$ with respect to c_1 . Similar notation exists for c_2 and c_3 , respectively $\frac{\partial}{\partial c_2}(f(c_1, c_2, c_3))$ and $\frac{\partial}{\partial c_3}(f(c_1, c_2, c_3))$.

More specifically,

$$\frac{\partial}{\partial c_1}(f(c_1, c_2, c_3)) = \frac{f(c_1, c_2, c_3) - f(c_1 - \Delta c_1, c_2, c_3)}{\Delta c_1}$$

is the change in $f(c_1, c_2, c_3)$ between **adjacent cells** in principal direction 1 divided by the change in c_1 .

$$\frac{\partial}{\partial c_2}(f(c_1, c_2, c_3)) = \frac{f(c_1, c_2, c_3) - f(c_1, c_2 - \Delta c_2, c_3)}{\Delta c_2}$$

is the change in $f(c_1, c_2, c_3)$ between **adjacent cells** in principal direction 2 divided by the change in c_2 .

$$\frac{\partial}{\partial c_3}(f(c_1, c_2, c_3)) = \frac{f(c_1, c_2, c_3) - f(c_1, c_2, c_3 - \Delta c_3)}{\Delta c_3}$$

is the change in $f(c_1, c_2, c_3)$ between **adjacent cells** in principal direction 3 divided by the change in c_3 .

7.8.1 Computing path endpoints

Consider the multi-path $\mathbf{J} = [i : J_i] = \begin{bmatrix} J_1 \\ J_2 \\ J_3 \end{bmatrix}$. The multi-point end points $\nabla \bullet \mathbf{J}$ can be computed as follows:

Let (c_1, c_2, c_3) denote an arbitrary position, and let (k_1, k_2, k_3) index the cell that contains (c_1, c_2, c_3) . The lattice line segments $\alpha_{1,(k_1, k_2, k_3)}$, $\alpha_{1,(k_1-1, k_2, k_3)}$, $\alpha_{2,(k_1, k_2, k_3)}$, $\alpha_{2,(k_1, k_2-1, k_3)}$, $\alpha_{3,(k_1, k_2, k_3)}$, and $\alpha_{3,(k_1, k_2, k_3-1)}$ have endpoints at $\theta_{(k_1, k_2, k_3)}$.

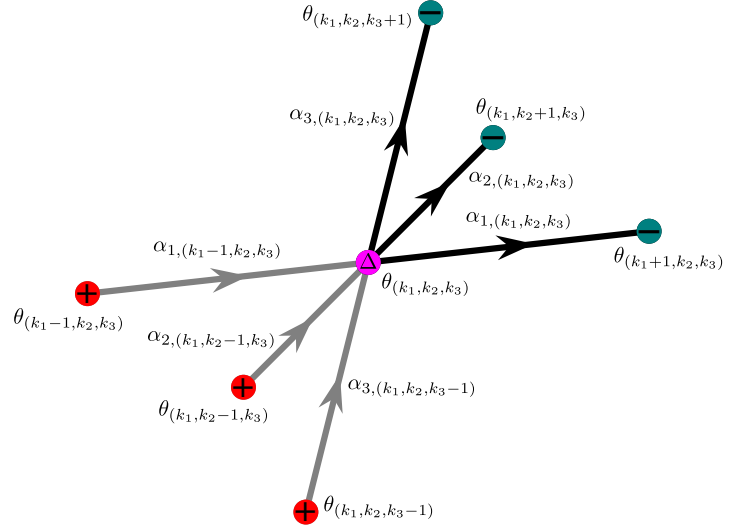
The weights of these paths are:

- The weight of $\alpha_{1,(k_1, k_2, k_3)}$ is $J_1(c_1, c_2, c_3)B_1(c_1, c_2, c_3)\Delta c_2\Delta c_3$
- The weight of $\alpha_{1,(k_1-1, k_2, k_3)}$ is $J_1(c_1 - \Delta c_1, c_2, c_3)B_1(c_1 - \Delta c_1, c_2, c_3)\Delta c_2\Delta c_3$
- The weight of $\alpha_{2,(k_1, k_2, k_3)}$ is $J_2(c_1, c_2, c_3)B_2(c_1, c_2, c_3)\Delta c_3\Delta c_1$
- The weight of $\alpha_{2,(k_1, k_2-1, k_3)}$ is $J_2(c_1, c_2 - \Delta c_2, c_3)B_2(c_1, c_2 - \Delta c_2, c_3)\Delta c_3\Delta c_1$
- The weight of $\alpha_{3,(k_1, k_2, k_3)}$ is $J_3(c_1, c_2, c_3)B_3(c_1, c_2, c_3)\Delta c_1\Delta c_2$
- The weight of $\alpha_{3,(k_1, k_2, k_3-1)}$ is $J_3(c_1, c_2, c_3 - \Delta c_3)B_3(c_1, c_2, c_3 - \Delta c_3)\Delta c_1\Delta c_2$

The total endpoint weight at $\theta_{(k_1, k_2, k_3)}$ is

$$\begin{aligned}
& J_1(c_1, c_2, c_3)B_1(c_1, c_2, c_3)\Delta c_2\Delta c_3 - J_1(c_1 - \Delta c_1, c_2, c_3)B_1(c_1 - \Delta c_1, c_2, c_3)\Delta c_2\Delta c_3 \\
& + J_2(c_1, c_2, c_3)B_2(c_1, c_2, c_3)\Delta c_3\Delta c_1 - J_2(c_1, c_2 - \Delta c_2, c_3)B_2(c_1, c_2 - \Delta c_2, c_3)\Delta c_3\Delta c_1 \\
& + J_3(c_1, c_2, c_3)B_3(c_1, c_2, c_3)\Delta c_1\Delta c_2 - J_3(c_1, c_2, c_3 - \Delta c_3)B_3(c_1, c_2, c_3 - \Delta c_3)\Delta c_1\Delta c_2 \\
& = (J_1(c_1, c_2, c_3)B_1(c_1, c_2, c_3) - J_1(c_1 - \Delta c_1, c_2, c_3)B_1(c_1 - \Delta c_1, c_2, c_3))\Delta c_2\Delta c_3 \\
& + (J_2(c_1, c_2, c_3)B_2(c_1, c_2, c_3) - J_2(c_1, c_2 - \Delta c_2, c_3)B_2(c_1, c_2 - \Delta c_2, c_3))\Delta c_3\Delta c_1 \\
& + (J_3(c_1, c_2, c_3)B_3(c_1, c_2, c_3) - J_3(c_1, c_2, c_3 - \Delta c_3)B_3(c_1, c_2, c_3 - \Delta c_3))\Delta c_1\Delta c_2
\end{aligned}$$

On the right is shown how the endpoint weights of the line segment pairs $\alpha_{1, (k_1, k_2, k_3)}$ and $\alpha_{1, (k_1-1, k_2, k_3)}$; $\alpha_{2, (k_1, k_2, k_3)}$ and $\alpha_{2, (k_1, k_2-1, k_3)}$; and $\alpha_{3, (k_1, k_2, k_3)}$ and $\alpha_{3, (k_1, k_2, k_3-1)}$ partially cancel out at the vertex $\theta_{(k_1, k_2, k_3)}$.



Spreading the weight of $\theta_{(k_1, k_2, k_3)}$ over the volume of cell (k_1, k_2, k_3) gives:

$$\begin{aligned}
\nabla \bullet \mathbf{J} &= \frac{1}{V\Delta c_1\Delta c_2\Delta c_3} \left((J_1(c_1, c_2, c_3)B_1(c_1, c_2, c_3) - J_1(c_1 - \Delta c_1, c_2, c_3)B_1(c_1 - \Delta c_1, c_2, c_3))\Delta c_2\Delta c_3 \right. \\
&\quad + (J_2(c_1, c_2, c_3)B_2(c_1, c_2, c_3) - J_2(c_1, c_2 - \Delta c_2, c_3)B_2(c_1, c_2 - \Delta c_2, c_3))\Delta c_3\Delta c_1 \\
&\quad \left. + (J_3(c_1, c_2, c_3)B_3(c_1, c_2, c_3) - J_3(c_1, c_2, c_3 - \Delta c_3)B_3(c_1, c_2, c_3 - \Delta c_3))\Delta c_1\Delta c_2 \right) \\
&= \frac{1}{V} \left(\frac{J_1(c_1, c_2, c_3)B_1(c_1, c_2, c_3) - J_1(c_1 - \Delta c_1, c_2, c_3)B_1(c_1 - \Delta c_1, c_2, c_3)}{\Delta c_1} \right. \\
&\quad + \frac{J_2(c_1, c_2, c_3)B_2(c_1, c_2, c_3) - J_2(c_1, c_2 - \Delta c_2, c_3)B_2(c_1, c_2 - \Delta c_2, c_3)}{\Delta c_2} \\
&\quad \left. + \frac{J_3(c_1, c_2, c_3)B_3(c_1, c_2, c_3) - J_3(c_1, c_2, c_3 - \Delta c_3)B_3(c_1, c_2, c_3 - \Delta c_3)}{\Delta c_3} \right) \\
&= \frac{1}{V} \left(\frac{\partial}{\partial c_1}(J_1B_1) + \frac{\partial}{\partial c_2}(J_2B_2) + \frac{\partial}{\partial c_3}(J_3B_3) \right)
\end{aligned}$$

Therefore:

Theorem 30. The endpoints of multi-path $\mathbf{J} = [i : J_i] = \begin{bmatrix} J_1 \\ J_2 \\ J_3 \end{bmatrix}$ is the multi-point:

$$\nabla \bullet \mathbf{J} = \nabla \bullet \begin{bmatrix} J_1 \\ J_2 \\ J_3 \end{bmatrix} = \frac{1}{V} \left(\frac{\partial}{\partial c_1}(B_1J_1) + \frac{\partial}{\partial c_2}(B_2J_2) + \frac{\partial}{\partial c_3}(B_3J_3) \right) = \frac{1}{V} \sum_i \frac{\partial}{\partial c_i}(B_iJ_i)$$

7.8.2 Computing surface boundaries

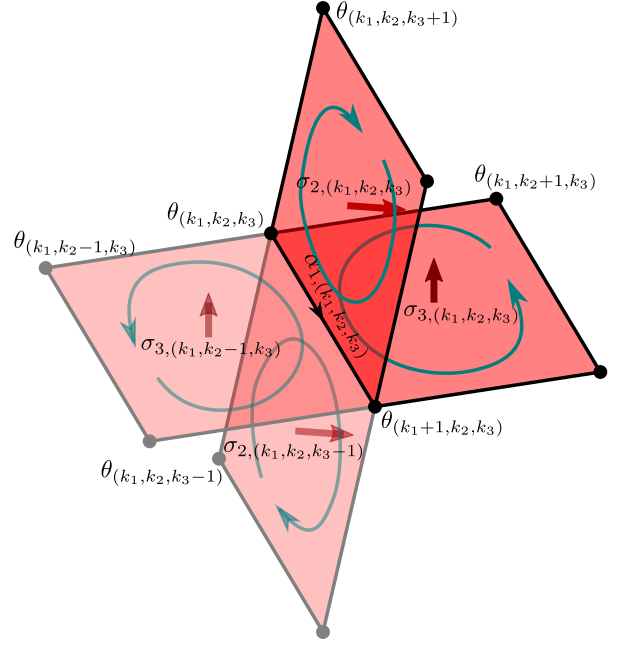
Consider the multi-surface $\mathbf{F} = [i : F_i] = \begin{bmatrix} F_1 \\ F_2 \\ F_3 \end{bmatrix}$. The multi-path boundary $\nabla \times \mathbf{F}$ can be computed as follows:

Let (c_1, c_2, c_3) denote an arbitrary position, and let (k_1, k_2, k_3) index the cell that contains (c_1, c_2, c_3) . For notational simplicity, the weight that the counter-clockwise boundary assigns to the lattice line segment $\alpha_{1,(k_1,k_2,k_3)}$ will be computed. The weights assigned to $\alpha_{2,(k_1,k_2,k_3)}$ and $\alpha_{3,(k_1,k_2,k_3)}$ can be computed in an exactly analogous manner.

The lattice tiles $\sigma_{3,(k_1,k_2,k_3)}$; $\sigma_{3,(k_1,k_2-1,k_3)}$; $\sigma_{2,(k_1,k_2,k_3)}$; and $\sigma_{2,(k_1,k_2,k_3-1)}$ have the lattice line segment $\alpha_{1,(k_1,k_2,k_3)}$ as part of their boundary, as depicted on the right. The weights of these tiles are respectively

- $F_3(c_1, c_2, c_3)h_3(c_1, c_2, c_3)\Delta c_3$
- $F_3(c_1, c_2 - \Delta c_2, c_3)h_3(c_1, c_2 - \Delta c_2, c_3)\Delta c_3$
- $F_2(c_1, c_2, c_3)h_2(c_1, c_2, c_3)\Delta c_2$
- $F_2(c_1, c_2, c_3 - \Delta c_3)h_2(c_1, c_2, c_3 - \Delta c_3)\Delta c_2$

From the image of the right, the counterclockwise boundaries of these tiles add to the weight of $\alpha_{1,(k_1,k_2,k_3)}$ in the case of $\sigma_{3,(k_1,k_2,k_3)}$ and $\sigma_{2,(k_1,k_2,k_3-1)}$, and subtract from the weight of $\alpha_{1,(k_1,k_2,k_3)}$ in the case of $\sigma_{3,(k_1,k_2-1,k_3)}$ and $\sigma_{2,(k_1,k_2,k_3)}$



The total weight of $\alpha_{1,(k_1,k_2,k_3)}$ is:

$$\begin{aligned} & F_3(c_1, c_2, c_3)h_3(c_1, c_2, c_3)\Delta c_3 - F_3(c_1, c_2 - \Delta c_2, c_3)h_3(c_1, c_2 - \Delta c_2, c_3)\Delta c_3 \\ & - F_2(c_1, c_2, c_3)h_2(c_1, c_2, c_3)\Delta c_2 + F_2(c_1, c_2, c_3 - \Delta c_3)h_2(c_1, c_2, c_3 - \Delta c_3)\Delta c_2 \\ & = (F_3(c_1, c_2, c_3)h_3(c_1, c_2, c_3) - F_3(c_1, c_2 - \Delta c_2, c_3)h_3(c_1, c_2 - \Delta c_2, c_3))\Delta c_3 \\ & - (F_2(c_1, c_2, c_3)h_2(c_1, c_2, c_3) - F_2(c_1, c_2, c_3 - \Delta c_3)h_2(c_1, c_2, c_3 - \Delta c_3))\Delta c_2 \end{aligned}$$

Spreading the weight of $\alpha_{1,(k_1,k_2,k_3)}$ over the cross sectional area of cell (k_1, k_2, k_3) gives:

$$\begin{aligned} & \frac{1}{B_1\Delta c_2\Delta c_3} \left((F_3(c_1, c_2, c_3)h_3(c_1, c_2, c_3) - F_3(c_1, c_2 - \Delta c_2, c_3)h_3(c_1, c_2 - \Delta c_2, c_3))\Delta c_3 \right. \\ & \quad \left. - (F_2(c_1, c_2, c_3)h_2(c_1, c_2, c_3) - F_2(c_1, c_2, c_3 - \Delta c_3)h_2(c_1, c_2, c_3 - \Delta c_3))\Delta c_2 \right) \\ & = \frac{1}{B_1} \left(\frac{F_3(c_1, c_2, c_3)h_3(c_1, c_2, c_3) - F_3(c_1, c_2 - \Delta c_2, c_3)h_3(c_1, c_2 - \Delta c_2, c_3)}{\Delta c_2} \right. \\ & \quad \left. - \frac{F_2(c_1, c_2, c_3)h_2(c_1, c_2, c_3) - F_2(c_1, c_2, c_3 - \Delta c_3)h_2(c_1, c_2, c_3 - \Delta c_3)}{\Delta c_3} \right) \\ & = \frac{1}{B_1} \left(\frac{\partial}{\partial c_2}(F_3h_3) - \frac{\partial}{\partial c_3}(F_2h_2) \right) \end{aligned}$$

Performing analogous calculations for $\alpha_{2,(k_1,k_2,k_3)}$ and $\alpha_{3,(k_1,k_2,k_3)}$ yields the general expression for the

path weight density at $\alpha_{i,(k_1,k_2,k_3)}$:

$$\frac{1}{B_i} \left(\frac{\partial}{\partial c_{i+1}} (F_{i+2} h_{i+2}) - \frac{\partial}{\partial c_{i+2}} (F_{i+1} h_{i+1}) \right)$$

Therefore:

Theorem 31. *The counterclockwise boundary of multi-surface $\mathbf{F} = [i : F_i] = \begin{bmatrix} F_1 \\ F_2 \\ F_3 \end{bmatrix}$ is the multi-path:*

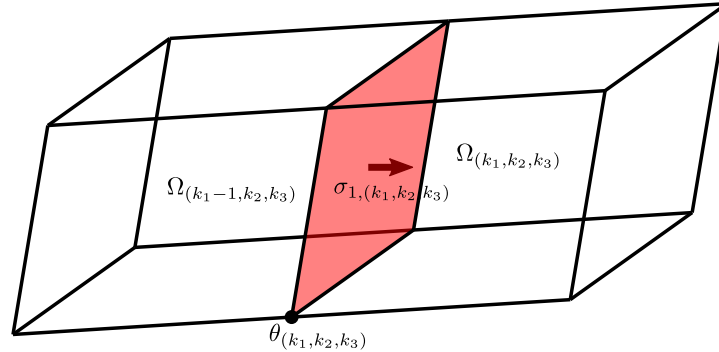
$$\nabla \times \mathbf{F} = \nabla \times \begin{bmatrix} F_1 \\ F_2 \\ F_3 \end{bmatrix} = \begin{bmatrix} \frac{1}{B_1} \left(\frac{\partial}{\partial c_2} (h_3 F_3) - \frac{\partial}{\partial c_3} (h_2 F_2) \right) \\ \frac{1}{B_2} \left(\frac{\partial}{\partial c_3} (h_1 F_1) - \frac{\partial}{\partial c_1} (h_3 F_3) \right) \\ \frac{1}{B_3} \left(\frac{\partial}{\partial c_1} (h_2 F_2) - \frac{\partial}{\partial c_2} (h_1 F_1) \right) \end{bmatrix} = \left[i : \frac{1}{B_i} \left(\frac{\partial}{\partial c_{i+1}} (h_{i+2} F_{i+2}) - \frac{\partial}{\partial c_{i+2}} (h_{i+1} F_{i+1}) \right) \right]$$

7.8.3 Computing volume surfaces

Consider the multi-volume U . The multi-surface inwards oriented surface ∇U can be computed as follows:

Let (c_1, c_2, c_3) denote an arbitrary position, and let (k_1, k_2, k_3) index the cell that contains (c_1, c_2, c_3) . For notational simplicity, the weight that the inwards-oriented surface assigns to the lattice tile $\sigma_{1,(k_1,k_2,k_3)}$ will be computed. The weights assigned to $\sigma_{2,(k_1,k_2,k_3)}$ and $\sigma_{3,(k_1,k_2,k_3)}$ can be computed in an exactly analogous manner.

The cell volumes $\Omega_{(k_1,k_2,k_3)}$ and $\Omega_{(k_1-1,k_2,k_3)}$ have the lattice tile $\sigma_{1,(k_1,k_2,k_3)}$ as part of their boundary, as depicted below.



The weights of these volumes are respectively $U(c_1, c_2, c_3)$ and $U(c_1 - \Delta c_1, c_2, c_3)$. The total weight of $\sigma_{1,(k_1,k_2,k_3)}$ is:

$$U(c_1, c_2, c_3) - U(c_1 - \Delta c_1, c_2, c_3)$$

Spreading the weight of $\sigma_{1,(k_1,k_2,k_3)}$ over the thickness of cell (k_1, k_2, k_3) gives:

$$\frac{1}{h_1 \Delta c_1} (U(c_1, c_2, c_3) - U(c_1 - \Delta c_1, c_2, c_3)) = \frac{1}{h_1} \frac{U(c_1, c_2, c_3) - U(c_1 - \Delta c_1, c_2, c_3)}{\Delta c_1} = \frac{1}{h_1} \frac{\partial}{\partial c_1} (U)$$

Performing analogous calculations for $\sigma_{2,(k_1,k_2,k_3)}$ and $\sigma_{3,(k_1,k_2,k_3)}$ yields the general expression for the surface weight density at $\sigma_{i,(k_1,k_2,k_3)}$:

$$\frac{1}{h_i} \frac{\partial}{\partial c_i} (U)$$

Therefore:

Theorem 32. *The inwards oriented surface of multi-volume U is the multi-surface:*

$$\nabla U = \begin{bmatrix} \frac{1}{h_1} \frac{\partial}{\partial c_1}(U) \\ \frac{1}{h_2} \frac{\partial}{\partial c_2}(U) \\ \frac{1}{h_3} \frac{\partial}{\partial c_3}(U) \end{bmatrix} = \left[i : \frac{1}{h_i} \frac{\partial}{\partial c_i}(U) \right]$$

Summary

- The endpoints of multi-path $\mathbf{J} = [i : J_i] = \begin{bmatrix} J_1 \\ J_2 \\ J_3 \end{bmatrix}$ is the multi-point:

$$\nabla \bullet \mathbf{J} = \nabla \bullet \begin{bmatrix} J_1 \\ J_2 \\ J_3 \end{bmatrix} = \frac{1}{V} \left(\frac{\partial}{\partial c_1}(B_1 J_1) + \frac{\partial}{\partial c_2}(B_2 J_2) + \frac{\partial}{\partial c_3}(B_3 J_3) \right) = \frac{1}{V} \sum_i \frac{\partial}{\partial c_i}(B_i J_i)$$

- The counterclockwise boundary of multi-surface $\mathbf{F} = [i : F_i] = \begin{bmatrix} F_1 \\ F_2 \\ F_3 \end{bmatrix}$ is the multi-path:

$$\nabla \times \mathbf{F} = \nabla \times \begin{bmatrix} F_1 \\ F_2 \\ F_3 \end{bmatrix} = \begin{bmatrix} \frac{1}{B_1} \left(\frac{\partial}{\partial c_2}(h_3 F_3) - \frac{\partial}{\partial c_3}(h_2 F_2) \right) \\ \frac{1}{B_2} \left(\frac{\partial}{\partial c_3}(h_1 F_1) - \frac{\partial}{\partial c_1}(h_3 F_3) \right) \\ \frac{1}{B_3} \left(\frac{\partial}{\partial c_1}(h_2 F_2) - \frac{\partial}{\partial c_2}(h_1 F_1) \right) \end{bmatrix} = \left[i : \frac{1}{B_i} \left(\frac{\partial}{\partial c_{i+1}}(h_{i+2} F_{i+2}) - \frac{\partial}{\partial c_{i+2}}(h_{i+1} F_{i+1}) \right) \right]$$

- The inwards oriented surface of multi-volume U is the multi-surface:

$$\nabla U = \begin{bmatrix} \frac{1}{h_1} \frac{\partial}{\partial c_1}(U) \\ \frac{1}{h_2} \frac{\partial}{\partial c_2}(U) \\ \frac{1}{h_3} \frac{\partial}{\partial c_3}(U) \end{bmatrix} = \left[i : \frac{1}{h_i} \frac{\partial}{\partial c_i}(U) \right]$$

7.9 Select Coordinate systems

The coordinate systems that will be considered are all **orthogonal**. This means that:

- The parallelepipeds are rectangular prisms: the principal directions are all mutually orthogonal.
- For each $i = 1, 2, 3$, the principal direction i is equivalent to the co-principal direction i .
- For each $i = 1, 2, 3$,

$$h_i = l_i$$

- For each $i = 1, 2, 3$,

$$B_i = A_i = l_{i+1} l_{i+2}$$

-

$$V = l_1 l_2 l_3$$

Only the quantities l_1 , l_2 , and l_3 need to be known.

The formulas for computing intersections and boundaries can be simplified in the case of orthogonal coordinate systems:

- Given a multi-path $\mathbf{J} = [i : J_i] = \begin{bmatrix} J_1 \\ J_2 \\ J_3 \end{bmatrix}$ and a multi-surface $\mathbf{F} = [i : F_i] = \begin{bmatrix} F_1 \\ F_2 \\ F_3 \end{bmatrix}$, then the intersection is the multi-point:

$$\mathbf{J} \bullet \mathbf{F} = \begin{bmatrix} J_1 \\ J_2 \\ J_3 \end{bmatrix} \bullet \begin{bmatrix} F_1 \\ F_2 \\ F_3 \end{bmatrix} = \frac{B_1 h_1}{V} J_1 F_1 + \frac{B_2 h_2}{V} J_2 F_2 + \frac{B_3 h_3}{V} J_3 F_3 = \sum_i \frac{B_i h_i}{V} J_i F_i$$

in the case of orthogonality,

$$\mathbf{J} \bullet \mathbf{F} = \begin{bmatrix} J_1 \\ J_2 \\ J_3 \end{bmatrix} \bullet \begin{bmatrix} F_1 \\ F_2 \\ F_3 \end{bmatrix} = J_1 F_1 + J_2 F_2 + J_3 F_3 = \sum_i J_i F_i$$

- Given multi-surfaces $\mathbf{F} = [i : F_i] = \begin{bmatrix} F_1 \\ F_2 \\ F_3 \end{bmatrix}$ and $\mathbf{G} = [i : G_i] = \begin{bmatrix} G_1 \\ G_2 \\ G_3 \end{bmatrix}$, then the intersection is the multi-path:

$$\mathbf{F} \times \mathbf{G} = \begin{bmatrix} F_1 \\ F_2 \\ F_3 \end{bmatrix} \times \begin{bmatrix} G_1 \\ G_2 \\ G_3 \end{bmatrix} = \begin{bmatrix} \frac{h_2 h_3}{B_1} (F_2 G_3 - F_3 G_2) \\ \frac{h_3 h_1}{B_2} (F_3 G_1 - F_1 G_3) \\ \frac{h_1 h_2}{B_3} (F_1 G_2 - F_2 G_1) \end{bmatrix} = \left[i : \frac{h_{i+1} h_{i+2}}{B_i} (F_{i+1} G_{i+2} - F_{i+2} G_{i+1}) \right]$$

in the case of orthogonality,

$$\mathbf{F} \times \mathbf{G} = \begin{bmatrix} F_1 \\ F_2 \\ F_3 \end{bmatrix} \times \begin{bmatrix} G_1 \\ G_2 \\ G_3 \end{bmatrix} = \begin{bmatrix} F_2 G_3 - F_3 G_2 \\ F_3 G_1 - F_1 G_3 \\ F_1 G_2 - F_2 G_1 \end{bmatrix} = [i : F_{i+1} G_{i+2} - F_{i+2} G_{i+1}]$$

- The endpoints of multi-path $\mathbf{J} = [i : J_i] = \begin{bmatrix} J_1 \\ J_2 \\ J_3 \end{bmatrix}$ is the multi-point:

$$\nabla \bullet \mathbf{J} = \nabla \bullet \begin{bmatrix} J_1 \\ J_2 \\ J_3 \end{bmatrix} = \frac{1}{V} \left(\frac{\partial}{\partial c_1} (B_1 J_1) + \frac{\partial}{\partial c_2} (B_2 J_2) + \frac{\partial}{\partial c_3} (B_3 J_3) \right) = \frac{1}{V} \sum_i \frac{\partial}{\partial c_i} (B_i J_i)$$

in the case of orthogonality,

$$\nabla \bullet \mathbf{J} = \nabla \bullet \begin{bmatrix} J_1 \\ J_2 \\ J_3 \end{bmatrix} = \frac{1}{l_1 l_2 l_3} \left(\frac{\partial}{\partial c_1} (l_2 l_3 J_1) + \frac{\partial}{\partial c_2} (l_3 l_1 J_2) + \frac{\partial}{\partial c_3} (l_1 l_2 J_3) \right) = \frac{1}{l_1 l_2 l_3} \sum_i \frac{\partial}{\partial c_i} (l_{i+1} l_{i+2} J_i)$$

- The counterclockwise boundary of multi-surface $\mathbf{F} = [i : F_i] = \begin{bmatrix} F_1 \\ F_2 \\ F_3 \end{bmatrix}$ is the multi-path:

$$\nabla \times \mathbf{F} = \nabla \times \begin{bmatrix} F_1 \\ F_2 \\ F_3 \end{bmatrix} = \begin{bmatrix} \frac{1}{B_1} \left(\frac{\partial}{\partial c_2} (h_3 F_3) - \frac{\partial}{\partial c_3} (h_2 F_2) \right) \\ \frac{1}{B_2} \left(\frac{\partial}{\partial c_3} (h_1 F_1) - \frac{\partial}{\partial c_1} (h_3 F_3) \right) \\ \frac{1}{B_3} \left(\frac{\partial}{\partial c_1} (h_2 F_2) - \frac{\partial}{\partial c_2} (h_1 F_1) \right) \end{bmatrix} = \left[i : \frac{1}{B_i} \left(\frac{\partial}{\partial c_{i+1}} (h_{i+2} F_{i+2}) - \frac{\partial}{\partial c_{i+2}} (h_{i+1} F_{i+1}) \right) \right]$$

in the case of orthogonality,

$$\nabla \times \mathbf{F} = \nabla \times \begin{bmatrix} F_1 \\ F_2 \\ F_3 \end{bmatrix} = \begin{bmatrix} \frac{1}{l_2 l_3} \left(\frac{\partial}{\partial c_2} (l_3 F_3) - \frac{\partial}{\partial c_3} (l_2 F_2) \right) \\ \frac{1}{l_3 l_1} \left(\frac{\partial}{\partial c_3} (l_1 F_1) - \frac{\partial}{\partial c_1} (l_3 F_3) \right) \\ \frac{1}{l_1 l_2} \left(\frac{\partial}{\partial c_1} (l_2 F_2) - \frac{\partial}{\partial c_2} (l_1 F_1) \right) \end{bmatrix} = \left[i : \frac{1}{l_{i+1} l_{i+2}} \left(\frac{\partial}{\partial c_{i+1}} (l_{i+2} F_{i+2}) - \frac{\partial}{\partial c_{i+2}} (l_{i+1} F_{i+1}) \right) \right]$$

- The inwards oriented surface of multi-volume U is the multi-surface:

$$\nabla U = \begin{bmatrix} \frac{1}{h_1} \frac{\partial}{\partial c_1} (U) \\ \frac{1}{h_2} \frac{\partial}{\partial c_2} (U) \\ \frac{1}{h_3} \frac{\partial}{\partial c_3} (U) \end{bmatrix} = \left[i : \frac{1}{h_i} \frac{\partial}{\partial c_i} (U) \right]$$

in the case of orthogonality,

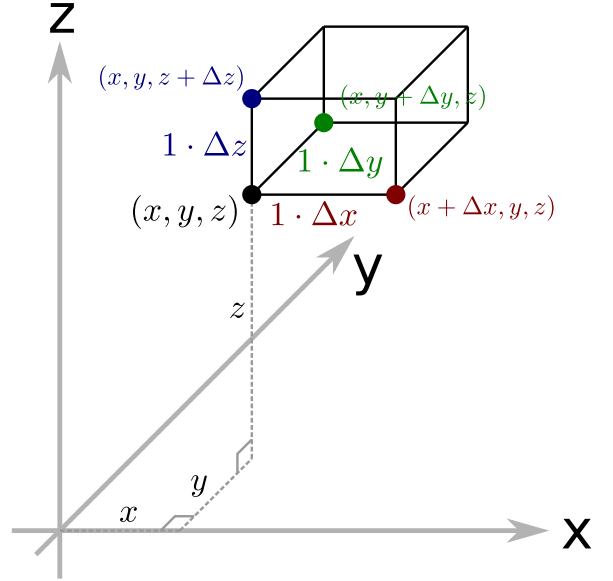
$$\nabla U = \begin{bmatrix} \frac{1}{l_1} \frac{\partial}{\partial c_1} (U) \\ \frac{1}{l_2} \frac{\partial}{\partial c_2} (U) \\ \frac{1}{l_3} \frac{\partial}{\partial c_3} (U) \end{bmatrix} = \left[i : \frac{1}{l_i} \frac{\partial}{\partial c_i} (U) \right]$$

7.9.1 Cartesian coordinates

The 3 coordinates used in **Cartesian coordinates** are $c_1 = x$, $c_2 = y$, and $c_3 = z$. Coordinate x is the displacement parallel to the x axis. Coordinate y is the displacement parallel to the y axis. Coordinate z is the displacement parallel to the z axis.

If (x, y, z) are the coordinates of a lattice vertex, then the dimensions of the cell prism at (x, y, z) are respectively: $1 \cdot \Delta x$; $1 \cdot \Delta y$; and $1 \cdot \Delta z$

From these dimensions, the following can be derived:



- Given a multi-path $\mathbf{J} = \begin{bmatrix} J_x \\ J_y \\ J_z \end{bmatrix}$ and a multi-surface $\mathbf{F} = \begin{bmatrix} F_x \\ F_y \\ F_z \end{bmatrix}$, then the intersection is the multi-point:

$$\mathbf{J} \bullet \mathbf{F} = \begin{bmatrix} J_x \\ J_y \\ J_z \end{bmatrix} \bullet \begin{bmatrix} F_x \\ F_y \\ F_z \end{bmatrix} = J_x F_x + J_y F_y + J_z F_z$$

- Given multi-surfaces $\mathbf{F} = \begin{bmatrix} F_x \\ F_y \\ F_z \end{bmatrix}$ and $\mathbf{G} = \begin{bmatrix} G_x \\ G_y \\ G_z \end{bmatrix}$, then the intersection is the multi-path:

$$\mathbf{F} \times \mathbf{G} = \begin{bmatrix} F_x \\ F_y \\ F_z \end{bmatrix} \times \begin{bmatrix} G_x \\ G_y \\ G_z \end{bmatrix} = \begin{bmatrix} F_y G_z - F_z G_y \\ F_z G_x - F_x G_z \\ F_x G_y - F_y G_x \end{bmatrix}$$

- The endpoints of multi-path $\mathbf{J} = \begin{bmatrix} J_x \\ J_y \\ J_z \end{bmatrix}$ is the multi-point:

$$\nabla \bullet \mathbf{J} = \nabla \bullet \begin{bmatrix} J_x \\ J_y \\ J_z \end{bmatrix} = \frac{\partial}{\partial x}(J_x) + \frac{\partial}{\partial y}(J_y) + \frac{\partial}{\partial z}(J_z)$$

- The counterclockwise boundary of multi-surface $\mathbf{F} = \begin{bmatrix} F_x \\ F_y \\ F_z \end{bmatrix}$ is the multi-path:

$$\nabla \times \mathbf{F} = \nabla \times \begin{bmatrix} F_x \\ F_y \\ F_z \end{bmatrix} = \begin{bmatrix} \frac{\partial}{\partial y}(F_z) - \frac{\partial}{\partial z}(F_y) \\ \frac{\partial}{\partial z}(F_x) - \frac{\partial}{\partial x}(F_z) \\ \frac{\partial}{\partial x}(F_y) - \frac{\partial}{\partial y}(F_x) \end{bmatrix}$$

- The inwards oriented surface of multi-volume U is the multi-surface:

$$\nabla U = \begin{bmatrix} \frac{\partial}{\partial x}(U) \\ \frac{\partial}{\partial y}(U) \\ \frac{\partial}{\partial z}(U) \end{bmatrix}$$

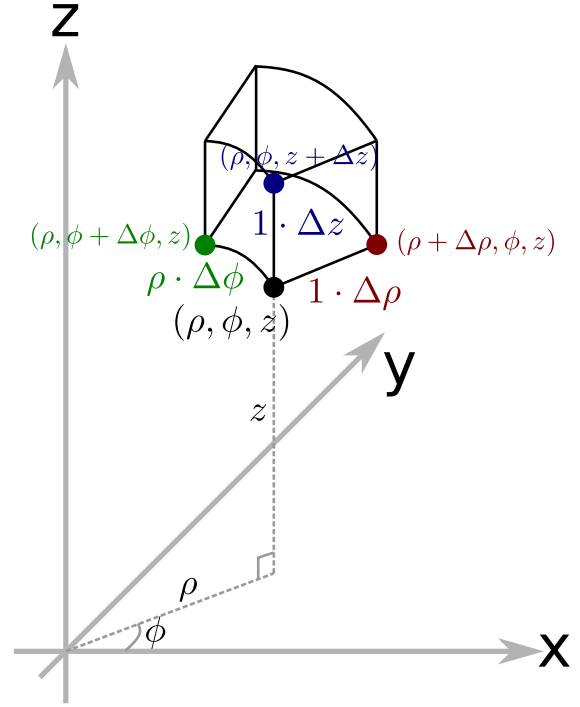
7.9.2 Cylindrical coordinates

The 3 coordinates used in **cylindrical coordinates** are $c_1 = \rho$, $c_2 = \phi$, and $c_3 = z$. Coordinate ρ is the perpendicular distance from the z -axis. Coordinate ϕ is the longitudinal coordinate (see the image on the right). Coordinate z is the displacement parallel to the z -axis, the same as the z coordinate from Cartesian coordinates.

If (ρ, ϕ, z) are the coordinates of a lattice vertex, then the dimensions of the cell prism at (ρ, ϕ, z) are respectively: $1 \cdot \Delta\rho$; $\rho \cdot \Delta\phi$; and $1 \cdot \Delta z$

When $\Delta\phi$ is large, the cell is not a prism, but has a curve as appears on the right. When $\Delta\phi$ is infinitely small however as is being assumed, then the cell becomes a rectangular prism.

From these dimensions, the following can be derived:



- Given a multi-path $\mathbf{J} = \begin{bmatrix} J_\rho \\ J_\phi \\ J_z \end{bmatrix}$ and a multi-surface $\mathbf{F} = \begin{bmatrix} F_\rho \\ F_\phi \\ F_z \end{bmatrix}$, then the intersection is the multi-point:

$$\mathbf{J} \bullet \mathbf{F} = \begin{bmatrix} J_\rho \\ J_\phi \\ J_z \end{bmatrix} \bullet \begin{bmatrix} F_\rho \\ F_\phi \\ F_z \end{bmatrix} = J_\rho F_\rho + J_\phi F_\phi + J_z F_z$$

- Given multi-surfaces $\mathbf{F} = \begin{bmatrix} F_x \\ F_y \\ F_z \end{bmatrix}$ and $\mathbf{G} = \begin{bmatrix} G_x \\ G_y \\ G_z \end{bmatrix}$, then the intersection is the multi-path:

$$\mathbf{F} \times \mathbf{G} = \begin{bmatrix} F_\rho \\ F_\phi \\ F_z \end{bmatrix} \times \begin{bmatrix} G_\rho \\ G_\phi \\ G_z \end{bmatrix} = \begin{bmatrix} F_\phi G_z - F_z G_\phi \\ F_z G_\rho - F_\rho G_z \\ F_\rho G_\phi - F_\phi G_\rho \end{bmatrix}$$

- The endpoints of multi-path $\mathbf{J} = \begin{bmatrix} J_\rho \\ J_\phi \\ J_z \end{bmatrix}$ is the multi-point:

$$\nabla \bullet \mathbf{J} = \nabla \bullet \begin{bmatrix} J_\rho \\ J_\phi \\ J_z \end{bmatrix} = \frac{1}{\rho} \left(\frac{\partial}{\partial \rho} (\rho \cdot J_\rho) + \frac{\partial}{\partial \phi} (J_\phi) + \frac{\partial}{\partial z} (\rho \cdot J_z) \right)$$

- The counterclockwise boundary of multi-surface $\mathbf{F} = \begin{bmatrix} F_\rho \\ F_\phi \\ F_z \end{bmatrix}$ is the multi-path:

$$\nabla \times \mathbf{F} = \nabla \times \begin{bmatrix} F_\rho \\ F_\phi \\ F_z \end{bmatrix} = \begin{bmatrix} \frac{1}{\rho} \left(\frac{\partial}{\partial \phi} (F_z) - \frac{\partial}{\partial z} (\rho \cdot F_\phi) \right) \\ \frac{\partial}{\partial z} (F_\rho) - \frac{\partial}{\partial \rho} (F_z) \\ \frac{1}{\rho} \left(\frac{\partial}{\partial \rho} (\rho \cdot F_\phi) - \frac{\partial}{\partial \phi} (F_\rho) \right) \end{bmatrix}$$

- The inwards oriented surface of multi-volume U is the multi-surface:

$$\nabla U = \begin{bmatrix} \frac{\partial}{\partial \rho} (U) \\ \frac{1}{\rho} \frac{\partial}{\partial \phi} (U) \\ \frac{\partial}{\partial z} (U) \end{bmatrix}$$

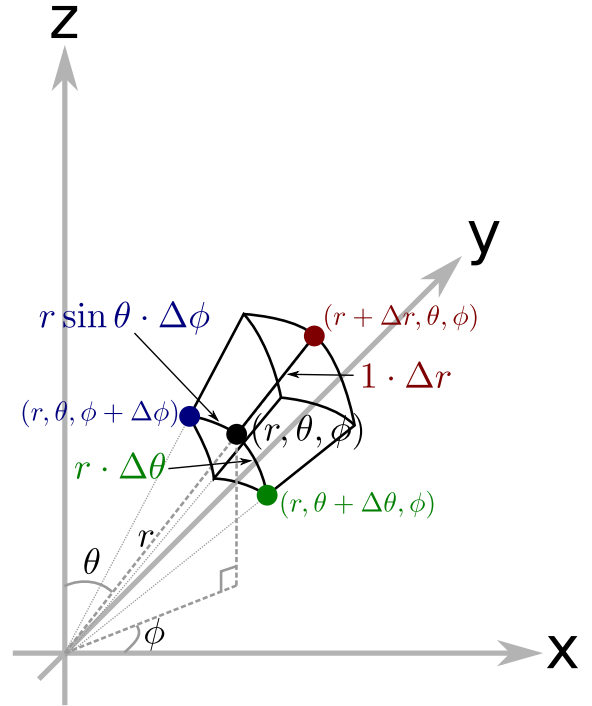
7.9.3 Spherical coordinates

The 3 coordinates used in **spherical coordinates** are $c_1 = r$, $c_2 = \theta$, and $c_3 = \phi$ (Here θ is a coordinate and does not refer to the vertex nodes from the lattice grid.). Coordinate r is the distance from the origin. Coordinate θ is the angle with the z axis (see the image on the right). Coordinate ϕ is the longitudinal coordinate, the same ϕ coordinate from cylindrical coordinates.

If (r, θ, ϕ) are the coordinates of a lattice vertex, then the dimensions of the cell prism at (r, θ, ϕ) are respectively: $1 \cdot \Delta r$; $r \cdot \Delta \theta$; and $r \sin \theta \cdot \Delta \phi$

When $\Delta \theta$ or $\Delta \phi$ is large, the cell is not a prism, but has a curve as appears on the right. When $\Delta \theta$ and $\Delta \phi$ are infinitely small however as is being assumed, then the cell becomes a rectangular prism.

From these dimensions, the following can be derived:



- Given a multi-path $\mathbf{J} = \begin{bmatrix} J_r \\ J_\theta \\ J_\phi \end{bmatrix}$ and a multi-surface $\mathbf{F} = \begin{bmatrix} F_r \\ F_\theta \\ F_\phi \end{bmatrix}$, then the intersection is the multi-point:

$$\mathbf{J} \bullet \mathbf{F} = \begin{bmatrix} J_r \\ J_\theta \\ J_\phi \end{bmatrix} \bullet \begin{bmatrix} F_r \\ F_\theta \\ F_\phi \end{bmatrix} = J_r F_r + J_\theta F_\theta + J_\phi F_\phi$$

- Given multi-surfaces $\mathbf{F} = \begin{bmatrix} F_r \\ F_\theta \\ F_\phi \end{bmatrix}$ and $\mathbf{G} = \begin{bmatrix} G_r \\ G_\theta \\ G_\phi \end{bmatrix}$, then the intersection is the multi-path:

$$\mathbf{F} \times \mathbf{G} = \begin{bmatrix} F_r \\ F_\theta \\ F_\phi \end{bmatrix} \times \begin{bmatrix} G_r \\ G_\theta \\ G_\phi \end{bmatrix} = \begin{bmatrix} F_\theta G_\phi - F_\phi G_\theta \\ F_\phi G_r - F_r G_\phi \\ F_r G_\theta - F_\theta G_r \end{bmatrix}$$

- The endpoints of multi-path $\mathbf{J} = \begin{bmatrix} J_r \\ J_\theta \\ J_\phi \end{bmatrix}$ is the multi-point:

$$\nabla \bullet \mathbf{J} = \nabla \bullet \begin{bmatrix} J_r \\ J_\theta \\ J_\phi \end{bmatrix} = \frac{1}{r^2 \sin \theta} \left(\frac{\partial}{\partial r} (r^2 \sin \theta \cdot J_r) + \frac{\partial}{\partial \theta} (r \sin \theta \cdot J_\theta) + \frac{\partial}{\partial \phi} (r \cdot J_\phi) \right)$$

- The counterclockwise boundary of multi-surface $\mathbf{F} = \begin{bmatrix} F_r \\ F_\theta \\ F_\phi \end{bmatrix}$ is the multi-path:

$$\nabla \times \mathbf{F} = \nabla \times \begin{bmatrix} F_r \\ F_\theta \\ F_\phi \end{bmatrix} = \begin{bmatrix} \frac{1}{r^2 \sin \theta} \left(\frac{\partial}{\partial \theta} (r \sin \theta \cdot F_\phi) - \frac{\partial}{\partial \phi} (r \cdot F_\theta) \right) \\ \frac{1}{r \sin \theta} \left(\frac{\partial}{\partial \phi} (F_r) - \frac{\partial}{\partial r} (r \sin \theta \cdot F_\phi) \right) \\ \frac{1}{r} \left(\frac{\partial}{\partial r} (r \cdot F_\theta) - \frac{\partial}{\partial \theta} (F_r) \right) \end{bmatrix}$$

- The inwards oriented surface of multi-volume U is the multi-surface:

$$\nabla U = \begin{bmatrix} \frac{\partial}{\partial r} (U) \\ \frac{1}{r} \frac{\partial}{\partial \theta} (U) \\ \frac{1}{r \sin \theta} \frac{\partial}{\partial \phi} (U) \end{bmatrix}$$

7.10 Summary

- Consider a multi-point that is quantified by the function $\rho(\mathbf{q})$. The weight assigned to the lattice node $\theta_{(k_1, k_2, k_3)}$ belonging to the cell that contains \mathbf{q} , is:

$$w_\theta = \rho(\mathbf{q}) \cdot (V \Delta c_1 \Delta c_2 \Delta c_3)$$

- Consider a multi-path that is quantified by the vector-valued function $\mathbf{J}(\mathbf{q}) = \begin{bmatrix} J_1(\mathbf{q}) \\ J_2(\mathbf{q}) \\ J_3(\mathbf{q}) \end{bmatrix}$. For each $i = 1, 2, 3$, the weight assigned to the lattice edge $\alpha_{i, (k_1, k_2, k_3)}$ belonging to the cell that contains \mathbf{q} , is:

$$w_{\alpha, i} = J_i(\mathbf{q}) \cdot (B_i \Delta c_{i+1} \Delta c_{i+2})$$

- Consider a multi-surface that is quantified by the vector-valued function $\mathbf{F}(\mathbf{q}) = \begin{bmatrix} F_1(\mathbf{q}) \\ F_2(\mathbf{q}) \\ F_3(\mathbf{q}) \end{bmatrix}$. For each $i = 1, 2, 3$, the weight assigned to the lattice tile $\sigma_{i, (k_1, k_2, k_3)}$ belonging to the cell that contains \mathbf{q} , is:

$$w_{\sigma, i} = F_i(\mathbf{q}) \cdot (h_i \Delta c_i)$$

- Consider a multi-volume that is quantified by the function $U(\mathbf{q})$. The weight assigned to the lattice cell $\Omega_{(k_1, k_2, k_3)}$ belonging to the cell that contains \mathbf{q} , is:

$$w_\Omega = U(\mathbf{q})$$

From these quantities, the following quantities were derived (the parameter \mathbf{q} will be omitted for simplicity):

| Quantity 1 | Quantity 2 | Computed quantity |
|---|---|--|
| Path $\mathbf{J} = \begin{bmatrix} J_1 \\ J_2 \\ J_3 \end{bmatrix}$ | Surface $\mathbf{F} = \begin{bmatrix} F_1 \\ F_2 \\ F_3 \end{bmatrix}$ | Intersection point (general): $\mathbf{J} \bullet \mathbf{F} = \sum_i \frac{B_i h_i}{V} J_i F_i = \frac{B_1 h_1}{V} J_1 F_1 + \frac{B_2 h_2}{V} J_2 F_2 + \frac{B_3 h_3}{V} J_3 F_3$ Intersection point (orthogonal): $\mathbf{J} \bullet \mathbf{F} = \sum_i J_i F_i = J_1 F_1 + J_2 F_2 + J_3 F_3$ |
| Surface $\mathbf{F} = \begin{bmatrix} F_1 \\ F_2 \\ F_3 \end{bmatrix}$ | Surface $\mathbf{G} = \begin{bmatrix} G_1 \\ G_2 \\ G_3 \end{bmatrix}$ | Intersection path (general): $\mathbf{F} \times \mathbf{G} = \left[i : \frac{h_{i+1} h_{i+2}}{B_i} (F_{i+1} G_{i+2} - F_{i+2} G_{i+1}) \right]$ $= \begin{bmatrix} \frac{h_2 h_3}{B_1} (F_2 G_3 - F_3 G_2) \\ \frac{h_3 h_1}{B_2} (F_3 G_1 - F_1 G_3) \\ \frac{h_1 h_2}{B_3} (F_1 G_2 - F_2 G_1) \end{bmatrix}$ Intersection path (orthogonal): $\mathbf{F} \times \mathbf{G} = [i : F_{i+1} G_{i+2} - F_{i+2} G_{i+1}]$ $= \begin{bmatrix} F_2 G_3 - F_3 G_2 \\ F_3 G_1 - F_1 G_3 \\ F_1 G_2 - F_2 G_1 \end{bmatrix}$ |

| Quantity | Computed quantity |
|--|---|
| Path $\mathbf{J} = \begin{bmatrix} J_1 \\ J_2 \\ J_3 \end{bmatrix}$ | Endpoints (general): $\nabla \bullet \mathbf{J} = \frac{1}{V} \sum_i \frac{\partial}{\partial c_i} (B_i J_i)$ $= \frac{1}{V} \left(\frac{\partial}{\partial c_1} (B_1 J_1) + \frac{\partial}{\partial c_2} (B_2 J_2) + \frac{\partial}{\partial c_3} (B_3 J_3) \right)$ Endpoints (orthogonal): $\nabla \bullet \mathbf{J} = \frac{1}{l_1 l_2 l_3} \sum_i \frac{\partial}{\partial c_i} (l_{i+1} l_{i+2} J_i)$ $= \frac{1}{l_1 l_2 l_3} \left(\frac{\partial}{\partial c_1} (l_2 l_3 J_1) + \frac{\partial}{\partial c_2} (l_3 l_1 J_2) + \frac{\partial}{\partial c_3} (l_1 l_2 J_3) \right)$ |

| | |
|---|--|
| <p>Surface</p> $\mathbf{F} = \begin{bmatrix} F_1 \\ F_2 \\ F_3 \end{bmatrix}$ | <p>Boundary (general):</p> $\begin{aligned} \nabla \times \mathbf{F} &= \left[i : \frac{1}{B_i} \left(\frac{\partial}{\partial c_{i+1}} (h_{i+2} F_{i+2}) - \frac{\partial}{\partial c_{i+2}} (h_{i+1} F_{i+1}) \right) \right] \\ &= \begin{bmatrix} \frac{1}{B_1} \left(\frac{\partial}{\partial c_2} (h_3 F_3) - \frac{\partial}{\partial c_3} (h_2 F_2) \right) \\ \frac{1}{B_2} \left(\frac{\partial}{\partial c_3} (h_1 F_1) - \frac{\partial}{\partial c_1} (h_3 F_3) \right) \\ \frac{1}{B_3} \left(\frac{\partial}{\partial c_1} (h_2 F_2) - \frac{\partial}{\partial c_2} (h_1 F_1) \right) \end{bmatrix} \end{aligned}$ <p>Boundary (orthogonal):</p> $\begin{aligned} \nabla \times \mathbf{F} &= \left[i : \frac{1}{l_{i+1} l_{i+2}} \left(\frac{\partial}{\partial c_{i+1}} (l_{i+2} F_{i+2}) - \frac{\partial}{\partial c_{i+2}} (l_{i+1} F_{i+1}) \right) \right] \\ &= \begin{bmatrix} \frac{1}{l_2 l_3} \left(\frac{\partial}{\partial c_2} (l_3 F_3) - \frac{\partial}{\partial c_3} (l_2 F_2) \right) \\ \frac{1}{l_3 l_1} \left(\frac{\partial}{\partial c_3} (l_1 F_1) - \frac{\partial}{\partial c_1} (l_3 F_3) \right) \\ \frac{1}{l_1 l_2} \left(\frac{\partial}{\partial c_1} (l_2 F_2) - \frac{\partial}{\partial c_2} (l_1 F_1) \right) \end{bmatrix} \end{aligned}$ |
| <p>Volume</p> U | <p>Surface (general):</p> $\nabla U = \left[i : \frac{1}{h_i} \frac{\partial}{\partial c_i} (U) \right] = \begin{bmatrix} \frac{1}{h_1} \frac{\partial}{\partial c_1} (U) \\ \frac{1}{h_2} \frac{\partial}{\partial c_2} (U) \\ \frac{1}{h_3} \frac{\partial}{\partial c_3} (U) \end{bmatrix}$ <p>Surface (orthogonal):</p> $\nabla U = \left[i : \frac{1}{l_i} \frac{\partial}{\partial c_i} (U) \right] = \begin{bmatrix} \frac{1}{l_1} \frac{\partial}{\partial c_1} (U) \\ \frac{1}{l_2} \frac{\partial}{\partial c_2} (U) \\ \frac{1}{l_3} \frac{\partial}{\partial c_3} (U) \end{bmatrix}$ |

Chapter 8

Duality

This section will now establish the connection that exists between multi-paths and multi-surfaces that will henceforth be referred to as “duality”.

8.1 Point-volume duality

To quantify a multi-point ρ , at each position \mathbf{q} only one value $\rho(\mathbf{q})$ is required.

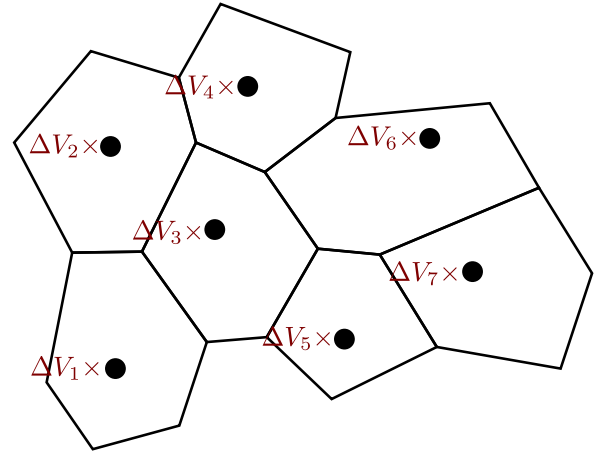
To quantify a multi-volume U , at each position \mathbf{q} only one value $U(\mathbf{q})$ is also required.

The fact that multi-points and multi-volumes both only require 1 value suggests that points and volumes can be “interchanged”. When a multi-point and a multi-volume are interchangeable, they will be referred to as being “dual” to each other.

Given a point P with an **infinitesimal** weight of w , then the volume that is “dual” to P is an infinitesimal volume Ω that both contains P and has a volume of w .

Given an **infinitesimal** volume Ω with a volume of ΔV , then the point that is “dual” to Ω is a point P that is contained by Ω and has a weight of ΔV .

Consider a multi-volume U . Multi-volume U consists of a single volume with a weight of 1. The multi-point ρ that is “dual” to Ω is a uniform “cloud” of points each with an infinitesimal weight. The average total weight per unit volume is 1. In the image on the right, a large volume is shattered into infinitesimal volumes, each shard of which is dual to point with a weight equal to the volume of said shard.



While there is no unique way of exactly placing the dual points or sketching the dual volumes, once “smoothing” has been applied none of this matters.

Given a multi-volume U , the multi-point ρ that is “dual” to U will be denoted via the notation:

$$\rho = \iota(U)$$

or conversely,

$$U = \iota^{-1}(\rho)$$

The following is important to note:

- The dual of the union is the union of the duals:

$$\iota(U_1 + U_2) = \iota(U_1) + \iota(U_2) \quad \text{and} \quad \iota^{-1}(\rho_1 + \rho_2) = \iota^{-1}(\rho_1) + \iota^{-1}(\rho_2)$$

If c is an arbitrary real valued coefficient, then:

$$\iota(c \cdot U) = c \cdot \iota(U) \quad \text{and} \quad \iota^{-1}(c \cdot \rho) = c \cdot \iota^{-1}(\rho)$$

8.2 Path-surface duality

To quantify a multi-path \mathbf{J} , at each position \mathbf{q} three values $\begin{bmatrix} J_1(\mathbf{q}) \\ J_2(\mathbf{q}) \\ J_3(\mathbf{q}) \end{bmatrix}$ are required.

To quantify a multi-surface \mathbf{F} , at each position \mathbf{q} three values $\begin{bmatrix} F_1(\mathbf{q}) \\ F_2(\mathbf{q}) \\ F_3(\mathbf{q}) \end{bmatrix}$ are also required.

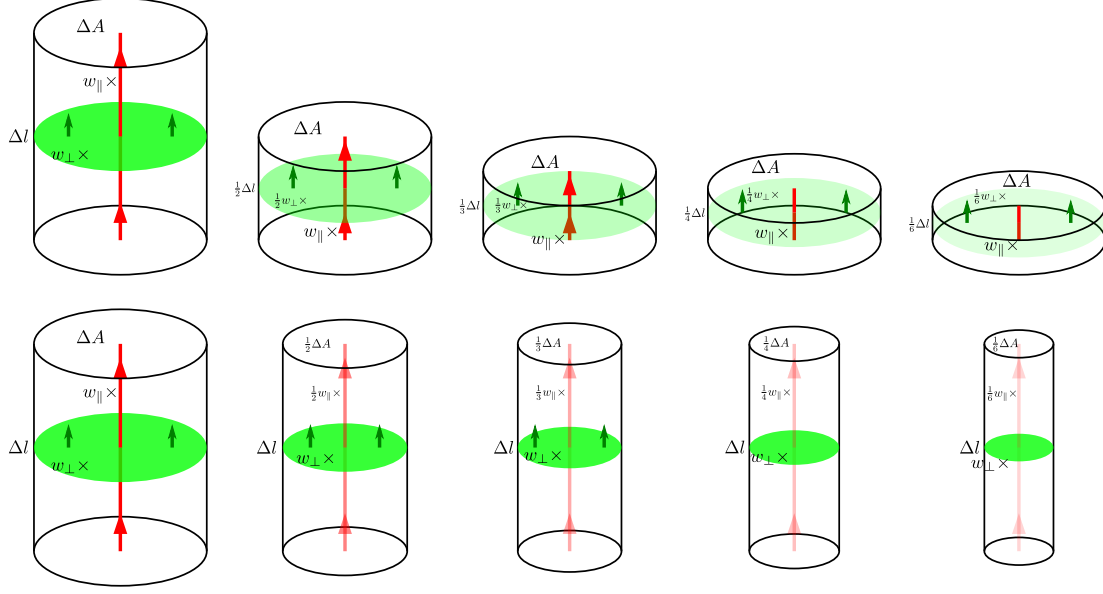
The fact that multi-paths and multi-surface both require 3 values suggests that paths and surfaces can be “interchanged”. When a multi-path and multi-surface are interchangeable, they will be referred to as being “dual” to each other.

Given an infinitesimal segment of path C with an infinitesimal weight, the surface σ that is “dual” to C is:

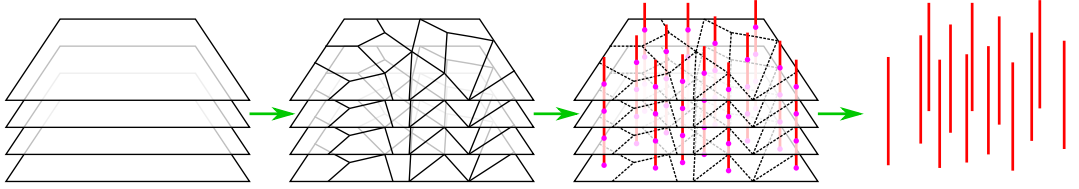
- Infinitesimal in both size and weight.
- Perpendicular to C .
- The direction of C passes through σ in the preferred direction. This gives the intersections of dual paths and surfaces positive weight.

To visualize a smoothed multi-path and its smoothed dual surface, sheath the infinitesimal path fibers in a cylinder. The path fibers are parallel to the sides of the cylinder, and are perpendicular to the end caps. The dual surfaces are perpendicular to the sides of the cylinder and are parallel to the end caps. The total path weight passing through the cylinder is proportional to the cross-sectional area of the cylinder, while the total surface weight slicing through the cylinder is proportional to its length.

In the image below, the leftmost cylinders contain a path with a total weight of w_{\parallel} , and a surface with a total weight of w_{\perp} . These paths and surfaces are dual to each other. In the top row of images, when the cylinder decreases in length, the contained surface weight decreases proportionally, while the contained path weight remains constant. In the bottom row of images, when the cylinder decreases in cross-sectional area, the contained path weight decreases proportionally, while the contained surface weight remains constant.



To determine the multi-path \mathbf{J} that is dual to a multi-surface \mathbf{F} , break the multi-surface \mathbf{F} into infinitesimal sections with equal weight and area, replace each section of surface with its dual path, and lastly stitch the path segments together leaving as little endpoints as possible. While there is no unique way of performing this process, once “smoothing” has been applied none of this matters.



Given a multi-surface \mathbf{F} , the multi-path \mathbf{J} that is “dual” to \mathbf{F} will be denoted via the notation:

$$\mathbf{J} = \epsilon(\mathbf{F})$$

or conversely,

$$\mathbf{F} = \epsilon^{-1}(\mathbf{J})$$

The following is important to note:

- The dual of the union is the union of the duals:

$$\epsilon(\mathbf{F}_1 + \mathbf{F}_2) = \epsilon(\mathbf{F}_1) + \epsilon(\mathbf{F}_2) \quad \text{and} \quad \epsilon^{-1}(\mathbf{J}_1 + \mathbf{J}_2) = \epsilon^{-1}(\mathbf{J}_1) + \epsilon^{-1}(\mathbf{J}_2)$$

If c is an arbitrary real valued coefficient, then:

$$\epsilon(c \cdot \mathbf{F}) = c \cdot \epsilon(\mathbf{F}) \quad \text{and} \quad \epsilon^{-1}(c \cdot \mathbf{J}) = c \cdot \epsilon^{-1}(\mathbf{J})$$

8.3 Duality and intersections

Theorem 33. Given multi-point ρ and multi-volume V ,

$$\iota^{-1}(\rho \cdot V) = \iota^{-1}(\rho) \cdot V$$

Given multi-point \mathbf{J} and multi-volume V ,

$$\epsilon^{-1}(\mathbf{J} \cdot V) = \epsilon^{-1}(\mathbf{J}) \cdot V$$

Given multi-surface \mathbf{F} and multi-volume V ,

$$\epsilon(\mathbf{F} \cdot V) = \epsilon(\mathbf{F}) \cdot V$$

Given multi-volume U and multi-volume V ,

$$\iota(U \cdot V) = \iota(U) \cdot V$$

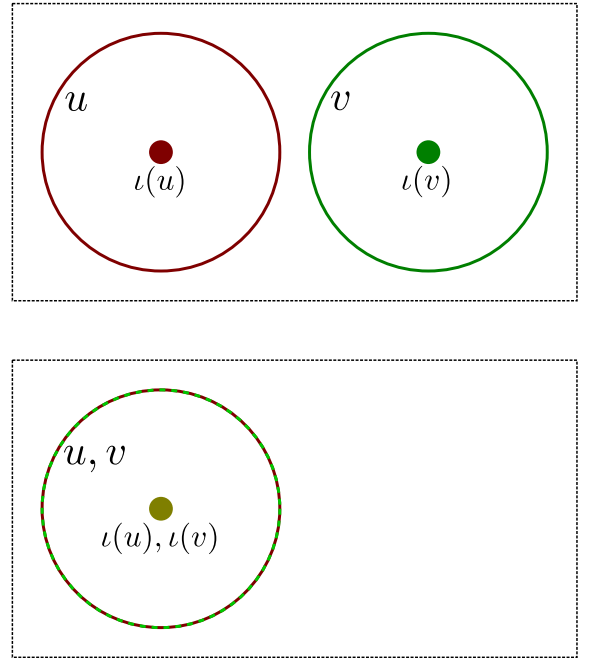
Theorem 34. Given multi-volumes U and V ,

$$\iota(U) \cdot V = U \cdot \iota(V)$$

Proof:

Let u and v be infinitesimally small single volumes with weights of 1, and whose volumes are equivalent. There are two scenarios. In the first scenario, $\iota(u)$ and $\iota(v)$ are at different positions. In the second scenario, $\iota(u) = \iota(v)$. These scenarios are depicted on the right.

- In case 1, $\iota(u) \cdot v = 0$ and $u \cdot \iota(v) = 0$ so $\iota(u) \cdot v = u \cdot \iota(v)$.
- In case 2, $\iota(u) = \iota(v)$ implies $u = v$. Therefore $\iota(u) \cdot v = u \cdot \iota(v)$.



For infinitesimal single volumes u and v with equal volumes and weights of 1, $\iota(u) \cdot v = u \cdot \iota(v)$. Generalizing to non-infinitesimal scales, let U and V denote non-infinitesimal volumes comprised of infinitesimal volumes:

$$U = u_1 + u_2 + \dots + u_\infty$$

$$V = v_1 + v_2 + \dots + v_\infty$$

Next:

$$\begin{aligned} \iota(U) \cdot V &= \iota(u_1 + u_2 + \dots + u_\infty) \cdot (v_1 + v_2 + \dots + v_\infty) \\ &= (\iota(u_1) + \iota(u_2) + \dots + \iota(u_\infty)) \cdot (v_1 + v_2 + \dots + v_\infty) \\ &= \iota(u_1) \cdot v_1 + \iota(u_1) \cdot v_2 + \dots + \iota(u_1) \cdot v_\infty \\ &\quad + \iota(u_2) \cdot v_1 + \iota(u_2) \cdot v_2 + \dots + \iota(u_2) \cdot v_\infty \\ &\quad \dots \\ &\quad + \iota(u_\infty) \cdot v_1 + \iota(u_\infty) \cdot v_2 + \dots + \iota(u_\infty) \cdot v_\infty \end{aligned}$$

$$\begin{aligned}
&= u_1 \cdot \iota(v_1) + u_1 \cdot \iota(v_2) + \dots + u_1 \cdot \iota(v_\infty) \\
&\quad + u_2 \cdot \iota(v_1) + u_2 \cdot \iota(v_2) + \dots + u_2 \cdot \iota(v_\infty) \\
&\quad \dots \\
&\quad + u_\infty \cdot \iota(v_1) + u_\infty \cdot \iota(v_2) + \dots + u_\infty \cdot \iota(v_\infty) \\
&= (u_1 + u_2 + \dots + u_\infty) \cdot (\iota(v_1) + \iota(v_2) + \dots + \iota(v_\infty)) \\
&= (u_1 + u_2 + \dots + u_\infty) \cdot \iota(v_1 + v_2 + \dots + v_\infty) \\
&= U \cdot \iota(V)
\end{aligned}$$

Therefore:

$$\iota(U) \cdot V = U \cdot \iota(V)$$

□

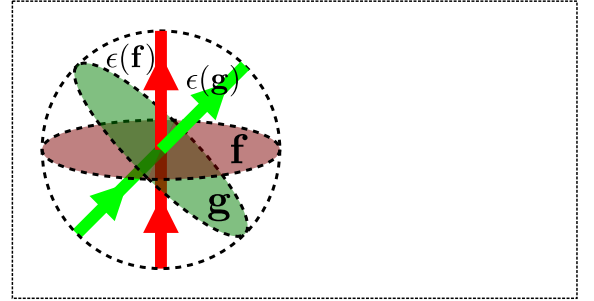
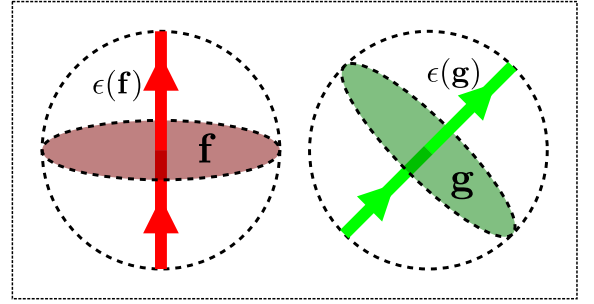
Theorem 35. *Given multi-surfaces \mathbf{F} and \mathbf{G} ,*

$$\epsilon(\mathbf{F}) \bullet \mathbf{G} = \mathbf{F} \bullet \epsilon(\mathbf{G})$$

Proof:

Let \mathbf{f} and \mathbf{g} be infinitesimally small surfaces with weights of w_\perp . Let the dual paths $\epsilon(\mathbf{f})$ and $\epsilon(\mathbf{g})$ have weights of w_\parallel . There are two scenarios. In the first scenario, \mathbf{f} and \mathbf{g} are at different positions. In the second scenario, \mathbf{f} and \mathbf{g} are at the same position. These scenarios are depicted on the right.

- In case 1, $\epsilon(\mathbf{f}) \bullet \mathbf{g} = 0$ and $\mathbf{f} \bullet \epsilon(\mathbf{g}) = 0$ so $\epsilon(\mathbf{f}) \bullet \mathbf{g} = \mathbf{f} \bullet \epsilon(\mathbf{g})$.
- In case 2, the intersection point $\epsilon(\mathbf{f}) \bullet \mathbf{g}$ has a weight of $w_\parallel w_\perp$. The intersection point $\mathbf{f} \bullet \epsilon(\mathbf{g})$ also has a weight of $w_\parallel w_\perp$, and has the same position. Therefore $\epsilon(\mathbf{f}) \bullet \mathbf{g} = \mathbf{f} \bullet \epsilon(\mathbf{g})$.



For infinitesimal surfaces \mathbf{f} and \mathbf{g} with equal weights, $\epsilon(\mathbf{f}) \bullet \mathbf{g} = \mathbf{f} \bullet \epsilon(\mathbf{g})$. Generalizing to non-infinitesimal scales, let \mathbf{F} and \mathbf{G} denote non-infinitesimal volumes comprised of infinitesimal volumes:

$$\mathbf{F} = \mathbf{f}_1 + \mathbf{f}_2 + \dots + \mathbf{f}_\infty$$

$$\mathbf{G} = \mathbf{g}_1 + \mathbf{g}_2 + \dots + \mathbf{g}_\infty$$

Next:

$$\begin{aligned}
\epsilon(\mathbf{F}) \bullet \mathbf{G} &= \epsilon(\mathbf{f}_1 + \mathbf{f}_2 + \dots + \mathbf{f}_\infty) \bullet (\mathbf{g}_1 + \mathbf{g}_2 + \dots + \mathbf{g}_\infty) \\
&= (\epsilon(\mathbf{f}_1) + \epsilon(\mathbf{f}_2) + \dots + \epsilon(\mathbf{f}_\infty)) \bullet (\mathbf{g}_1 + \mathbf{g}_2 + \dots + \mathbf{g}_\infty) \\
&= \epsilon(\mathbf{f}_1) \bullet \mathbf{g}_1 + \epsilon(\mathbf{f}_1) \bullet \mathbf{g}_2 + \dots + \epsilon(\mathbf{f}_1) \bullet \mathbf{g}_\infty \\
&\quad + \epsilon(\mathbf{f}_2) \bullet \mathbf{g}_1 + \epsilon(\mathbf{f}_2) \bullet \mathbf{g}_2 + \dots + \epsilon(\mathbf{f}_2) \bullet \mathbf{g}_\infty \\
&\quad \dots \\
&\quad + \epsilon(\mathbf{f}_\infty) \bullet \mathbf{g}_1 + \epsilon(\mathbf{f}_\infty) \bullet \mathbf{g}_2 + \dots + \epsilon(\mathbf{f}_\infty) \bullet \mathbf{g}_\infty
\end{aligned}$$

$$\begin{aligned}
&= \mathbf{f}_1 \bullet \epsilon(\mathbf{g}_1) + \mathbf{f}_1 \bullet \epsilon(\mathbf{g}_2) + \dots + \mathbf{f}_1 \bullet \epsilon(\mathbf{g}_\infty) \\
&\quad + \mathbf{f}_2 \bullet \epsilon(\mathbf{g}_1) + \mathbf{f}_2 \bullet \epsilon(\mathbf{g}_2) + \dots + \mathbf{f}_2 \bullet \epsilon(\mathbf{g}_\infty) \\
&\quad \dots \\
&\quad + \mathbf{f}_\infty \bullet \epsilon(\mathbf{g}_1) + \mathbf{f}_\infty \bullet \epsilon(\mathbf{g}_2) + \dots + \mathbf{f}_\infty \bullet \epsilon(\mathbf{g}_\infty) \\
&= (\mathbf{f}_1 + \mathbf{f}_2 + \dots + \mathbf{f}_\infty) \bullet (\epsilon(\mathbf{g}_1) + \epsilon(\mathbf{g}_2) + \dots + \epsilon(\mathbf{g}_\infty)) \\
&= (\mathbf{f}_1 + \mathbf{f}_2 + \dots + \mathbf{f}_\infty) \bullet \epsilon(\mathbf{g}_1 + \mathbf{g}_2 + \dots + \mathbf{g}_\infty) \\
&= \mathbf{F} \bullet \epsilon(\mathbf{G})
\end{aligned}$$

Therefore:

$$\epsilon(\mathbf{F}) \bullet \mathbf{G} = \mathbf{F} \bullet \epsilon(\mathbf{G})$$

□

8.4 Simplifying notation

In the discussions that will follow, duality conversions will begin to happen rapidly, and to avoid notational clutter, the following abbreviations will be made:

- Given multi-points ρ_1 and ρ_2 , the expression $\rho_1 \cdot \rho_2$ will be defined by

$$\rho_1 \cdot \rho_2 = \iota^{-1}(\rho_1) \cdot \rho_2 = \rho_1 \cdot \iota^{-1}(\rho_2)$$

Thanks to theorem 34, $\iota^{-1}(\rho_1) \cdot \rho_2 = \rho_1 \cdot \iota^{-1}(\rho_2)$

- Given multi-point ρ and multi-path \mathbf{J} , the expression $\rho \cdot \mathbf{J}$ will be defined by

$$\rho \cdot \mathbf{J} = \iota^{-1}(\rho) \cdot \mathbf{J}$$

- Given multi-point ρ and multi-surface \mathbf{F} , the expression $\rho \cdot \mathbf{F}$ will be defined by

$$\rho \cdot \mathbf{F} = \iota^{-1}(\rho) \cdot \mathbf{F}$$

- Given multi-paths \mathbf{J}_1 and \mathbf{J}_2 , the expression $\mathbf{J}_1 \bullet \mathbf{J}_2$ will be defined by

$$\mathbf{J}_1 \bullet \mathbf{J}_2 = \epsilon^{-1}(\mathbf{J}_1) \bullet \mathbf{J}_2 = \mathbf{J}_1 \bullet \epsilon^{-1}(\mathbf{J}_2)$$

Thanks to theorem 35, $\epsilon^{-1}(\mathbf{J}_1) \bullet \mathbf{J}_2 = \mathbf{J}_1 \bullet \epsilon^{-1}(\mathbf{J}_2)$

- Given multi-surfaces \mathbf{F}_1 and \mathbf{F}_2 , the expression $\mathbf{F}_1 \bullet \mathbf{F}_2$ will be defined by

$$\mathbf{F}_1 \bullet \mathbf{F}_2 = \epsilon(\mathbf{F}_1) \bullet \mathbf{F}_2 = \mathbf{F}_1 \bullet \epsilon(\mathbf{F}_2)$$

Thanks to theorem 35, $\epsilon(\mathbf{F}_1) \bullet \mathbf{F}_2 = \mathbf{F}_1 \bullet \epsilon(\mathbf{F}_2)$

- Given multi-paths \mathbf{J}_1 and \mathbf{J}_2 , the expression $\mathbf{J}_1 \times \mathbf{J}_2$ will be defined by

$$\mathbf{J}_1 \times \mathbf{J}_2 = \epsilon^{-1}(\mathbf{J}_1) \times \epsilon^{-1}(\mathbf{J}_2)$$

- Given multi-path \mathbf{J} and multi-surface \mathbf{F} , the expression $\mathbf{J} \times \mathbf{F}$ will be defined by

$$\mathbf{J} \times \mathbf{F} = \epsilon^{-1}(\mathbf{J}) \times \mathbf{F}$$

- Given multi-surface \mathbf{F} and multi-path \mathbf{J} , the expression $\mathbf{F} \times \mathbf{J}$ will be defined by

$$\mathbf{F} \times \mathbf{J} = \mathbf{F} \times \epsilon^{-1}(\mathbf{J})$$

- Given multi-point ρ , the expression $\nabla \rho$ will be defined by

$$\nabla \rho = \nabla \iota^{-1}(\rho)$$

- Given multi-path \mathbf{J} , the expression $\nabla \times \mathbf{J}$ will be defined by

$$\nabla \times \mathbf{J} = \nabla \times \epsilon^{-1}(\mathbf{J})$$

- Given multi-surface \mathbf{F} , the expression $\nabla \bullet \mathbf{F}$ will be defined by

$$\nabla \bullet \mathbf{F} = \nabla \bullet \epsilon(\mathbf{F})$$

- Given multi-volume U , the expression $\int U$ will be defined by

$$\int U = \int \iota(U)$$

This expression computes the total volume of U .

In summary, if an operation cannot be performed, compute the dual of one (or both) of the operands until the operation is possible.

8.5 Quantifying duality

Now that the concept of duality has been established, the relationship between the functions that quantify dual multi-structures is now to be addressed.

Firstly, consider a multi-volume U quantified by the function $U(\mathbf{q})$, and the dual multi-point $\rho = \iota(U)$. The function $\rho(\mathbf{q})$ that quantifies ρ is exactly the same as the function that quantifies U :

For all positions \mathbf{q} ,

$$\rho(\mathbf{q}) = U(\mathbf{q})$$

The relationship between multi-surfaces and their dual multi-paths is far less trivial however. Let \mathbf{D} be a multi-path, and \mathbf{E} be the dual multi-surface: $\mathbf{D} = \epsilon(\mathbf{E})$. If $\mathbf{D}(\mathbf{q}) = \begin{bmatrix} D_1(\mathbf{q}) \\ D_2(\mathbf{q}) \\ D_3(\mathbf{q}) \end{bmatrix}$ is the vector

valued function that quantifies \mathbf{D} and $\mathbf{E}(\mathbf{q}) = \begin{bmatrix} E_1(\mathbf{q}) \\ E_2(\mathbf{q}) \\ E_3(\mathbf{q}) \end{bmatrix}$ is the vector valued function that quantifies \mathbf{E} , then for all positions \mathbf{q} ,

$$\begin{cases} D_1(\mathbf{q}) = \epsilon_{1,1}(\mathbf{q})E_1(\mathbf{q}) + \epsilon_{1,2}(\mathbf{q})E_2(\mathbf{q}) + \epsilon_{1,3}(\mathbf{q})E_3(\mathbf{q}) = \sum_j \epsilon_{1,j}(\mathbf{q})E_j(\mathbf{q}) \\ D_2(\mathbf{q}) = \epsilon_{2,1}(\mathbf{q})E_1(\mathbf{q}) + \epsilon_{2,2}(\mathbf{q})E_2(\mathbf{q}) + \epsilon_{2,3}(\mathbf{q})E_3(\mathbf{q}) = \sum_j \epsilon_{2,j}(\mathbf{q})E_j(\mathbf{q}) \\ D_3(\mathbf{q}) = \epsilon_{3,1}(\mathbf{q})E_1(\mathbf{q}) + \epsilon_{3,2}(\mathbf{q})E_2(\mathbf{q}) + \epsilon_{3,3}(\mathbf{q})E_3(\mathbf{q}) = \sum_j \epsilon_{3,j}(\mathbf{q})E_j(\mathbf{q}) \end{cases}$$

Where all of the $\epsilon_{i,j}(\mathbf{q})$ are coefficients that quantify the relationship $\mathbf{D} = \epsilon(\mathbf{E})$.

This relationship can be abbreviated using “matrix form”:

$$\begin{bmatrix} D_1(\mathbf{q}) \\ D_2(\mathbf{q}) \\ D_3(\mathbf{q}) \end{bmatrix} = \begin{bmatrix} \epsilon_{1,1}(\mathbf{q}) & \epsilon_{1,2}(\mathbf{q}) & \epsilon_{1,3}(\mathbf{q}) \\ \epsilon_{2,1}(\mathbf{q}) & \epsilon_{2,2}(\mathbf{q}) & \epsilon_{2,3}(\mathbf{q}) \\ \epsilon_{3,1}(\mathbf{q}) & \epsilon_{3,2}(\mathbf{q}) & \epsilon_{3,3}(\mathbf{q}) \end{bmatrix} \begin{bmatrix} E_1(\mathbf{q}) \\ E_2(\mathbf{q}) \\ E_3(\mathbf{q}) \end{bmatrix}$$

In order for the relationship $\epsilon(\mathbf{F}) \bullet \mathbf{G} = \mathbf{F} \bullet \epsilon(\mathbf{G})$ to hold, the matrix must be “symmetric”:

$$\epsilon_{1,2}(\mathbf{q}) = \epsilon_{2,1}(\mathbf{q}) \quad \text{and} \quad \epsilon_{1,3}(\mathbf{q}) = \epsilon_{3,1}(\mathbf{q}) \quad \text{and} \quad \epsilon_{2,3}(\mathbf{q}) = \epsilon_{3,2}(\mathbf{q})$$

All of the coefficients have units of m^{-1} .

8.6 Energy

8.6.1 Path energy

Given a multi-path \mathbf{D} , the “energy” of \mathbf{D} is $1/2$ the total number of intersections that the path has with its own dual:

$$E = \frac{1}{2} \int (\mathbf{D} \bullet \mathbf{D}) = \frac{1}{2} \int (\mathbf{D} \bullet \epsilon^{-1}(\mathbf{D}))$$

The multiplier of $\frac{1}{2}$ exists to remain consistent with physics.

The energy is always strictly positive except for the 0 multi-path where the energy is 0.

8.6.2 Surface energy

Given a multi-surface \mathbf{E} , the “energy” of \mathbf{E} is $1/2$ the total number of intersections that the surface has with its own dual:

$$E = \frac{1}{2} \int (\mathbf{E} \bullet \mathbf{E}) = \frac{1}{2} \int (\epsilon(\mathbf{E}) \bullet \mathbf{E})$$

Again, the multiplier of $\frac{1}{2}$ exists to remain consistent with physics.

The energy is always strictly positive except for the 0 multi-surface where the energy is 0.

8.6.3 Loop-bubble duality

If a multi-bubble is dual to a multi-loop, then both are 0. This can be proven from the fact that the energy of a nonzero path or surface is always positive.

Theorem 36. *Assume that \mathbf{E} is a multi-bubble: $\nabla \times \mathbf{E} = 0$. Also assume that the dual multi-path $\mathbf{D} = \epsilon(\mathbf{E})$ is also a multi-loop: $\nabla \bullet \mathbf{D} = 0$. It must then be the case that $\mathbf{E} = 0$ and $\mathbf{D} = 0$.*

Proof:

Since \mathbf{E} is a multi-bubble, there must exist some multi-volume U whose inwards oriented surface is \mathbf{E} .
The energy of both \mathbf{D} and \mathbf{E} is:

$$E = \frac{1}{2} \int (\mathbf{D} \bullet \mathbf{E}) = \frac{1}{2} \int (\mathbf{D} \bullet (\nabla U))$$

As established by theorem 21, the number of times \mathbf{D} enters U is the total number of finishing points \mathbf{D} leaves in U so:

$$\int (\mathbf{D} \bullet (\nabla U)) = - \int ((\nabla \bullet \mathbf{D}) U)$$

therefore continuing the derivation yields:

$$E = \frac{1}{2} \int (\mathbf{D} \bullet (\nabla U)) = -\frac{1}{2} \int ((\nabla \bullet \mathbf{D}) U) = -\frac{1}{2} \int (0 \cdot U) = 0$$

The energy is 0, and this only occurs if $\mathbf{D} = 0$ and $\mathbf{E} = 0$. **Non-zero multi-bubbles can never be dual to a multi-loop and vice versa.** \square

A consequence of this fact is that if two path-surface pairs have the same end-points and counterclockwise boundaries, then they are equivalent:

Corollary:

Let \mathbf{D}_1 and \mathbf{E}_1 be a multi-path and a multi-surface pair that are dual to each other: $\mathbf{D}_1 = \epsilon(\mathbf{E}_1)$

Let \mathbf{D}_2 and \mathbf{E}_2 also be a multi-path and a multi-surface pair that are dual to each other: $\mathbf{D}_2 = \epsilon(\mathbf{E}_2)$

If $\nabla \bullet \mathbf{D}_1 = \nabla \bullet \mathbf{D}_2$ and $\nabla \times \mathbf{E}_1 = \nabla \times \mathbf{E}_2$, then $\mathbf{D}_1 = \mathbf{D}_2$ and $\mathbf{E}_1 = \mathbf{E}_2$.

Proof:

Let $\mathbf{D}_{\text{loop}} = \mathbf{D}_1 - \mathbf{D}_2$. \mathbf{D}_{loop} is a multi-loop:

$$\nabla \bullet \mathbf{D}_{\text{loop}} = \nabla \bullet (\mathbf{D}_1 - \mathbf{D}_2) = \nabla \bullet \mathbf{D}_1 - \nabla \bullet \mathbf{D}_2 = 0$$

Let $\mathbf{E}_{\text{bubble}} = \mathbf{E}_1 - \mathbf{E}_2$. $\mathbf{E}_{\text{bubble}}$ is a multi-bubble:

$$\nabla \times \mathbf{E}_{\text{bubble}} = \nabla \times (\mathbf{E}_1 - \mathbf{E}_2) = \nabla \times \mathbf{E}_1 - \nabla \times \mathbf{E}_2 = 0$$

\mathbf{D}_{loop} and $\mathbf{E}_{\text{bubble}}$ are a dual pair:

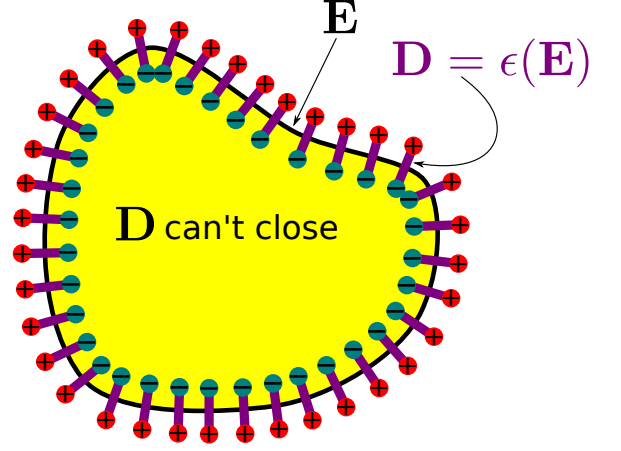
$$\epsilon(\mathbf{E}_{\text{bubble}}) = \epsilon(\mathbf{E}_1 - \mathbf{E}_2) = \epsilon(\mathbf{E}_1) - \epsilon(\mathbf{E}_2) = \mathbf{D}_1 - \mathbf{D}_2 = \mathbf{D}_{\text{loop}}$$

From theorem 36, $\mathbf{D}_{\text{loop}} = 0$ and $\mathbf{E}_{\text{bubble}} = 0$. Therefore $\mathbf{D}_1 = \mathbf{D}_2$ and $\mathbf{E}_1 = \mathbf{E}_2$. \square

8.6.4 Low energy multi-path

Given a balanced multi-point ρ , it is known via theorem 14 from section 5.1 that there must exist a multi-path \mathbf{D} such that $\nabla \bullet \mathbf{D} = \rho$. However, the choice of \mathbf{D} is **not unique**. A unique choice of multi-path \mathbf{D} is the choice that minimizes the energy $\frac{1}{2} \int (\mathbf{D} \bullet \mathbf{D})$. It will now be demonstrated that the energy minimizing choice is both unique and is dual to a multi-bubble:

Theorem 37. *Given a balanced multi-point ρ , the multi-path \mathbf{D} that satisfies $\nabla \bullet \mathbf{D} = \rho$ and minimizes the energy $\frac{1}{2} \int (\mathbf{D} \bullet \epsilon^{-1}(\mathbf{D}))$ is both **unique** and is dual to a multi-bubble: i.e. $\nabla \times \epsilon^{-1}(\mathbf{D}) = 0$.*



Proof:

Let \mathbf{D} denote any multi-path whose endpoints are ρ : $\nabla \bullet \mathbf{D} = \rho$. It will be demonstrated that unless $\nabla \times \mathbf{D} = 0$, that there will exist another multi-path \mathbf{D}_{next} whose endpoints are also ρ : $\nabla \bullet \mathbf{D}_{\text{next}} = \rho$, and has a lower energy than \mathbf{D} .

The approach that will be used here is referred to as the **method of variations**. The method of variations involves proposing a change to \mathbf{D} , and then determining conditions such that no changes result in lower energy. Choose any multi-surface \mathbf{F} , referred to as a “test surface”. The boundary $\nabla \times \mathbf{F}$ is a closed loop, and adding any multiple of $\nabla \times \mathbf{F}$ to \mathbf{D} does not change the endpoints.

Let t be a small number (that is close to 0), and then propose the change:

$$\mathbf{D}_{\text{new}} = \mathbf{D} + t(\nabla \times \mathbf{F})$$

The endpoints are unchanged:

$$\begin{aligned}\nabla \bullet \mathbf{D}_{\text{new}} &= \nabla \bullet \mathbf{D} + t(\nabla \bullet (\nabla \times \mathbf{F})) \\ &= \nabla \bullet \mathbf{D} - t(0) = \rho\end{aligned}$$

The current energy is $E_{\text{old}} = \frac{1}{2} \int (\mathbf{D} \bullet \mathbf{D})$

The new energy is:

$$\begin{aligned}E_{\text{new}} &= \frac{1}{2} \int (\mathbf{D}_{\text{new}} \bullet \mathbf{D}_{\text{new}}) \\ &= \frac{1}{2} \int (\mathbf{D} + t(\nabla \times \mathbf{F})) \bullet (\mathbf{D} + t(\nabla \times \mathbf{F})) \\ &= \frac{1}{2} \int (\mathbf{D} \bullet \mathbf{D} + t(\mathbf{D} \bullet (\nabla \times \mathbf{F}) + (\nabla \times \mathbf{F}) \bullet \mathbf{D}) + t^2((\nabla \times \mathbf{F}) \bullet (\nabla \times \mathbf{F}))) \\ &= \frac{1}{2} \int (\mathbf{D} \bullet \mathbf{D}) + t \int (\mathbf{D} \bullet (\nabla \times \mathbf{F})) + \frac{t^2}{2} \int ((\nabla \times \mathbf{F}) \bullet (\nabla \times \mathbf{F})) \\ &= E_{\text{old}} + t \int (\mathbf{D} \bullet (\nabla \times \mathbf{F})) + \frac{t^2}{2} \int ((\nabla \times \mathbf{F}) \bullet (\nabla \times \mathbf{F}))\end{aligned}$$

Of interest is the term $\int (\mathbf{D} \bullet (\nabla \times \mathbf{F}))$. If this term is 0, then no choice of t results in lower energy. Contrariwise, if this term is non-zero, then t can be chosen to decrease the energy further.

$\int (\mathbf{D} \bullet (\nabla \times \mathbf{F}))$ is the total point weight of the intersection of the surface $\epsilon^{-1}(\mathbf{D})$ with the counterclockwise boundary of \mathbf{F} . Using Stokes’ theorem (theorem 23),

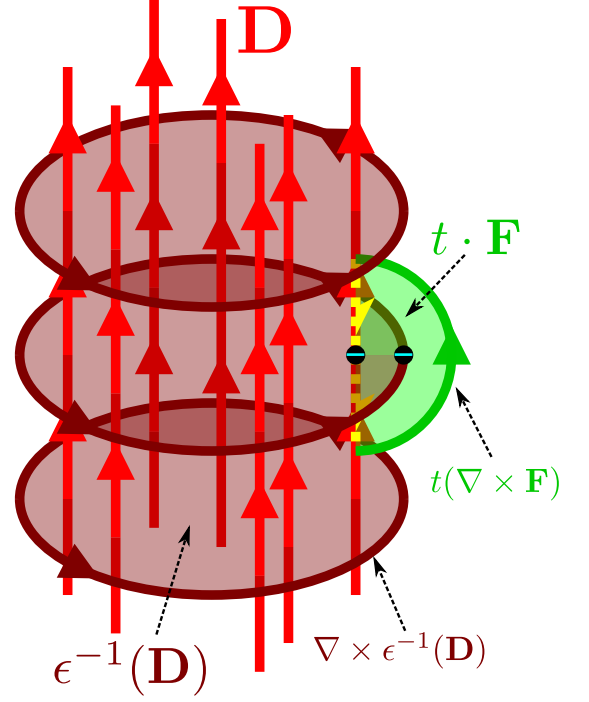
$$\int (\mathbf{D} \bullet (\nabla \times \mathbf{F})) = 0 \iff \int ((\nabla \times \mathbf{D}) \bullet \mathbf{F}) = 0 \iff \int ((\nabla \times \mathbf{D}) \bullet \mathbf{F}) = \int (0 \bullet \mathbf{F})$$

The energy cannot be reduced further if and only if $\int (\mathbf{D} \bullet (\nabla \times \mathbf{F})) = 0$ for every choice of test surface \mathbf{F} . Equivalently, the energy cannot be reduced further if and only if $\int ((\nabla \times \mathbf{D}) \bullet \mathbf{F}) = \int (0 \bullet \mathbf{F})$ for every choice of test surface \mathbf{F} .

Treat \mathbf{F} as a “scanning window” from theorem 6. From this theorem, $\int ((\nabla \times \mathbf{D}) \bullet \mathbf{F}) = \int (0 \bullet \mathbf{F})$ for every choice of scanning window \mathbf{F} if and only if $\nabla \times \mathbf{D} = 0$. The energy cannot be reduced further if and only if \mathbf{D} is dual to a multi-bubble: i.e. $\nabla \times \mathbf{D} = 0$.

It lastly needs to be demonstrated that the optimal choice of \mathbf{D} is unique. Let \mathbf{D}_1 and \mathbf{D}_2 denote two optimal choices of \mathbf{D} . This means that $\nabla \bullet \mathbf{D}_1 = \nabla \bullet \mathbf{D}_2 = \rho$ and $\nabla \times \epsilon^{-1}(\mathbf{D}_1) = \nabla \times \epsilon^{-1}(\mathbf{D}_2) = 0$. From the corollary of theorem 36, $\mathbf{D}_1 = \mathbf{D}_2$. \square

In the image to the right, the scanning window surface \mathbf{F} is chosen to intersect the counterclockwise boundary of $\epsilon^{-1}(\mathbf{D})$ in the reverse direction. Let $t > 0$. When $t(\nabla \times \mathbf{F})$ is added to \mathbf{D} , the paths that comprise \mathbf{D} spread out past the current boundary of $\epsilon^{-1}(\mathbf{D})$. Keeping t small so that the contribution of the term $\frac{t^2}{2} \int ((\nabla \times \mathbf{F}) \bullet (\nabla \times \mathbf{F}))$ remains small, it can be seen that the total intersection of $t(\nabla \times \mathbf{F})$ with the current surface $\epsilon^{-1}(\mathbf{D})$ is negative, i.e. $\int (\epsilon^{-1}(\mathbf{D}) \bullet t(\nabla \times \mathbf{F})) < 0$, resulting in a net decrease in energy.



Corollary:

Given the balanced multi-points ρ_1 and ρ_2 , if \mathbf{D}_1 and \mathbf{D}_2 are the minimum energy multi-paths that satisfy $\nabla \bullet \mathbf{D}_1 = \rho_1$ and $\nabla \bullet \mathbf{D}_2 = \rho_2$, then $\mathbf{D}_{1+2} = \mathbf{D}_1 + \mathbf{D}_2$ is the minimum energy multi-path that satisfies $\nabla \bullet \mathbf{D}_{1+2} = \rho_1 + \rho_2$. Moreover, given any real number c , $\mathbf{D}_{c1} = c \cdot \mathbf{D}_1$ is the minimum energy multi-path that satisfies $\nabla \bullet \mathbf{D}_{c1} = c \cdot \rho_1$.

Proof:

Firstly,

$$\nabla \bullet \mathbf{D}_{1+2} = \nabla \bullet \mathbf{D}_1 + \nabla \bullet \mathbf{D}_2 = \rho_1 + \rho_2$$

and

$$\nabla \bullet \mathbf{D}_{c1} = c \cdot (\nabla \bullet \mathbf{D}_1) = c \cdot \rho_1$$

so \mathbf{D}_{1+2} and \mathbf{D}_{c1} satisfy their respective equations.

From theorem 37, \mathbf{D}_1 and \mathbf{D}_2 are multi-bubbles, and \mathbf{D}_{1+2} and \mathbf{D}_{c1} must also be multi-bubbles to be minimum energy multi-paths.

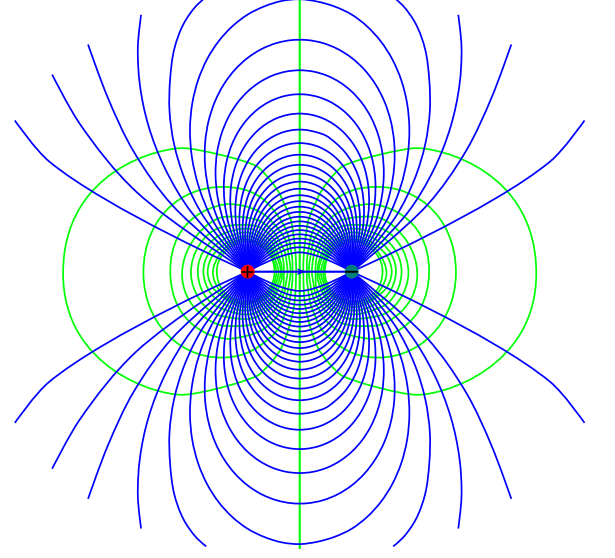
$$\nabla \times \mathbf{D}_{1+2} = \nabla \times (\mathbf{D}_1 + \mathbf{D}_2) = \nabla \times \mathbf{D}_1 + \nabla \times \mathbf{D}_2 = 0 + 0 = 0$$

and

$$\nabla \times \mathbf{D}_{c1} = \nabla \times (c \cdot \mathbf{D}_1) = c \cdot (\nabla \times \mathbf{D}_1) = c \cdot 0 = 0$$

Therefore \mathbf{D}_{1+2} and \mathbf{D}_{c1} are multi-bubbles and are hence minimum energy multi-paths. \square

On the right is shown a minimum energy multi-path that connects a multi-point that consists of a single point with a weight of +1 and a single point with a weight of -1. The low energy multi-path is depicted in blue, while the dual multi-bubble is depicted in the background using green. While some paths seem to be missing in this image, primarily near the center, this is due to the fact that this image is a 2D cross section of a 3D scenario.



8.6.5 Low energy multi-surface

Given a multi-loop \mathbf{J} , it is known via theorem 15 from section 5.2 that there must exist a multi-surface \mathbf{E} such that $\nabla \times \mathbf{E} = \mathbf{J}$. However, the choice of \mathbf{E} is **not unique**. A unique choice of multi-surface \mathbf{E} is the choice that minimizes the energy $\frac{1}{2} \int (\mathbf{E} \bullet \mathbf{E})$. It will now be demonstrated that the energy minimizing choice is both unique and is dual to a multi-loop: i.e. $\nabla \bullet \epsilon(\mathbf{E}) = 0$.

Theorem 38. *Given a multi-loop \mathbf{J} , the multi-surface \mathbf{E} that satisfies $\nabla \times \mathbf{E} = \mathbf{J}$ and minimizes the energy $\frac{1}{2} \int (\epsilon(\mathbf{E}) \bullet \mathbf{E})$ is both **unique** and is dual to a multi-loop: i.e. $\nabla \bullet \epsilon(\mathbf{E}) = 0$.*

Proof:

Let \mathbf{E} denote any multi-surface whose boundary is \mathbf{J} : $\nabla \times \mathbf{E} = \mathbf{J}$. It will be demonstrated that unless $\nabla \bullet \mathbf{E} = 0$, that there will exist another multi-surface \mathbf{E}_{next} whose boundary is also \mathbf{J} : $\nabla \times \mathbf{E}_{\text{next}} = \mathbf{J}$, and has a lower energy than \mathbf{E} .

The approach that will be used here is referred to as the **method of variations**. The method of variations involves proposing a change to \mathbf{E} , and then determining conditions such that no changes result in lower energy. Choose any multi-volume U , referred to as a “test volume”. The surface ∇U is a closed surface, and adding any multiple of ∇U to \mathbf{E} does not change the boundary.

Let t be a small number (that is close to 0), and then propose the change:

$$\mathbf{E}_{\text{new}} = \mathbf{E} + t(\nabla U)$$

The boundary is unchanged:

$$\begin{aligned} \nabla \times \mathbf{E}_{\text{new}} &= \nabla \times \mathbf{E} + t(\nabla \times (\nabla U)) \\ &= \nabla \times \mathbf{E} - t(0) = \mathbf{J} \end{aligned}$$

The current energy is $E_{\text{old}} = \frac{1}{2} \int (\mathbf{E} \bullet \mathbf{E})$

The new energy is:

$$\begin{aligned}
E_{\text{new}} &= \frac{1}{2} \int (\mathbf{E}_{\text{new}} \bullet \mathbf{E}_{\text{new}}) \\
&= \frac{1}{2} \int (\mathbf{E} + t(\nabla U)) \bullet (\mathbf{E} + t(\nabla U)) \\
&= \frac{1}{2} \int (\mathbf{E} \bullet \mathbf{E} + t(\mathbf{E} \bullet (\nabla U) + (\nabla U) \bullet \mathbf{E}) + t^2((\nabla U) \bullet (\nabla U))) \\
&= \frac{1}{2} \int (\mathbf{E} \bullet \mathbf{E}) + t \int (\mathbf{E} \bullet (\nabla U)) + \frac{t^2}{2} \int ((\nabla U) \bullet (\nabla U)) \\
&= E_{\text{old}} + t \int (\mathbf{E} \bullet (\nabla U)) + \frac{t^2}{2} \int ((\nabla U) \bullet (\nabla U))
\end{aligned}$$

Of interest is the term $\int (\mathbf{E} \bullet (\nabla U))$. If this term is 0, then no choice of t results in lower energy. Contrariwise, if this term is non-zero, then t can be chosen to decrease the energy further.

$\int (\mathbf{E} \bullet (\nabla U))$ is the total point weight of the intersection of the path $\epsilon(\mathbf{E})$ with the inwards oriented surface of U . Using the gradient theorem (theorem 21),

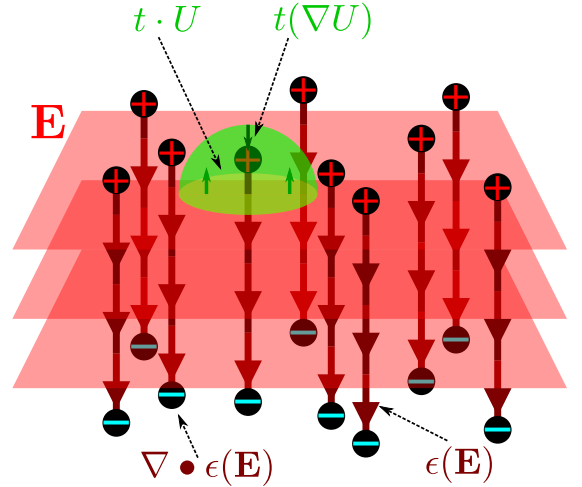
$$\int (\mathbf{E} \bullet (\nabla U)) = 0 \iff - \int ((\nabla \bullet \mathbf{E}) \cdot U) = 0 \iff \int ((\nabla \bullet \mathbf{E}) \cdot U) = \int (0 \cdot U)$$

The energy cannot be reduced further if and only if $\int (\mathbf{E} \bullet (\nabla U)) = 0$ for every choice of test volume U . Equivalently, the energy cannot be reduced further if and only if $\int ((\nabla \bullet \mathbf{E}) \cdot U) = \int (0 \cdot U)$ for every choice of test volume U .

Treat U as a “scanning window” from theorem 5. From this theorem, $\int ((\nabla \bullet \mathbf{E}) \cdot U) = \int (0 \cdot U)$ for every choice of scanning window U if and only if $\nabla \bullet \mathbf{E} = 0$. The energy cannot be reduced further if and only if \mathbf{E} is dual to a multi-loop: i.e. $\nabla \bullet \mathbf{E} = 0$.

It lastly needs to be demonstrated that the optimal choice of \mathbf{E} is unique. Let \mathbf{E}_1 and \mathbf{E}_2 denote two optimal choices of \mathbf{E} . This means that $\nabla \times \mathbf{E}_1 = \nabla \times \mathbf{E}_2 = \mathbf{J}$ and $\nabla \bullet \epsilon(\mathbf{E}_1) = \nabla \bullet \epsilon(\mathbf{E}_2) = 0$. From the corollary of theorem 36, $\mathbf{E}_1 = \mathbf{E}_2$. \square

In the image to the right, the scanning window volume U is chosen to contain a starting point of $\epsilon(\mathbf{E})$. Let $t > 0$. When $t(\nabla U)$ is added to \mathbf{E} , the surfaces that comprise \mathbf{E} spread out past the current endpoints of $\epsilon(\mathbf{E})$. Keeping t small so that the contribution of the term $\frac{t^2}{2} \int ((\nabla U) \bullet (\nabla U))$ remains small, it can be seen that the total intersection of $t(\nabla U)$ with the current path $\epsilon(\mathbf{E})$ is negative, i.e. $\int (\epsilon(\mathbf{E}) \bullet t(\nabla U)) < 0$, resulting in a net decrease in energy.



Corollary:

Given the multi-loops \mathbf{J}_1 and \mathbf{J}_2 , if \mathbf{E}_1 and \mathbf{E}_2 are the minimum energy multi-surfaces that satisfy $\nabla \times \mathbf{E}_1 = \mathbf{J}_1$ and $\nabla \times \mathbf{E}_2 = \mathbf{J}_2$, then $\mathbf{E}_{1+2} = \mathbf{E}_1 + \mathbf{E}_2$ is the minimum energy multi-surface that satisfies $\nabla \times \mathbf{E}_{1+2} = \mathbf{J}_1 + \mathbf{J}_2$. Moreover, given any real number c , $\mathbf{E}_{c1} = c \cdot \mathbf{E}_1$ is the minimum energy multi-surface that satisfies $\nabla \times \mathbf{E}_{c1} = c \cdot \mathbf{J}_1$.

Proof:

Firstly,

$$\nabla \times \mathbf{E}_{1+2} = \nabla \times \mathbf{E}_1 + \nabla \times \mathbf{E}_2 = \mathbf{J}_1 + \mathbf{J}_2$$

and

$$\nabla \times \mathbf{E}_{c1} = c \cdot (\nabla \times \mathbf{E}_1) = c \cdot \mathbf{J}_1$$

so \mathbf{E}_{1+2} and \mathbf{E}_{c1} satisfy their respective equations.

From theorem 38, \mathbf{E}_1 and \mathbf{E}_2 are multi-loops, and \mathbf{E}_{1+2} and \mathbf{E}_{c1} must also be multi-loops to be minimum energy multi-surfaces.

$$\nabla \bullet \mathbf{E}_{1+2} = \nabla \bullet (\mathbf{E}_1 + \mathbf{E}_2) = \nabla \bullet \mathbf{E}_1 + \nabla \bullet \mathbf{E}_2 = 0 + 0 = 0$$

and

$$\nabla \bullet \mathbf{E}_{c1} = \nabla \bullet (c \cdot \mathbf{E}_1) = c \cdot (\nabla \bullet \mathbf{E}_1) = c \cdot 0 = 0$$

Therefore $\mathbf{E}_{1,2}$ and \mathbf{E}_{c1} are multi-loops and are hence minimum energy multi-surfaces. \square

8.6.6 The Helmholtz decomposition theorem

Theorem 39. *Given an arbitrary balanced multi-point ρ , and an arbitrary multi-loop \mathbf{J} , then there exists a unique multi-path \mathbf{D} with dual multi-surface \mathbf{E} such that $\nabla \bullet \mathbf{D} = \rho$ and $\nabla \times \mathbf{E} = \mathbf{J}$.*

Proof:

From theorem 37, there exists a unique multi-path \mathbf{D}_0 such that $\nabla \bullet \mathbf{D}_0 = \rho$ and $\nabla \times \epsilon^{-1}(\mathbf{D}_0) = 0$.

From theorem 38, there exists a unique multi-surface \mathbf{E}_0 such that $\nabla \times \mathbf{E}_0 = \mathbf{J}$ and $\nabla \bullet \epsilon(\mathbf{E}_0) = 0$.

Let multi-path $\mathbf{D} = \mathbf{D}_0 + \epsilon(\mathbf{E}_0)$ and multi-surface $\mathbf{E} = \epsilon^{-1}(\mathbf{D}_0) + \mathbf{E}_0$. It is clear that \mathbf{D} and \mathbf{E} are dual to each other. It is also easy to confirm that:

$$\nabla \bullet \mathbf{D} = \nabla \bullet (\mathbf{D}_0 + \epsilon(\mathbf{E}_0)) = \nabla \bullet \mathbf{D}_0 + \nabla \bullet \epsilon(\mathbf{E}_0) = \rho + 0 = \rho$$

and

$$\nabla \times \mathbf{E} = \nabla \times (\epsilon^{-1}(\mathbf{D}_0) + \mathbf{E}_0) = \nabla \times \epsilon^{-1}(\mathbf{D}_0) + \nabla \times \mathbf{E}_0 = 0 + \mathbf{J} = \mathbf{J}$$

From the corollary of theorem 36, \mathbf{D} and \mathbf{E} are unique. \square

Theorem 40. *Given an arbitrary multi-path \mathbf{J} , then there exists a unique multi-loop \mathbf{D} ($\nabla \bullet \mathbf{D} = 0$) and a unique multi-bubble \mathbf{E} ($\nabla \times \mathbf{E} = 0$) such that $\mathbf{J} = \mathbf{D} + \epsilon(\mathbf{E})$. This is referred to as the **Helmholtz decomposition theorem**, which states that any multi-path or multi-surface is the sum of a multi-loop and a multi-bubble.*

Proof:

$\nabla \bullet \mathbf{J}$ is a balanced multi-point. From theorem 37, let $\mathbf{D}_{\text{bubble}}$ denote the unique multi-path such that $\nabla \bullet \mathbf{D}_{\text{bubble}} = \nabla \bullet \mathbf{J}$ and $\nabla \times \epsilon^{-1}(\mathbf{D}_{\text{bubble}}) = 0$.

Let $\mathbf{D} = \mathbf{J} - \mathbf{D}_{\text{bubble}}$, and let $\mathbf{E} = \epsilon^{-1}(\mathbf{D}_{\text{bubble}})$. It is already known that \mathbf{E} is a multi-bubble. Since $\nabla \bullet \mathbf{D} = \nabla \bullet \mathbf{J} - \nabla \bullet \mathbf{D}_{\text{bubble}} = \nabla \bullet \mathbf{J} - \nabla \bullet \mathbf{J} = 0$, \mathbf{D} is a multi-loop.

\mathbf{D} is a multi-loop and \mathbf{E} is a multi-bubble such that $\mathbf{J} = \mathbf{D} + \epsilon(\mathbf{E})$. Since the choice of $\mathbf{D}_{\text{bubble}}$ is unique, \mathbf{D} and \mathbf{E} are unique also. \square

8.7 Inductance

8.7.1 Balanced multi-point inductance

Self inductance

Given a balanced multi-point ρ , the “self inductance” of ρ , often denoted by $L(\rho)$, is the $2\times$ the minimum possible energy of the multi-path whose endpoints are ρ . If \mathbf{D}_{\min} is the minimum energy multi-path that satisfies $\nabla \bullet \mathbf{D}_{\min} = \rho$, then

$$L(\rho) = \int (\mathbf{D}_{\min} \bullet \mathbf{D}_{\min})$$

If \mathbf{J} were an arbitrary multi-path whose endpoints are ρ , $\nabla \bullet \mathbf{J} = \rho$, then $L(\rho)$ can also be interpreted as follows. Since $\epsilon^{-1}(\mathbf{D}_{\min})$ is a multi-bubble (see theorem 37) and \mathbf{D}_{\min} and \mathbf{J} have the same endpoints, it then follows from theorem 18 that

$$L(\rho) = \int (\mathbf{D}_{\min} \bullet \epsilon^{-1}(\mathbf{D}_{\min})) = \int (\mathbf{J} \bullet \epsilon^{-1}(\mathbf{D}_{\min}))$$

In other words, $L(\rho)$ is the total number of surfaces from $\epsilon^{-1}(\mathbf{D}_{\min})$ that any path connecting the points from ρ will have to pass through.

Mutual inductance

Given two balanced multi-points ρ_1 and ρ_2 , the “mutual inductance” between ρ_1 and ρ_2 , often demoted by $M(\rho_1, \rho_2)$, is defined as follows. Let $\mathbf{D}_{\min,1}$ be the minimum energy multi-path that satisfies $\nabla \bullet \mathbf{D}_{\min,1} = \rho_1$. Let $\mathbf{D}_{\min,2}$ be the minimum energy multi-path that satisfies $\nabla \bullet \mathbf{D}_{\min,2} = \rho_2$. The mutual inductance is

$$M(\rho_1, \rho_2) = \int (\mathbf{D}_{\min,1} \bullet \mathbf{D}_{\min,2})$$

One immediate observation is that $M(\rho_1, \rho_2) = M(\rho_2, \rho_1)$. It is also worth noting that $L(\rho) = M(\rho, \rho)$.

If \mathbf{J}_1 and \mathbf{J}_2 are arbitrary multi-paths whose endpoints are ρ_1 and ρ_2 respectively, $\nabla \bullet \mathbf{J}_1 = \rho_1$ and $\nabla \bullet \mathbf{J}_2 = \rho_2$, then $M(\rho_1, \rho_2)$ can be interpreted as follows.

Since $\epsilon^{-1}(\mathbf{D}_{\min,2})$ is a multi-bubble, it then follows from theorem 18 that

$$M(\rho_1, \rho_2) = \int (\mathbf{D}_{\min,1} \bullet \epsilon^{-1}(\mathbf{D}_{\min,2})) = \int (\mathbf{J}_1 \bullet \epsilon^{-1}(\mathbf{D}_{\min,2}))$$

In other words, $M(\rho_1, \rho_2)$ is the total number of surfaces from $\epsilon^{-1}(\mathbf{D}_{\min,2})$ that any path connecting the points from ρ_1 will have to pass through.

Similarly, since $\epsilon^{-1}(\mathbf{D}_{\min,1})$ is a multi-bubble, it then follows from theorem 18 that

$$M(\rho_1, \rho_2) = \int (\mathbf{D}_{\min,2} \bullet \epsilon^{-1}(\mathbf{D}_{\min,1})) = \int (\mathbf{J}_2 \bullet \epsilon^{-1}(\mathbf{D}_{\min,1}))$$

In other words, $M(\rho_1, \rho_2)$ is the total number of surfaces from $\epsilon^{-1}(\mathbf{D}_{\min,1})$ that any path connecting the points from ρ_2 will have to pass through.

Properties of the inductance

Theorem 41. *Let ρ_1 , ρ_2 , and ρ_3 be arbitrary balanced multi-points. Let c be an arbitrary real number. It is then the case that:*

a)

$$M(\rho_1 + \rho_2, \rho_3) = M(\rho_1, \rho_3) + M(\rho_2, \rho_3)$$

b)

$$M(c \cdot \rho_1, \rho_3) = c \cdot M(\rho_1, \rho_3)$$

c)

$$L(\rho_1 + \rho_2) = L(\rho_1) + 2M(\rho_1, \rho_2) + L(\rho_2)$$

d)

$$L(c \cdot \rho_1) = c^2 \cdot L(\rho_1)$$

Proof:

Let \mathbf{D}_1 , \mathbf{D}_2 , and \mathbf{D}_3 be the minimum energy multi-paths that satisfy $\nabla \bullet \mathbf{D}_1 = \rho_1$; $\nabla \bullet \mathbf{D}_2 = \rho_2$; and $\nabla \bullet \mathbf{D}_3 = \rho_3$ respectively. The following can then be computed:

- a) The minimum energy multi-path \mathbf{D}_{1+2} that satisfies $\nabla \bullet \mathbf{D}_{1+2} = \rho_1 + \rho_2$ is $\mathbf{D}_{1+2} = \mathbf{D}_1 + \mathbf{D}_2$

$$\begin{aligned} M(\rho_1 + \rho_2, \rho_3) &= \int (\mathbf{D}_{1+2} \bullet \mathbf{D}_3) = \int ((\mathbf{D}_1 + \mathbf{D}_2) \bullet \mathbf{D}_3) = \int (\mathbf{D}_1 \bullet \mathbf{D}_3) + \int (\mathbf{D}_2 \bullet \mathbf{D}_3) \\ &= M(\rho_1, \rho_3) + M(\rho_2, \rho_3) \end{aligned}$$

- b) The minimum energy multi-path \mathbf{D}_{c1} that satisfies $\nabla \bullet \mathbf{D}_{c1} = c \cdot \rho_1$ is $\mathbf{D}_{c1} = c \cdot \mathbf{D}_1$

$$\begin{aligned} M(c \cdot \rho_1, \rho_3) &= \int (\mathbf{D}_{c1} \bullet \mathbf{D}_3) = \int ((c \cdot \mathbf{D}_1) \bullet \mathbf{D}_3) = c \int (\mathbf{D}_1 \bullet \mathbf{D}_3) \\ &= c \cdot M(\rho_1, \rho_3) \end{aligned}$$

- c) The minimum energy multi-path \mathbf{D}_{1+2} that satisfies $\nabla \bullet \mathbf{D}_{1+2} = \rho_1 + \rho_2$ is $\mathbf{D}_{1+2} = \mathbf{D}_1 + \mathbf{D}_2$

$$\begin{aligned} L(\rho_1 + \rho_2) &= \int (\mathbf{D}_{1+2} \bullet \mathbf{D}_{1+2}) = \int ((\mathbf{D}_1 + \mathbf{D}_2) \bullet (\mathbf{D}_1 + \mathbf{D}_2)) \\ &= \int ((\mathbf{D}_1 \bullet \mathbf{D}_1) + (\mathbf{D}_1 \bullet \mathbf{D}_2) + (\mathbf{D}_2 \bullet \mathbf{D}_1) + (\mathbf{D}_2 \bullet \mathbf{D}_2)) \\ &= \int (\mathbf{D}_1 \bullet \mathbf{D}_1) + 2 \int (\mathbf{D}_1 \bullet \mathbf{D}_2) + \int (\mathbf{D}_2 \bullet \mathbf{D}_2) = L(\rho_1) + 2M(\rho_1, \rho_2) + L(\rho_2) \end{aligned}$$

- d) The minimum energy multi-path \mathbf{D}_{c1} that satisfies $\nabla \bullet \mathbf{D}_{c1} = c \cdot \rho_1$ is $\mathbf{D}_{c1} = c \cdot \mathbf{D}_1$

$$\begin{aligned} L(c \cdot \rho_1) &= \int (\mathbf{D}_{c1} \bullet \mathbf{D}_{c1}) = \int ((c \cdot \mathbf{D}_1) \bullet (c \cdot \mathbf{D}_1)) = c^2 \int (\mathbf{D}_1 \bullet \mathbf{D}_1) \\ &= c^2 \cdot L(\rho_1) \end{aligned}$$

8.7.2 Multi-loop inductance

Inductance involving closed loops is nearly an identical concept to inductance involving balanced multi-points.

Self inductance

Given a multi-loop \mathbf{J} , the “self inductance” of \mathbf{J} , often denoted by $L(\mathbf{J})$, is the $2\times$ the minimum possible energy of the multi-surface whose boundary is \mathbf{J} . If \mathbf{E}_{\min} is the minimum energy multi-surface that satisfies $\nabla \times \mathbf{E}_{\min} = \mathbf{J}$, then

$$L(\mathbf{J}) = \int (\mathbf{E}_{\min} \bullet \mathbf{E}_{\min})$$

If \mathbf{F} were an arbitrary multi-surface whose boundary is \mathbf{J} , $\nabla \times \mathbf{F} = \mathbf{J}$, then $L(\mathbf{J})$ can also be interpreted as follows. Since $\epsilon(\mathbf{E}_{\min})$ is a multi-loop (see theorem 38) and \mathbf{E}_{\min} and \mathbf{F} have the same boundary, it then follows from theorem 19 that

$$L(\mathbf{J}) = \int (\epsilon(\mathbf{E}_{\min}) \bullet \mathbf{E}_{\min}) = \int (\epsilon(\mathbf{E}_{\min}) \bullet \mathbf{F})$$

In other words, $L(\mathbf{J})$ is the total number of loops from $\epsilon(\mathbf{E}_{\min})$ that pass through \mathbf{F} , therefore linking through \mathbf{J} .

Mutual inductance

Given two multi-loops \mathbf{J}_1 and \mathbf{J}_2 , the “mutual inductance” between \mathbf{J}_1 and \mathbf{J}_2 , often demoted by $M(\mathbf{J}_1, \mathbf{J}_2)$, is defined as follows. Let $\mathbf{E}_{\min,1}$ be the minimum energy multi-surface that satisfies $\nabla \times \mathbf{E}_{\min,1} = \mathbf{J}_1$. Let $\mathbf{E}_{\min,2}$ be the minimum energy multi-surface that satisfies $\nabla \times \mathbf{E}_{\min,2} = \mathbf{J}_2$. The mutual inductance is

$$M(\mathbf{J}_1, \mathbf{J}_2) = \int (\mathbf{E}_{\min,1} \bullet \mathbf{E}_{\min,2})$$

One immediate observation is that $M(\mathbf{J}_1, \mathbf{J}_2) = M(\mathbf{J}_2, \mathbf{J}_1)$. It is also worth noting that $L(\mathbf{J}) = M(\mathbf{J}, \mathbf{J})$.

If \mathbf{F}_1 and \mathbf{F}_2 are arbitrary multi-surfaces whose boundaries are \mathbf{J}_1 and \mathbf{J}_2 respectively, $\nabla \times \mathbf{F}_1 = \mathbf{J}_1$ and $\nabla \times \mathbf{F}_2 = \mathbf{J}_2$, then $M(\mathbf{J}_1, \mathbf{J}_2)$ can be interpreted as follows.

Since $\epsilon(\mathbf{E}_{\min,2})$ is a multi-loop, it then follows from theorem 19 that

$$M(\mathbf{J}_1, \mathbf{J}_2) = \int (\epsilon(\mathbf{E}_{\min,2}) \bullet \mathbf{E}_{\min,1}) = \int (\epsilon(\mathbf{E}_{\min,2}) \bullet \mathbf{F}_1)$$

In other words, $M(\mathbf{J}_1, \mathbf{J}_2)$ is the total number of loops from $\epsilon(\mathbf{E}_{\min,2})$ that pass through \mathbf{F}_1 , therefore linking through \mathbf{J}_1 .

Since $\epsilon(\mathbf{E}_{\min,1})$ is a multi-loop, it then follows from theorem 19 that

$$M(\mathbf{J}_1, \mathbf{J}_2) = \int (\epsilon(\mathbf{E}_{\min,1}) \bullet \mathbf{E}_{\min,2}) = \int (\epsilon(\mathbf{E}_{\min,1}) \bullet \mathbf{F}_2)$$

In other words, $M(\mathbf{J}_1, \mathbf{J}_2)$ is the total number of loops from $\epsilon(\mathbf{E}_{\min,1})$ that pass through \mathbf{F}_2 , therefore linking through \mathbf{J}_2 .

Properties of the inductance

Theorem 42. *Let \mathbf{J}_1 , \mathbf{J}_2 , and \mathbf{J}_3 be arbitrary multi-loops. Let c be an arbitrary real number. It is then the case that:*

a)

$$M(\mathbf{J}_1 + \mathbf{J}_2, \mathbf{J}_3) = M(\mathbf{J}_1, \mathbf{J}_3) + M(\mathbf{J}_2, \mathbf{J}_3)$$

b)

$$M(c \cdot \mathbf{J}_1, \mathbf{J}_3) = c \cdot M(\mathbf{J}_1, \mathbf{J}_3)$$

c)

$$L(\mathbf{J}_1 + \mathbf{J}_2) = L(\mathbf{J}_1) + 2M(\mathbf{J}_1, \mathbf{J}_2) + L(\mathbf{J}_2)$$

d)

$$L(c \cdot \mathbf{J}_1) = c^2 \cdot L(\mathbf{J}_1)$$

Proof:

Let \mathbf{E}_1 , \mathbf{E}_2 , and \mathbf{E}_3 be the minimum energy multi-surfaces that satisfy $\nabla \times \mathbf{E}_1 = \mathbf{J}_1$; $\nabla \times \mathbf{E}_2 = \mathbf{J}_2$; and $\nabla \times \mathbf{E}_3 = \mathbf{J}_3$ respectively. The following can then be computed:

a) The minimum energy multi-surface \mathbf{E}_{1+2} that satisfies $\nabla \times \mathbf{E}_{1+2} = \mathbf{J}_1 + \mathbf{J}_2$ is $\mathbf{E}_{1+2} = \mathbf{E}_1 + \mathbf{E}_2$

$$\begin{aligned} M(\mathbf{J}_1 + \mathbf{J}_2, \mathbf{J}_3) &= \int (\mathbf{E}_{1+2} \bullet \mathbf{E}_3) = \int ((\mathbf{E}_1 + \mathbf{E}_2) \bullet \mathbf{E}_3) = \int (\mathbf{E}_1 \bullet \mathbf{E}_3) + \int (\mathbf{E}_2 \bullet \mathbf{E}_3) \\ &= M(\mathbf{J}_1, \mathbf{J}_3) + M(\mathbf{J}_2, \mathbf{J}_3) \end{aligned}$$

b) The minimum energy multi-surface \mathbf{E}_{c1} that satisfies $\nabla \times \mathbf{E}_{c1} = c \cdot \mathbf{J}_1$ is $\mathbf{E}_{c1} = c \cdot \mathbf{E}_1$

$$\begin{aligned} M(c \cdot \mathbf{J}_1, \mathbf{J}_3) &= \int (\mathbf{E}_{c1} \bullet \mathbf{E}_3) = \int ((c \cdot \mathbf{E}_1) \bullet \mathbf{E}_3) = c \int (\mathbf{E}_1 \bullet \mathbf{E}_3) \\ &= c \cdot M(\mathbf{J}_1, \mathbf{J}_3) \end{aligned}$$

c) The minimum energy multi-surface \mathbf{E}_{1+2} that satisfies $\nabla \times \mathbf{E}_{1+2} = \mathbf{J}_1 + \mathbf{J}_2$ is $\mathbf{E}_{1+2} = \mathbf{E}_1 + \mathbf{E}_2$

$$\begin{aligned} L(\mathbf{J}_1 + \mathbf{J}_2) &= \int (\mathbf{E}_{1+2} \bullet \mathbf{E}_{1+2}) = \int ((\mathbf{E}_1 + \mathbf{E}_2) \bullet (\mathbf{E}_1 + \mathbf{E}_2)) \\ &= \int ((\mathbf{E}_1 \bullet \mathbf{E}_1) + (\mathbf{E}_1 \bullet \mathbf{E}_2) + (\mathbf{E}_2 \bullet \mathbf{E}_1) + (\mathbf{E}_2 \bullet \mathbf{E}_2)) \\ &= \int (\mathbf{E}_1 \bullet \mathbf{E}_1) + 2 \int (\mathbf{E}_1 \bullet \mathbf{E}_2) + \int (\mathbf{E}_2 \bullet \mathbf{E}_2) = L(\mathbf{J}_1) + 2M(\mathbf{J}_1, \mathbf{J}_2) + L(\mathbf{J}_2) \end{aligned}$$

d) The minimum energy multi-surface \mathbf{E}_{c1} that satisfies $\nabla \times \mathbf{E}_{c1} = c \cdot \mathbf{J}_1$ is $\mathbf{E}_{c1} = c \cdot \mathbf{E}_1$

$$\begin{aligned} L(c \cdot \mathbf{J}_1) &= \int (\mathbf{E}_{c1} \bullet \mathbf{E}_{c1}) = \int ((c \cdot \mathbf{E}_1) \bullet (c \cdot \mathbf{E}_1)) = c^2 \int (\mathbf{E}_1 \bullet \mathbf{E}_1) \\ &= c^2 \cdot L(\mathbf{J}_1) \end{aligned}$$

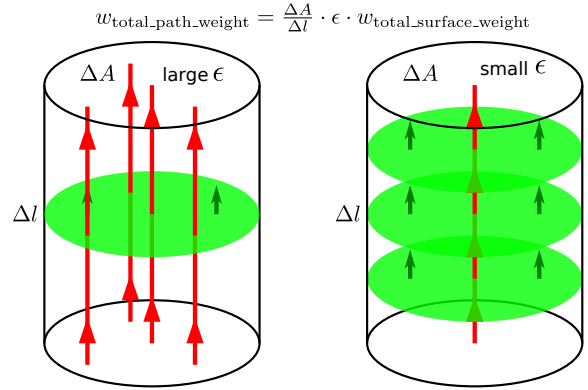
8.8 Scalar ϵ

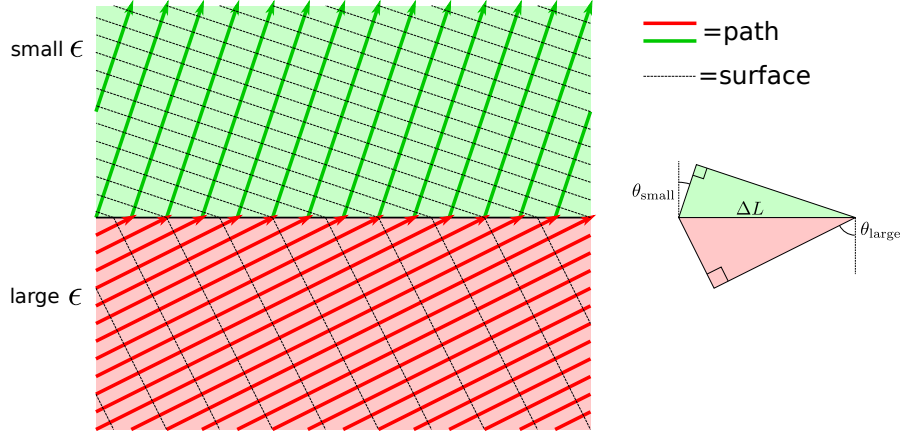
In many scenarios, the duality relationship ϵ is simply the following: Let \mathbf{E} denote an arbitrary multi-surface. At an arbitrary position \mathbf{q} , consider a cylinder that is parallel to the dual multi-path $\mathbf{D} = \epsilon(\mathbf{E})$. Let ΔA denote the area of this cylinder, and let Δl denote the length of this cylinder. Let $w_{\text{total_path_weight}}$ denote the total path weight from \mathbf{D} that runs the length of the cylinder. Let $w_{\text{total_surface_weight}}$ denote the total surface weight from \mathbf{E} that slices through the cylinder, perpendicular to the length. Duality is quantified by a single number ϵ , such that the path weight per unit area is ϵ times the surface weight per unit length:

$$\frac{w_{\text{total_path_weight}}}{\Delta A} = \epsilon \cdot \frac{w_{\text{total_surface_weight}}}{\Delta l}$$

The number ϵ has units of m^{-1} .

It should be noted that the number ϵ can change from position to position. In the image below, a dual multi-path/multi-surface pair $\mathbf{D} = \epsilon(\mathbf{E})$ is shown crossing between two regions where ϵ is different. When the conditions that \mathbf{D} has no endpoints ($\nabla \bullet \mathbf{D} = 0$) and \mathbf{E} has no boundaries ($\nabla \times \mathbf{E} = 0$) are enforced, the following conditions must hold to ensure no break in the paths' and surfaces' continuity.





The values of ϵ in the two regions are denoted by ϵ_{small} and ϵ_{large} .

Consider a stretch of boundary with a length of ΔL , as depicted above.

Let Δt denote the depth of this segment of boundary, not shown in the 2D image.

Let θ_{small} denote the angle that the paths make with the direction perpendicular to the boundary in the ϵ_{small} region, and let θ_{large} denote the angle that the paths make with the direction perpendicular to the boundary in the ϵ_{large} region. These are also the angles that the surfaces make with the boundary in their respective regions.

Let D_{total} denote the total path weight that crosses this segment.

Let E_{total} denote the total surface weight that crosses this segment.

In the region with the small ϵ ,

$$\frac{D_{\text{total}}}{\Delta L \cos \theta_{\text{small}} \cdot \Delta t} = \epsilon_{\text{small}} \cdot \frac{E_{\text{total}}}{\Delta L \sin \theta_{\text{small}}}$$

In the region with the large ϵ ,

$$\frac{D_{\text{total}}}{\Delta L \cos \theta_{\text{large}} \cdot \Delta t} = \epsilon_{\text{large}} \cdot \frac{E_{\text{total}}}{\Delta L \sin \theta_{\text{large}}}$$

These equations respectively give:

$$E_{\text{total}} = \tan \theta_{\text{small}} \cdot \frac{D_{\text{total}}}{\Delta t \cdot \epsilon_{\text{small}}} \quad \text{and} \quad E_{\text{total}} = \tan \theta_{\text{large}} \cdot \frac{D_{\text{total}}}{\Delta t \cdot \epsilon_{\text{large}}}$$

so

$$\tan \theta_{\text{small}} \cdot \frac{D_{\text{total}}}{\Delta t \cdot \epsilon_{\text{small}}} = \tan \theta_{\text{large}} \cdot \frac{D_{\text{total}}}{\Delta t \cdot \epsilon_{\text{large}}} \iff \frac{\tan \theta_{\text{large}}}{\tan \theta_{\text{small}}} = \frac{\epsilon_{\text{large}}}{\epsilon_{\text{small}}}$$

Therefore:

$$\frac{\tan \theta_{\text{large}}}{\tan \theta_{\text{small}}} = \frac{\epsilon_{\text{large}}}{\epsilon_{\text{small}}}$$

From this equation, it can be observed that the angle that paths make to a direction perpendicular to the boundary increases when the paths pass from a region with low ϵ to a region with high ϵ , and vice versa.

Theorem 43. Consider two regions 1 and 2 separated by a flat boundary. Inside region 1, the duality relationship is defined by the single number ϵ_1 , and inside region 2, the duality relationship is defined by the single number ϵ_2 . Let multi-path \mathbf{D} and multi-surface \mathbf{E} be dual to each other, and be continuous and unbroken along the boundary between regions 1 and 2: $\nabla \bullet \mathbf{D} = 0$ and $\nabla \times \mathbf{E} = 0$. Let θ_1 denote the angle

that the paths from \mathbf{D} make with the direction that is perpendicular to the boundary between regions 1 and 2, inside of region 1. Similarly, let θ_2 denote the angle that the paths from \mathbf{D} make with the direction that is perpendicular to the boundary between regions 1 and 2, inside of region 2. It is then the case that these angles are related via the equation:

$$\frac{\tan \theta_2}{\tan \theta_1} = \frac{\epsilon_2}{\epsilon_1}$$

8.9 Electrostatics and magnetostatics

Now the behavior of electric and magnetic fields **when there are no changes with respect to time** will be quantified. When there are no changes with respect to time, the electromagnetic field consists of the following:

- A **multi-point** ρ_e that describes the electric charges.
- A **multi-point** ρ_m that describes the “magnetic charges”.
- A **multi-path** \mathbf{J}_e that describes the electric current.
- A **multi-path** \mathbf{J}_m that describes the “magnetic current”.
- A **multi-path** \mathbf{D} that describes the electric field lines.
- A **multi-path** \mathbf{B} that describes the magnetic field lines.
- A **multi-surface** \mathbf{E} that describes the electric field.
- A **multi-surface** \mathbf{H} that describes the magnetic field.

While “magnetic charge” a.k.a. “magnetic monopoles” are not known to exist, Maxwell’s equations are more symmetric assuming their existence.

There are **two** path-surface duality relationships. Multi-path \mathbf{D} and multi-surface \mathbf{E} are dual to each other, and multi-path \mathbf{B} and multi-surface \mathbf{H} are dual to each other. **However, the duality relationships are different for \mathbf{D} and \mathbf{E} vs \mathbf{B} and \mathbf{H} .**

The symbol ϵ used in the previous discussions will describe the duality between \mathbf{D} and \mathbf{E} :

$$\mathbf{D} = \epsilon(\mathbf{E})$$

Since the duality relationship between \mathbf{B} and \mathbf{H} differs from the relationship between \mathbf{D} and \mathbf{E} , a different symbol μ will describe the duality between \mathbf{B} and \mathbf{H} :

$$\mathbf{B} = \mu(\mathbf{H})$$

The equations that describe unchanging electric and magnetic fields are:

| | |
|--|---|
| $\nabla \bullet \mathbf{D} = \rho_e$ | (Electric charges are the endpoints of the electric field lines.) |
| $\nabla \bullet \mathbf{B} = \rho_m$ | (Magnetic charges are the endpoints of the magnetic field lines.) |
| $\nabla \times \mathbf{E} = -\mathbf{J}_m$ | (The magnetic current is the clockwise boundary of the electric field surfaces.) |
| $\nabla \times \mathbf{H} = \mathbf{J}_e$ | (The electric current is the counterclockwise boundary of the magnetic field surfaces.) |

What units are weights measured in for each of these multi-structures?

- With regards to multi-point ρ_e and multi-path \mathbf{D} , weight is measured using “Coulombs” (C), which are units of electric charge.

- With regards to multi-point ρ_m and multi-path \mathbf{B} , weight is measured using “Webers” (Wb), which are effectively units of magnetic charge.
- With regards to the multi-path \mathbf{J}_m and the multi-surface \mathbf{E} , weight is measured using “Volts” (V), which are units of energy per unit electric charge, or alternately, units of magnetic current.
- With regards to the multi-path \mathbf{J}_e and the multi-surface \mathbf{H} , weight is measured using “Amperes” (A), which are units of electric current, or alternately, units of energy per unit magnetic charge.

With magnetic monopoles not known to exist, it is always the case that $\rho_m = 0$ and $\mathbf{J}_m = 0$. This means that $\nabla \bullet \mathbf{B} = 0$ and $\nabla \times \mathbf{E} = 0$, implying that \mathbf{B} is a multi-loop and \mathbf{E} is a multi-bubble. Because \mathbf{E} is a multi-bubble, there exists some multi-volume V such that the outwards oriented surface of V is \mathbf{E} :

$$\nabla V = -\mathbf{E}$$

Multi-volume V is referred to as the “electric potential”. Given an arbitrary position \mathbf{q} , the net number of volumes from V that contain \mathbf{q} , a.k.a. $V(\mathbf{q})$, is the “electric potential” at position \mathbf{q} .

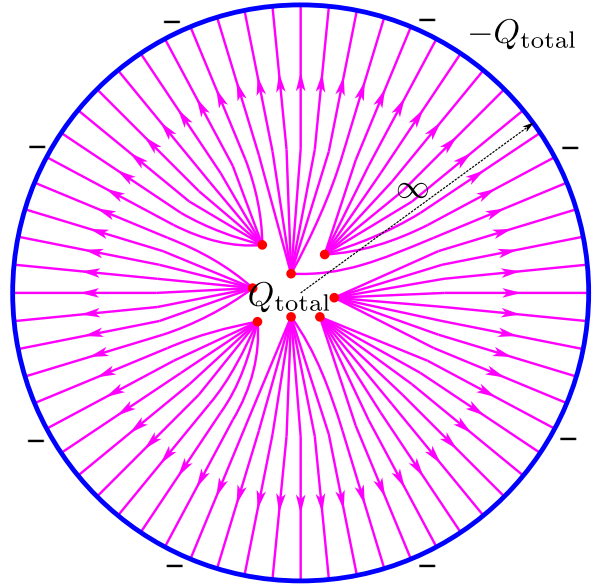
The function $\epsilon(\cdot)$ that converts the electric field multi-surface \mathbf{E} to the electric field lines \mathbf{D} is referred to as the “electric permittivity”. In many cases, ϵ is simply a scalar as discussed in section 8.8.

The function $\mu(\cdot)$ that converts the magnetic field multi-surface \mathbf{H} to the magnetic field lines \mathbf{B} is referred to as the “magnetic permeability”. In many cases, μ is simply a scalar as discussed in section 8.8.

8.9.1 Special scenarios

Point charges

The assumption that is being made from the equation $\nabla \bullet \mathbf{D} = \rho_e$ is that ρ_e is a balanced multi-point, $\int \rho_e = 0$. This means that the total charge in a system is 0. If the net charge in the system is nonzero, say $\int \rho_e = Q_{\text{total}}$, then an amount of charge equal to $-Q_{\text{total}}$ is distributed in a spherical shell at extremely far distances.



8.9.2 Nonuniform permittivity and permeability

Often, the permittivity and permeability are different at different positions.

8.9.3 Anisotropic mediums

Chapter 9

Finite element modeling

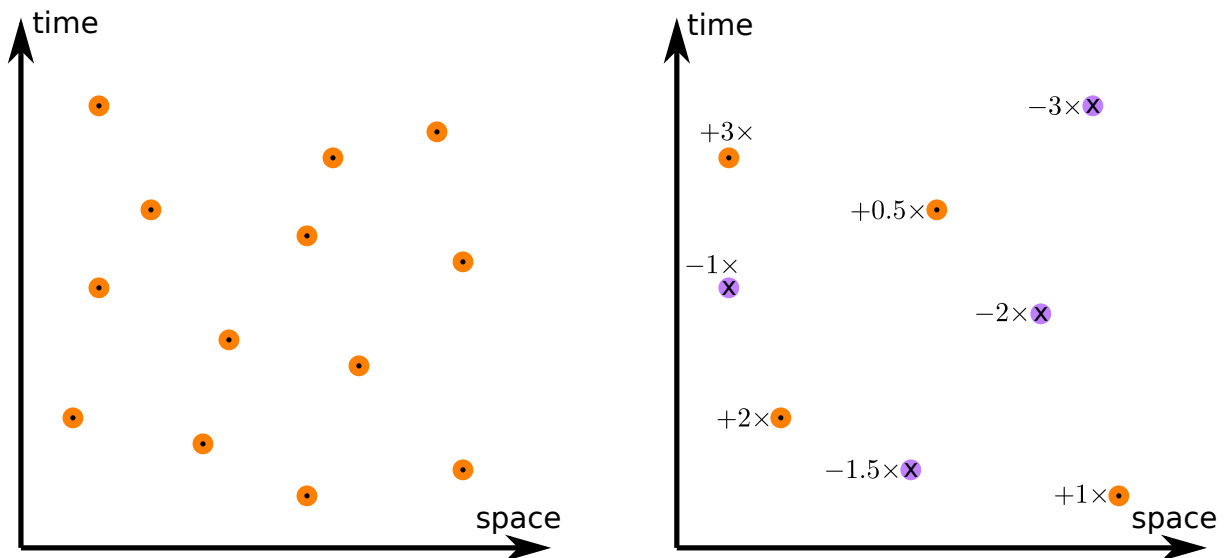
Chapter 10

Introducing time

10.1 A new multi-structure

In addition to the multi-structures of multi-points, multi-paths, multi-surfaces, and multi-volumes, utilizing time now introduces a new multi-structure: the **multi-event**.

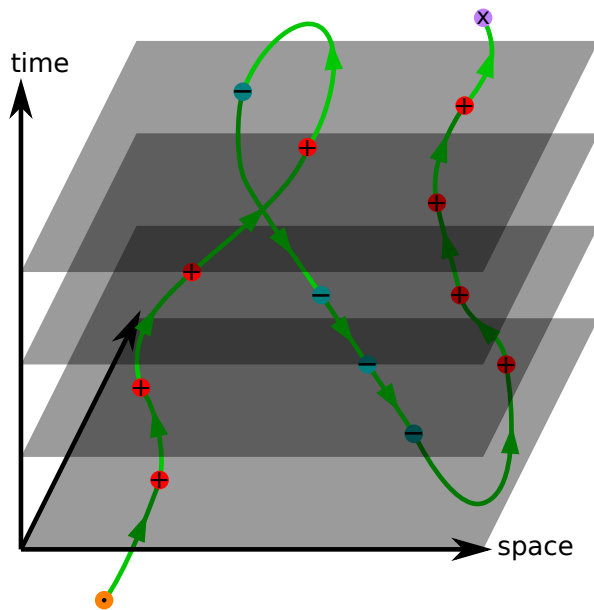
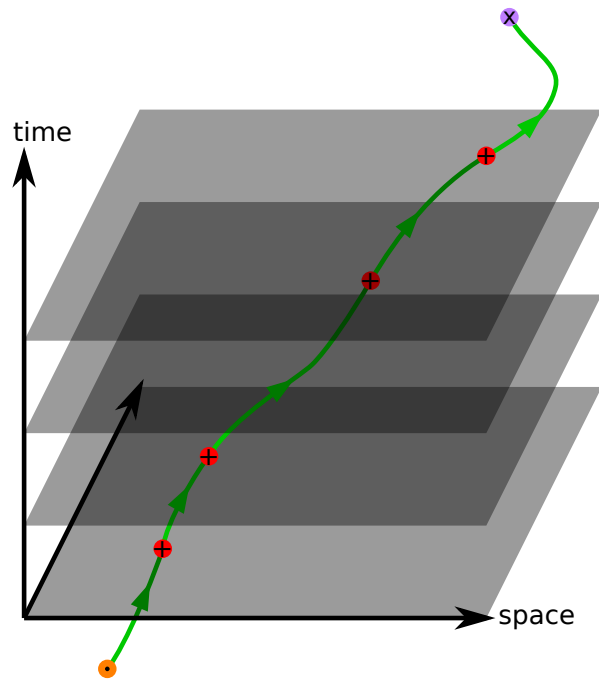
An “event” is the space-time equivalent of a point. An event is characterized by not just a position, but also by a time. In a similar manner to how copies of the same point occupying the same position creates points with different weights, multiple events occurring at the same position and time create events with different “weights”. In the image below, events with a positive weight are indicated using orange dots with a “.” in the center, while events with a negative weight are indicated using purple dots with a “X” in the center.

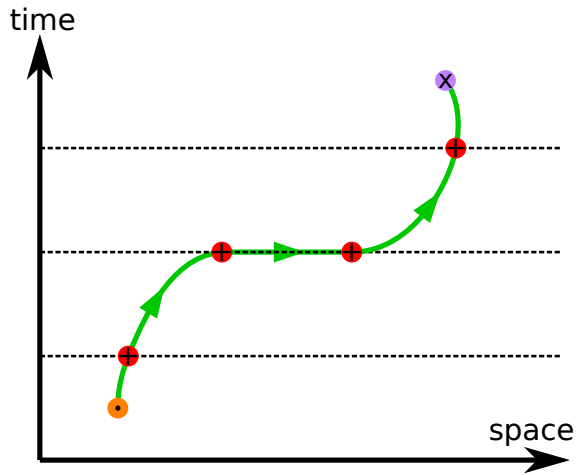
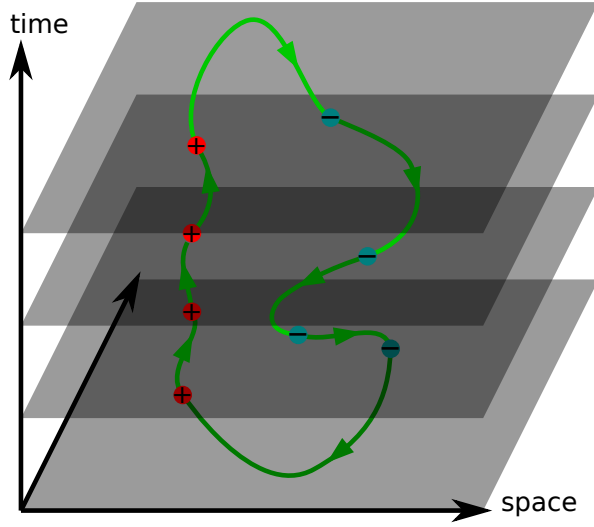


10.2 How multi-structures change with time

This section will detail the manner in which the previously introduced multi-structures, multi-points; multi-paths; multi-surfaces; and multi-volumes, evolve with time:

10.2.1 Moving points





10.3 New intersections

Theorem 44. *Given any multi-paths \mathbf{J}_1 and \mathbf{J}_2 , it is the case that:*

$$\mathbf{J}_1 \otimes \mathbf{J}_2 = \mathbf{J}_2 \otimes \mathbf{J}_1$$

Theorem 45. *Given multi-path \mathbf{J} and multi-surface \mathbf{F} , it is the case that:*

$$(\mathbf{J} \bullet \mathbf{F}) \odot \mathbf{F} = 0$$

A summary of the notations used for various intersections is given below:

| Intersections | event ξ_2 | point ρ_2 | path \mathbf{J}_2 | surface \mathbf{F}_2 | volume U_2 |
|------------------------|-------------------------|-----------------------------------|---|---|----------------------------------|
| event ξ_1 | N/A | N/A | N/A | N/A | $\xi_1 \cdot U_2$ |
| point ρ_1 | N/A | N/A | N/A | event $\rho_1 \odot \mathbf{F}_2$ | point $\rho_1 \cdot U_2$ |
| path \mathbf{J}_1 | N/A | N/A | event $\mathbf{J}_1 \otimes \mathbf{J}_2$ | point $\mathbf{J}_1 \bullet \mathbf{F}_2$ | path $\mathbf{J}_1 \cdot U_2$ |
| surface \mathbf{F}_1 | N/A | event $\mathbf{F}_1 \odot \rho_2$ | point $\mathbf{F}_1 \bullet \mathbf{J}_2$ | path $\mathbf{F}_1 \times \mathbf{F}_2$ | surface $\mathbf{F}_1 \cdot U_2$ |
| volume U_1 | event $U_1 \cdot \xi_2$ | point $U_1 \cdot \rho_2$ | path $U_1 \cdot \mathbf{J}_2$ | surface $U_1 \cdot \mathbf{F}_2$ | volume $U_1 \cdot U_2$ |

Event totals

Creation/destruction events

A summary of the notations used for the different boundaries is given below. In addition, we have observed that the boundaries have no boundaries themselves.

| multi-structure | boundary | orientation | no boundary of the boundary property |
|----------------------|-----------------------------------|---|---|
| event ξ | N/A | N/A | N/A |
| point ρ | event $\nabla \odot \rho$ | positive creation, negative destruction | $\int (\nabla \odot \rho) = 0$ |
| path \mathbf{J} | point $\nabla \bullet \mathbf{J}$ | positive start, negative end | $\nabla \odot (\nabla \bullet \mathbf{J}) = 0$ |
| surface \mathbf{F} | path $\nabla \times \mathbf{F}$ | counterclockwise | $\nabla \bullet (\nabla \times \mathbf{F}) = 0$ |
| volume U | surface ∇U | inwards-oriented | $\nabla \times (\nabla U) = 0$ |

Balanced multi-points redefined

Event totals